# IMPURITIES IN CRYSTALS FORMED BY EUTECTIC FREEZE CRYSTALLIZATION

by

Grant Apsey

A Thesis submitted in

Partial Fulfilment of the

Requirements for the Degree of

Masters in

Chemical Engineering

at

The University of Cape Town

November 2011

## Synopsis

A large concern facing South African industry, particularly the mining sector, is a suitable and sustainable means to deal with waste water streams. Large volumes of liquid waste are produced and no environmentally sound or economically viable means exist to adequately treat this waste. The waste is mostly comprised of effluent water streams containing a variety of dissolved salts.

Tightening legislation is forcing industries to recycle more of their water. To these ends the use of reverse osmosis, evaporating ponds and evaporative crystallizers is commonplace. These technologies have limitations however, and alternative methods must be devised. In addition to this, these existing technologies do not treat or reduce the resulting salt waste. Instead, the liquid waste is reduced in volume by the removal of water, and the concentrated product is disposed of. Because the salt component is never treated, it accumulates. Not only are dump sites dwindling, but they are known to represent environmental issues as well as having the potential to contaminate natural water systems.

A novel technique is being developed for the treatment of industrial waste brines. This technology, called Eutectic Freeze Crystallization (EFC), can potentially separate waste brines into pure water and its major constituent salts. In this way, not only is almost all water recovered, but the major salts are extracted as pure products. That is to say, EFC separates brines into its main components such that they may be reused or sold, and do not represent a costly disposal problem. This could represent a large reduction in salt waste.

The feasibility of this technology is heavily invested in its capacity to produce pure salts as a product from industrial waste brines. For this reason it is important to investigate the obtainable purity of these salts, before larger scale operations can begin. A major component of many South African waste brines is sodium sulphate. This work has therefore focused on the purity of sodium sulphate obtained from two different South African brines.

Up to this point, impurities that are intrinsic to the application of EFC to industrial waste brines have not been investigated. This study begins research into the most significant mechanisms by which impurities are manifested in the product salts. Two case studies are performed, and empirical evidence is extrapolated to form general observations about the relationship between industrial brine impurities and the salts formed in their presence. This work is novel in that little, if any, literature exists on the expected impurities in this form of crystallization. It is believed that findings made in this study will serve to focus future work on the most significant purity issues affecting the feasibility of EFC.

The first brine that was considered was that of the effluent from a platinum group metals (PGM) refinery. It was found that the sodium sulphate produced from this brine was reasonably pure at 99.5%. However, much of the impurity detected was found to be selenium. Selenium is regarded as toxic and environmentally unsafe. Though the purity of the product sodium sulphate is high, the presence of selenium represents a significant limitation to its saleability. It was therefore necessary to further investigate the nature of the selenium impurity, to see if it could be limited or avoided.

It was determined that selenium was present in the form of selenate, and that the similar structure and properties of selenate to sulphate allowed it to be isomorphously included in the sodium sulphate crystals.

Additionally, the high concentration of sodium chloride in the brine promoted the uptake of selenate. It was theorised that the common ion effect between sodium sulphate, sodium selenate and sodium chloride might have an impact on the solubility of sodium selenate relative to sodium sulphate. A theoretical analysis of this was performed with a simple model, and it illustrated that this is not likely to be the case. Both the solubilities of sodium sulphate and sodium selenate are similarly affected by the presence of sodium chloride. The solubility of one does not significantly change relative to the other.

It was also investigated if it was the common ion between sodium chloride and sodium sulphate that caused increased uptake of selenium, or the increased ionic strength of the solution. To establish this, tests were conducted where the ionic strength of the mother liquor was adjusted by adding either sodium chloride or potassium chloride. It was found that ionic strength does not appear to have an impact on the uptake of selenium, and that it is quite conclusively the presence of excess sodium that promotes the uptake of selenium.

It was believed that the uptake of selenium might also be a function of the mass deposition rate of sodium sulphate. Experiments were conducted whereby the selenium impurity uptake was measured against differing mass deposition rates of sodium sulphate. It was found that there did not appear to be any correlation between the mass deposition rate and the uptake of selenium.

It is believed, from the investigations, that the selenium impurity cannot be reduced simply by changing the process operating parameters. The uptake of selenium is facilitated by the similarity between selenate and sulphate ions, and therefore the selenate concentration in the brine must be reduced to prevent contamination of the sodium sulphate product.

The second brine investigated was that of a coal fired power station. This brine was treated using EFC and the sodium sulphate salt product was characterised. It was found that the purity was quite low at 94%. This was predominantly due to a high impurity of potassium in the salt (±5.5%). Closer inspection revealed that potassium is higher in concentration in the salt than it is in the brine, relative to sodium sulphate. From this is can be inferred that potassium is being concentrated in the salt. It is still unclear as to whether this impurity is due to isomorphous substitution, or the presence of an unknown sodium/potassium double salt.

Though this product is much less pure than the product of the PGM brine, the impurities can be considered to be more benign than selenium. It is more likely that 94% pure sodium sulphate with a potassium impurity will find a useful application than 99.5% pure sodium sulphate with a selenium impurity.

In addition to the potassium, an appreciable concentration of phosphate, 0.45%, was also detected. The phosphate concentration is also higher in the salt than it is in the brine, though is it not concentrated to the same degree as potassium. Though thermodynamic modelling predicted the formation of the double salt pentacalcium hydroxide phosphate, $Ca_5(OH)(PO_4)_3$, the detected concentrations of calcium were not high enough to support this. Phosphate can also be considered to be fairly benign for many applications, and is not considered to be of immediate concern. The nature of the phosphate inclusion is not known.

An additional concern of the treatment of the coal power plant brine is the presence of calcium sulphate. Calcium sulphate is sparingly soluble, and can precipitate along with the sodium sulphate in EFC. Part of this investigation was to examine how this might contaminate the product. It was found that, although calcium sulphate does form along with sodium sulphate, it does so in small amounts, not more than 2 ppm of the total salt product.

It was also found that in both brines considered, liquid inclusion was not a significant factor in the uptake of impurities. This is an important consideration in future studies into the purity of salts formed from industrial brines. When considering the wide range of dissolved components in industrial brine, this study has shown that it is likely that isomorphous substitution will be the main source of impurity in most cases. Thus the focus of future studies should be on minimising isomorphous substitution rather than liquid inclusion.

Acknowledgements

I would very much like to thank Professor Alison Lewis, both for the opportunity to work on such an interesting project, and for all the help she has given me over the last 18 months. As my supervisor she has always made an effort to be available and interested. This thesis would not have been possible without her.

Additionally, I am indebted to Traci Reddy for allowing me to continue her work, Dyllon Randall for his experience and expertise, and Sinethemba Nkukwana for his help in the lab. Also, thanks to Tracy-Anne Craig for her help in dealing with the ICP issues.

I am grateful too, to Dr Gerhard Venter, for the generous donation of his time and expertise.

# Contents

## Nomenclature

| | |
|---|---|
| EFC | Eutectic Freeze Crystallization |
| Agglomeration | Process whereby crystals attach themselves to each other |
| Brine | Water containing dissolved salts |
| Crystal lattice | The repeating molecular structure of a crystal |
| Desalination | The recovery of potable water from salt containing brine |
| Dislocations | A crystal defect resulting from a missing structural unit |
| Effluent | A waste stream from a process |
| Evaporative crystallization | The recovery of salts through the boiling off of water from a liquor |
| Exsolved | The extraction or separation of a substance from a solid crystal |
| Hydrological cycle | The cycle referring to the natural flow of moisture, from evaporation to precipitation to flow towards the ocean |
| Hypersaline | Brine containing a very high concentration of dissolved solids |
| Ionic radius | The size of an ion |
| Isomorphous inclusion | The random replacement of an ion with similar ion, without affecting the morphology of a crystal |
| Liquid inclusion | Mother liquor encapsulations within a crystal. Also known as occlusions |
| Mass deposition | Process whereby growth units are deposited on the growing surface of a crystal |
| Mass transfer | The movement of substance across a boundary layer |
| Membrane technologies | Processes using a semi-permeable membrane and a pressure gradient to desalinate water |
| Mother liquor | Liquid containing dissolved crystalline material |
| Occlusion | See liquid inclusion |
| PGM | Platinum Group Metal |
| Saturation | The thermodynamically stable point at which no more of a solute can be dissolved in a solvent |
| Solute | A substance that is dissolved in another |
| Solvent | A substance that contains a dissolved substance |
| Steric interactions | Interferences resulting from molecules occupying space |
| Supersaturation | A thermodynamically unstable state whereby a solvent contains an excess of solute, due to rapid cooling or evaporation |
| Synthetic Brine | An artificial brine made up to represent the main components of an industrial brine |

## Symbols

| | |
|---|---|
| $V$ | Total volume of inclusions per crystal in $\mu m^3$ |
| $d$ | Crystal size in μm |
| $x_{sol}$ | Concentration of impurity incorporated into crystal |
| $x_{liq}$ | Concentration of impurity in mother liquor |
| $K$ | Solid/liquid segregation coefficient |

# Table of Figures

# Table of Tables

# 1 Introduction

Crystallization has been used as a means to purify substances for centuries and is considered to be one of the oldest chemical engineering operations (Bohm, 1985). Earliest records indicate that crystallization was used to obtain sodium chloride and pigments. Initially crystallization was possibly used due the fact that it is a process that is easy to utilise without advanced technology. Since then however, crystallization has been favoured for its capacity to produce highly pure products. When crystallization was first used it could have been considered to be an art more than a science. Many advances have been made in understanding crystallization, but much is still considered to be a matter of feel rather than understanding. Like all mature processes, crystallization has evolved and diversified over centuries of use and is now used in a great number of industrial applications; sugar, table salt, optics, the food industry and desalination, to name a few. Recently however, as crystallization has become more advanced, different ways are being found to utilise this age old technology. One such way is a process called Eutectic Freeze Crystallization.

Eutectic Freeze Crystallization (EFC) is a novel technique that is showing potential in a number of processes, but possibly most notably in the arena of waste water treatment. EFC can be seen to be a combination of both cooling crystallization and solvent removal crystallization. A liquor is cooled to a point where both ice crystals and crystals of the solute form. A full description for this process can be found in section 3. It has been found however, that, when applying EFC to some real industrial brines, there is the propensity for the product crystals to be of unacceptably low purity. Because the feasibility of EFC is heavily invested in its potential to produce separate pure crystalline products from waste brines, it is important to understand how to prevent or control impurity uptake.

Much of the research to date that has been performed on Eutectic Freeze Crystallization has been on simple binary and ternary systems or synthetic brines, for example the work done by van der Ham et al (1997). So far this research has intentionally overlooked the influence of crystallizing products out of actual industrial brine. It has been necessary in this research of EFC to perform tests with synthetic or simple brines so that the influences of the microcomponents can be eliminated. The purpose of this was to investigate systems that could apply to a broader range of brines. By focusing on the major components of the brine, a more generally applicable understanding could be formulated.

In reality however, many brines, especially those produced by the mining industry, contain a variety of solutes that display a number of unpredictable interactions. Some prior research has

already been carried out to expand the pool of knowledge by modelling multi-component brine to better approximate real brines (Lewis et al., 2010) and some experiments have been performed on more realistic synthetic brines (Reddy et al., 2010). This research provides information about Eutectic Freeze Crystallization and has endeavoured to understand the complexities of industrial brine, but more research is required on genuine effluent brines before large scale operations can be considered.

Little is known of what impact the process of EFC might have on the purity of the product crystals, when compared to more established crystallization methods. This issue is compounded by the fact that impurity uptake in general is not well understood, even without the added complication of operating under eutectic conditions. The number of components in many waste brines and the current way in which Eutectic Freeze Crystallization is performed means that all known mechanisms for impurity uptake are possible. What this work attempts to ascertain is which mechanisms are the most influential on overall purity in the case of brine treatment. In so doing we can further add to the growing pool of knowledge about the feasibility of the process.

Because of the highly varied and dynamic nature of industrial brines, it is not possible to perform exhaustive analyses on all salts present in all brines. Therefore, within the time limits of this project, it was only possible to examine one salt from two brines. The salt selected for examination was sodium sulphate. Among the most prolific salts present in South African brines, sodium sulphate is expected to be the one of the main products of EFC. Sodium sulphate is most commonly used in the production of soaps and detergents as an inert filler, and in textile dying. It is also used in the pulp and paper industry, as well as in textiles and glass manufacture. A number of substitutes do, however, exist for sodium sulphate in all these industries and its use is thus mainly determined by economic factors. At the time of writing, most industrial sodium sulphate is obtained through the mining of natural sodium sulphate sources, and the remainder as a by-product of other chemical processes. The required purity of the product is dependent on both the nature of the impurity and the requirements of the industrial process.

The brine selected for analysis is motivated by a number of factors. The brines selected for investigation were those that were believed to represent the widest range of interest. To these ends, an industrial waste brine from a platinum operation, and the blended waste of a colliery and a coal power plant were selected for investigation.

Currently, the potential purity of sodium sulphate from the EFC of industrial waste brine is unknown, and predictions of its usefulness to industry cannot be made. For this reason, the investigation of sodium sulphate purity from different brines will have an important impact on

the predicted feasibility of EFC. In this project, impurities in general will be discussed, and the aforementioned case studies of impurity uptake by sodium sulphate will also be investigated. While it is understood that many factors must be omitted in this investigation, the purpose of this work is to begin building up a framework of understanding about the purity issues surrounding the treatment of hypersaline industrial brines with EFC.

"With the possible exception of the equator, everything begins somewhere."

CS Lewis

# 2 Problem statement

EFC is reaching a stage in development where pilot scale operations are being planned for the near future. However, before this happens, it is necessary to gather more information about EFC in a real system.

The main purpose of this work is to investigate impurities in salt formed from industrial brine by Eutectic Freeze Crystallization. This research is carried out by performing two case studies, and investigating impurities found in sodium sulphate produced from two different industrial brines.

This work should:

- Illustrate the most significant sources/mechanisms by which impurities are taken up in the EFC of industrial brines.
- Serve to provide general principles and guidelines, about impurities, that can be applied to other systems where industrial brines are crystallized with EFC.
- Justify how findings made here can be applied to other systems where EFC is to be applied.
- Provide recommendations on the most productive areas for further investigation into future research of impurities in the EFC of industrial brines.



## 2.1 Scope of work

This project will apply EFC to two real brines, each originating from a different industry. In this way it is believed that the beginnings of a broad cross-section of the efficacy of EFC can be developed. Additionally, problem areas can be identified before pilot scale operations begin. Brines are not only specific to the type of industry, but also to the particular operation in question. However, commonalities between brines and families of brines can be found such that general rules and statements can be made when treating them with EFC. As stated before, these investigations focus on the formation of sodium sulphate, as it is likely to be the primary product in many South African brines.

### *2.1.1 PGM brine*

The research into this particular brine follows a prior study done whereby appreciable amounts of selenium were detected in the sodium sulphate product. The selenium impurity could not be adequately explained in this previous work, and as such this project was conducted to further the understanding of impurities in salts formed from industrial brines. This previous study is summarised in the literature review in section 5.

This brine is produced by a PGM refinery, and is typified by very high concentrations of sodium sulphate and sodium chloride. Though these are the most prevalent dissolved substances, there are a large number of other dissolved microcomponents.

For EFC to be beneficial, the crystal products that it produces from the brine must be saleable. Before the salt can be considered for sale though, it must be proven that it is of high enough purity. To these ends, it is necessary to apply EFC to the waste brine, and investigate the purity of the products.

This brine represents the first investigation into an extended project on the purity of salts produced from EFC. For this reason, the impurity in sodium sulphate produced from this salt is investigated in such a way as to illuminate factors that are not of immediate importance. That is to say, the impact of the following factors will be investigated, and the less important ones will likely be removed from immediate future studies. The factors investigated are:

- Liquid inclusion (Section 5.3)
- Isomorphous substitution (Sections 5.3 and 6.1)
- Impact of other dissolved components (Sections 6.2, 6.3)
- Impact of mass deposition rate (Section 6.4)

### *2.1.2 Coal power plant brine*

This brine is a mixture of waste effluent from the cooling towers at a coal power plant and the effluent from a coal mining operation. The blended brine has been concentrated by reverse osmosis, but is still dilute when compared to the PGM brine. The strategy for this brine is to be sprayed over ash heaps, and the remainder pumped underground into disused mining caverns. This is not a sustainable solution, and alternatives must be considered.

This brine is comprised mostly of sodium sulphate and sodium chloride, but also contains appreciable amounts of calcium sulphate. Calcium sulphate is sparingly soluble and also displays inverse solubility. This means that it becomes less soluble with an increase in

temperature. Because of this, calcium sulphate often causes scaling in boilers and heat exchangers. Eutectic freeze may, therefore, prove to be a favoured option in the treatment of calcium sulphate containing brines.

This brine is of interest because it poses purity issues that are different to those encountered in the PGM brine. During the crystallization of sodium sulphate by EFC, calcium sulphate also precipitates out of the power plant brine. Experiments on this brine will investigate the impact that the precipitation of calcium sulphate has on the purity of the sodium sulphate salt, in addition to identifying other impurities.

Unlike the PGM brine salt, the nature of the impurities in the power plant brine salt will not be investigated further. The salt impurities from the power plant brine cannot be exhaustively investigated due to time constraints. Instead, impurities detected in the power plant salt will be discussed in terms of findings from the investigation into the PGM brine salt. This will serve to guide future studies into the impurities in EFC



## 2.2 Limitations of study

It has been mentioned that it is not possible to extensively investigate every salt product from every brine in one thesis. Nor is it possible to investigate every parameter that may have an effect on impurity uptake. As such, the following limitations of this study have been identified.

- The effect of agitation on the uptake of impurity was not investigated
- Only one type of salt, $Na_2SO4_4$, and two kinds of brine were investigated.
- 
- Only the selenium encountered in the PGM brine was investigated further.
- Methods to reduce the concentration of Selenium in the brine were not examined
- The specific nature of the impurities encountered in the coal brine sodium sulphate was not subjected to further testing.
- Study does not provide recommendations whether a salt can be classified as “pure” or “impure”, as this dependent on the specific requirements of industry utilising the salt.

# Literature Review

## 3 Eutectic Freeze Crystallization (EFC)

Water scarcity has been a growing concern for industries and constricting legislation is forcing them to recycle a larger percentage of their water. Though recycling decreases the load on the hydrological cycle, the techniques used to recover the water produce waste streams of hypersaline brine containing a large variety of dissolved substances. A popular method is to recover water through membrane technologies. There are limitations to the level of salinity and pH that this technology can manage, however, and the remaining concentrated waste brine must still be disposed of. Another common way in which industries treat salt-containing waste is to evaporate it in large solar ponds. From the ponds the concentrated brine is sometimes fed to an evaporative crystallizer and the water is boiled off. This leaves behind a mix of salt crystals that must be disposed of, usually in waste dumps. This is problematic for a number of reasons.

Apart from the fact that industries must pay to dispose of this solid effluent, the disposal sites are filling up, and are beginning to decline waste. With no alternatives for the disposal of the waste, operations may be forced to cease until a solution for this disposal issue can be found. There are also the additional issues of producing a mix of salts which is toxic and a significant environmental hazard.

These issues stem from the fact that, through evaporative crystallization, a mix of salts is produced, and with current means, there is no feasible way to separate them. Eutectic Freeze Crystallization (EFC) is a novel technique for the separation of aqueous salts from water, the products of which are salt crystals and ice. When operating at the eutectic temperature, ice and salt are formed as two separate phases (van der Ham et al., 1999). That is to say, salt and ice are formed separately and, due to their density difference, ice floats to the top and salt crystals sink to the bottom. This allows for an easily achievable separation. The potential for this technology is being recognised by industries with waste brine that must be disposed of.

In the case of EFC, due to the thermodynamics of some aqueous solutions, each salt contained in the mixture crystallizes out at a different temperature. This means that each salt contained in the brine can be removed sequentially at different temperatures and thus separate, pure products are recovered. This is advantageous as the produced pure salts could be considered to be by-products that may even be profitable, as opposed to a costly disposal problem.

Due the fact that heat of fusion is roughly six times less than that for evaporation, it has been shown that EFC can be significantly less energy intensive than evaporative crystallization, sometimes by as much as 70% (van der Ham et al., 1997). It must be noted that these values take into account the inherent energy differences between industrial heating and cooling. The research that has been performed has taken an overview of the processes, and despite the penalties related to freezing compared to heating, EFC is still more efficient.

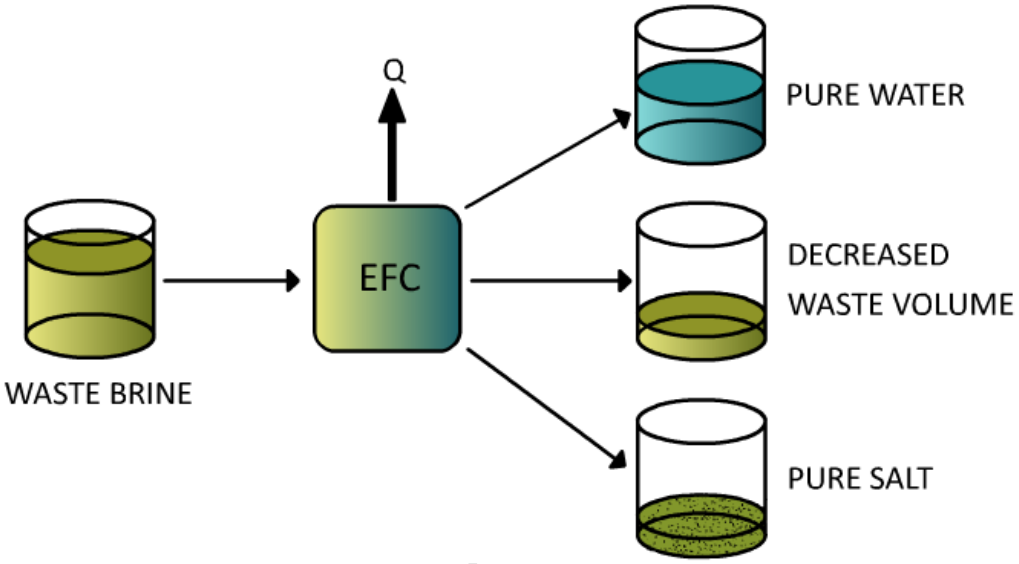


**Figure 1: The EFC process.**
**Waste brine is separated into its component salts, pure water and the residual brine**



Figure 1 represents the simplified EFC process. Waste brines are cooled to their eutectic point where ice and salt are produced simultaneously. The ice and salt are removed from the system, leaving behind residual brine. While it is practical and feasible to remove the major dissolved components, some dissolved micro-components remain. It is technically possible to remove these remaining salts, but, considering that each salt requires its own cooling stage, the marginal benefits are insignificant for this to be practical or feasible. Therefore, in any EFC process, there will be a small amount of residual brine.

The water that is extracted as ice can be recycled back into the system or used as the situation dictates. The usefulness of the produced salts is highly subject to the situation in question, but even if they are given away for free, it is a large improvement on the current system of paying for their disposal.

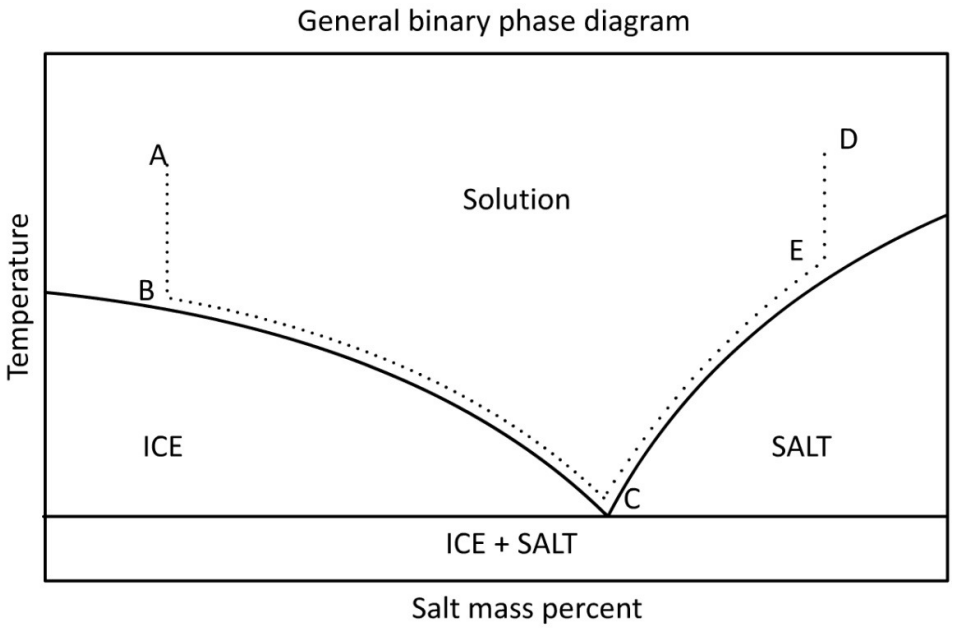


**Figure 2: A phase diagram for a binary salt/water solution**

A simplistic explanation for the theory behind Eutectic Freeze Crystallization is provided in Figure 2. If one were to begin with a dilute salt solution at point A and decrease the temperature to the ice solubility line at B, ice would start to crystallize out of the solution. If the temperature is further reduced, more ice is produced. As ice is crystallized the solution becomes more concentrated, following the ice solubility line to the eutectic point at C. At the eutectic point both ice and salt will be produced simultaneously. The density of ice and salt differ by about 1000 $kg/m^3$ and can thus be separated by gravity, as ice floats to the top and salt sinks to the bottom (van der Ham et al., 1999). The ice is washed and melted to produce pure water. A similar result is encountered when one begins with a concentrated salt solution, except the salt solubility line is reached first and initially salt crystallizes out. This is shown in Figure 2 by the path DEC.

Though this phase diagram only represents the separation of two substances, solutions with more dissolved components can be separated sequentially by the same process. By operating at the eutectic point, a salt is removed. Once this salt has been removed, the next eutectic point can be reached, representing the removal of more ice, and a different salt.

The potential for this technology is significant in that it represents a large decrease in the volume of effluent waste, while being more energy efficient than conventional means of hypersaline brine treatment. EFC is the only waste brine treatment that has the potential to concentrate the waste, as well as separate it into components that might no longer be referred to as waste.

## 3.1 Additional advantages of EFC

Apart from the energy savings mentioned before, EFC displays a number of additional characteristics that look to be promising in the treatment of hypersaline industrial brines. One of these characteristics is that EFC potentially operates best at very high dissolved salt concentrations, where many other brine treatment technologies fail and cannot be used.

Industrial crystallization is usually carried out in one of two ways; by cooling or by solvent removal. Components that have strongly temperature-dependent solubility like sodium sulphate lend themselves well to cooling crystallization. As the temperature of the solution is decreased the solubility of the salt decreases and it crystallizes out of solution. Alternatively, when the solubility of the salt is not very dependent on temperature, like sodium chloride for example, techniques that utilise the removal of solvent are favoured. For this evaporation is popular. The principle is that solvent is removed by evaporation until the solution becomes saturated. Further evaporation results in the forced crystallization of the salt. EFC combines these two principles in that cooling is required to reach the eutectic point, and once the eutectic point is reached the solvent is removed in the form of ice. In this way EFC combines the strengths and potential applications of these two principles and minimises the drawbacks. This should prove to be beneficial when treating brines with components that display a wide range of solubility behaviours.

Membranes used in desalination are sensitive to extreme pH. Thus brines that are strongly acidic or strongly alkaline cannot be treated with membrane technology. EFC is not affected by pH in this way, and can be used to treat these brines.

# 4 Impurities

EFC has in recent years been subject to renewed interest and research, but little testing has been performed on complex industrial brines. Work to date has focused on theoretical studies and lab work has been confined to synthetic systems, or very simple industrial brines. However, in reality, industrial waste brines contain a large number of aqueous components and it is necessary to establish how the complex interactions of these components influence the process. Considering that much of EFC's feasibility is invested in its potential to produce pure crystalline products, understanding the factors influencing the purity of these products is important.

Research has been completed on how some of these components influence the thermodynamics of the process (Reddy et al., 2010). This research was however still performed with synthetic brines and does not include how the different components in real brine might impact the purity of the crystalline product.

In addition to the abovementioned issues, the actual mechanical operation of EFC is still in its formative stages. The physical aspect of the crystallization process can have a bearing on the purity of the product, specifically with regard to the promotion of liquid inclusions. It thus becomes important to understand how this process will impact on the quality of the product so that design considerations can be implemented in the early stages of development.

Broadly speaking, the different ways in which impurities can occur are through liquid inclusions, isomorphous inclusions and adhesions. Liquid inclusions are chambers of mother liquor that are entrapped by the growing crystals. These liquid inclusions contain whatever impurities existed in the mother liquor and cannot be removed by washing. Isomorphous inclusions can be described as ionic substitutions or solid solutions. Sometimes when an impurity has a similar structure to one of the ions comprising the desired salt it can occupy a place in the lattice of the crystal. Alternatively the impurity can be incorporated interstitially, where the impurity is located in the spaces between ions. Adhesions refer to substances that are adsorbed onto the surface of the crystal. They are seldom discussed as impurities but are sometimes mentioned in papers discussing their ability to alter the growth pattern of the crystal.

## 4.1 Liquid inclusions

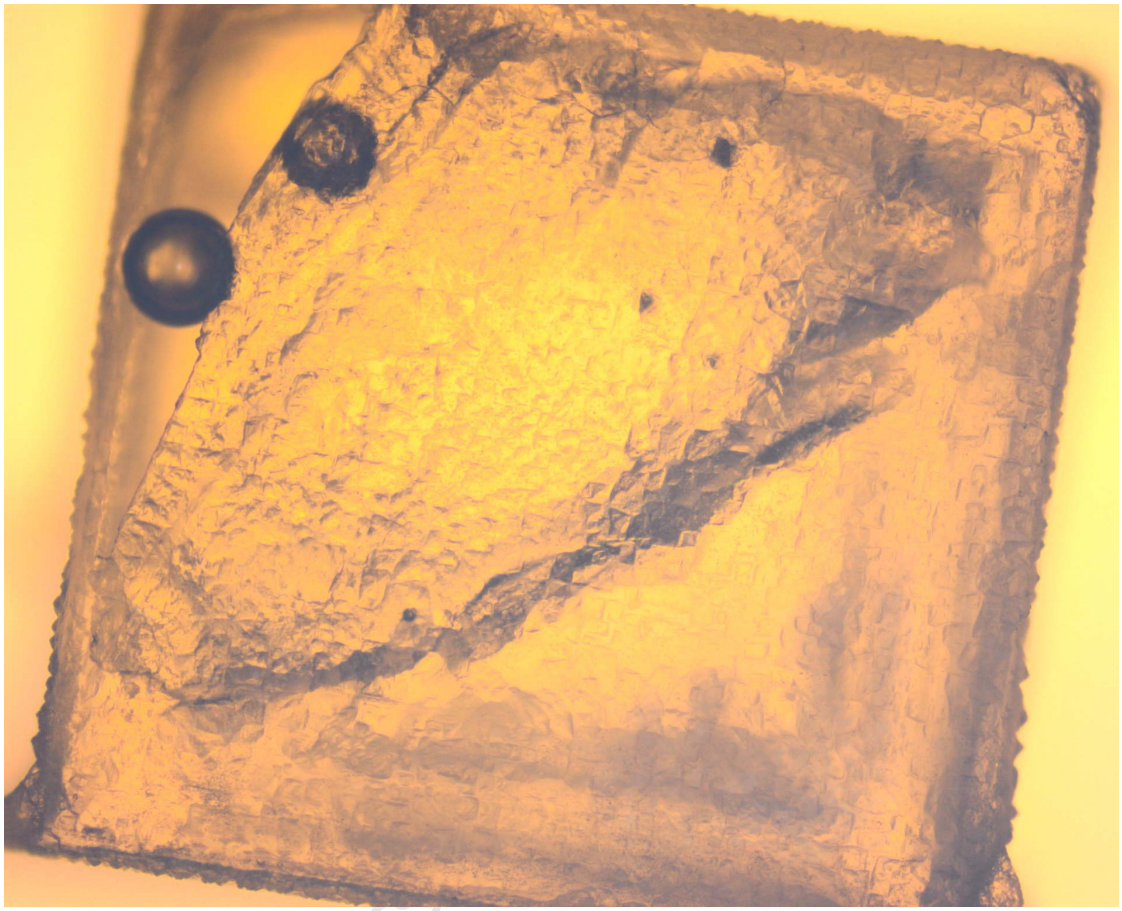

**Figure 3: Liquid inclusions in sodium chloride crystal**

Liquid inclusions or occlusions are encapsulated chambers of mother liquor that are retained within crystals. The nature of liquid occlusions has been investigated for many years by many notable authorities in crystallization(Brooks, Horton and Ferguson, 1968; Belyustin and Fridman, 1968; Denbigh and White, 1966). Despite this however, there are numerous theories on the subject, but there is little agreement in the literature and the phenomenon is poorly understood at best.

### *4.1.1 Classification of inclusions*

Before one can begin investigating liquid inclusions it is first necessary to break them down into groups. According to Saito et al (2001) liquid inclusions can be classified into two groups; type 1 and type 2 inclusions. Type 1 inclusions are chambers within single crystals that contain mother liquor. The exact mechanisms by which type 1 inclusions form are not fully understood

but literature indicates that they form as a result of damage to crystal surfaces, macro-step generation, mechanical impacts or adhesion of fine crystals onto larger crystal surfaces (Saito et al., 2001). There are also studies indicating that liquid inclusion is the result of the crystal interface becoming unstable and the crystal growing dendritically. The dendrite arms then impinge on each other to form occlusions (Edie and Kirwan, 1973). Type 2 inclusions form when mother liquor is trapped between agglomerating crystals (Saito et al., 2001). Alternatively, inclusions can be grouped into those that form during growth (primary) and those that occur after growth (secondary) (Zerfoss and Slawson, 1956). This primary and secondary classification is analogous to the type 1 and type 2 categories and it can be assumed that they mean roughly the same thing.

Early research into inclusions in crystals was essentially based exclusively on visual techniques and as a result primary inclusions are classified according to how they appear in the crystal. Primary inclusions are thus classified into one of the following groups (Zerfoss and Slawson, 1956)

- Bubbles – Amorphous shaped inclusions filled with either vapour or solution.
- Negative crystals – Inclusions that possess a crystalline shape
- Veils – Thin sheets of small inclusions
- Phantoms or ghosts – Oriented veils. An envelope of planar veils
- Clouds – Aggregates of fine bubbles or cavities.
- Solid crystals or mineral fragments. These are caused by
    - Foreign substances in the mother liquor that are incorporated into the crystal
    - Phases exsolved once growth has finished.
    - From crystals crystallised out of included mother liquor.

The fact that it is possible for inclusions to manifest themselves in such different forms has made researching them all the more difficult. No theory seems to adequately explain the formation of all types of inclusion and in most cases the explanation for the formation of one type of inclusion is mutually exclusive to any others, despite many efforts being made to find commonalities between them.

### *4.1.2 Causes and mechanisms for inclusions*

Wilcox (1968) believed that liquid inclusions begin as depressions on the surface of the crystal as it is growing. The cause of these depressions could be due to a foreign body preventing access of solution to the growth site, or possibly the adsorption of impurities onto the crystal surface.

These surface depressions are also believed to be a result of fluctuating supersaturation levels at the crystal surface. In the case of these depressions, the diffusion limited growth rate within the depression is slower than the growth rate at the corners. This exacerbates the depth of the depression as the crystal grows. Eventually there is the possibility for the depression to be closed over, and a liquid inclusion will result. In extreme cases of differing supersaturation levels, dendrites are formed, which later fill in to form inclusions. Dendritic growth within the context of EFC is not expected to be a problem, however, as frequent motion and collision with the impeller and other crystals is likely to break off any growing protrusions. Additionally, agitation is likely to limit the potential for different levels of supersaturation, which would also decrease the chance for dendritic growth.

The concept of differing local supersaturation levels is a common theme in discussions about the formation of inclusions. The cause of these differing supersaturation levels is however an area of disagreement, as can be seen in the theory on inclusion below.

Instead of foreign bodies causing sites of different supersaturation levels there is the theory that the growth of a crystal itself may be the source. Belyustin and Fridman (1968) believed that inclusions are a result of growth step heights of crystals. If the step height is above a critical value an inclusion will take the form of a large flat layer. The exact mechanism by which this occurs is not discussed. Other types of inclusions can be attributed to the fact that growth steps are not flat but often consist of lobes. See Figure 4. The base of these lobes is supplied with a lower supersaturation than the foot. Thus the foot advances more quickly than the base. If the height of the step is less than that required for the formation of the layers described above, then long channels are produced. Fluctuating supersaturation can result in the channel being broken up into separate, discrete inclusions.

Alternatively to the above, temperature changes may result in partial dissolution of the crystal, causing pitting in the crystal surface. These pits can then be overgrown to form liquid inclusions (Wilcox, 1968). Dissolution may also round the edges of the crystal. When growth continues again, strings of inclusions are seen to occur on the edges of the crystals. (Wilcox, 1968)

As a crystal grows, it incorporates growth units of the crystal and rejects impurities. Thus, impurities accumulate at the growing surface of the crystal. There is the potential that these impurities accumulate locally around the crystal to the extent where their concentration exceeds supersaturation. The impurities can then crystallise and potentially stick the growing crystal and may be incorporated into it (Wilcox, 1968). This is unlikely to occur in a well agitated system however.

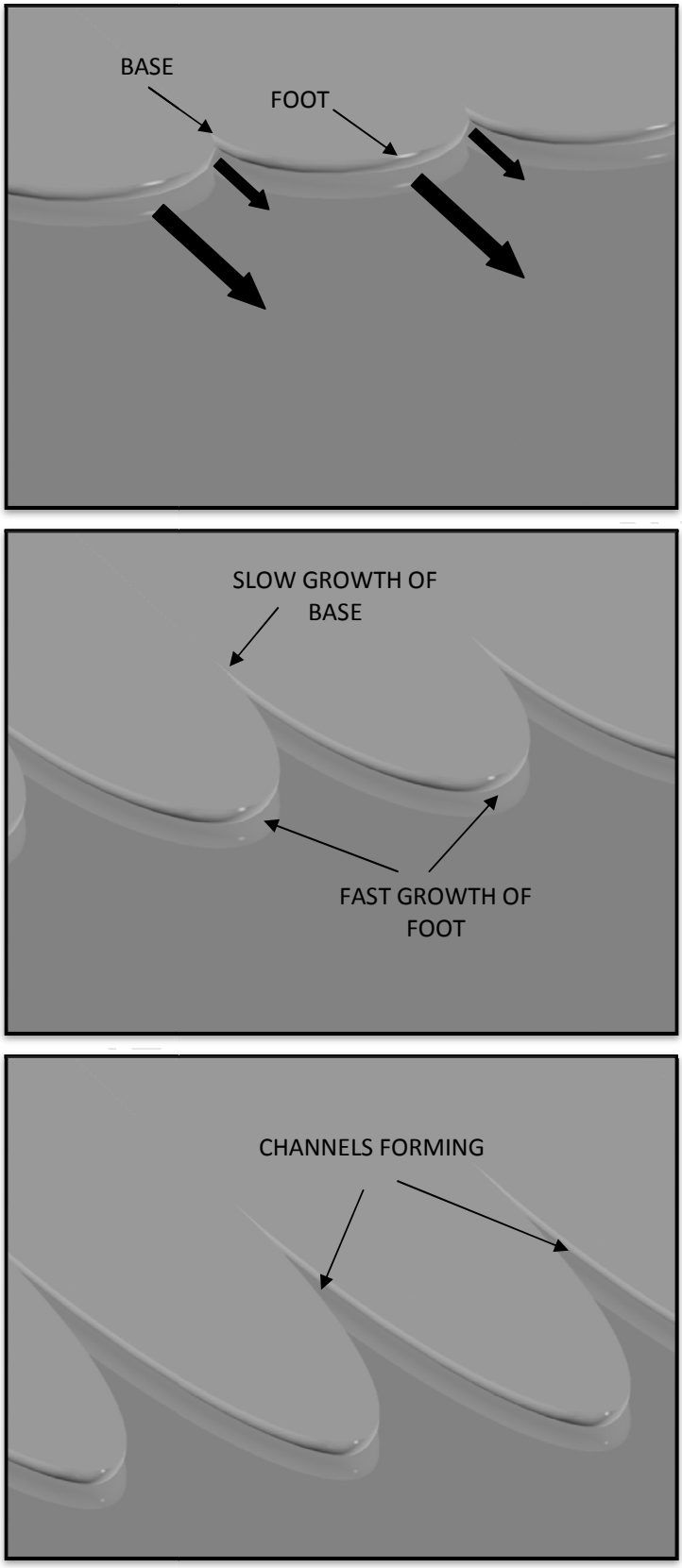


**Figure 4: Channel inclusions formed by growth of lobes on a crystal surface**

A number of papers have been written to investigate the influence of mechanical impacts on the growth of a crystal. Saito et al (1999) performed in situ tests on sodium chloride whereby a single crystal was contacted with a metal rod during growth. It was found that this contact sometimes enhanced the growth rate and the growth rate enhancement sometimes resulted in macrostep generation and subsequent inclusion. It was not indicated if the course of events following macrostep generation followed those described by Belyustin and Fridman (1968).

## 4.2 Prediction of inclusions and their impact on the product

Despite the lack of fundamental theoretical understanding of liquid inclusions, attempts have been made to find useable correlations and predictions. In tests performed by Saito et al (2000) it was found that the volume of type 1 liquid inclusion in NaCl in a suspension crystallization system increased according to the following equation

$$\boldsymbol{V = 4.0 \times 10^{-6} d^4} \quad (1)$$

where $V$ is the total volume of inclusions per crystal in μm$^3$ and $d$ is the crystal size in μm. It was also found that, when this laboratory data was extrapolated, it accurately predicted the results that were reported from plant data. This is interesting as the authors state that conditions, temperature, suspension density, supersaturation and agitation speed, for the plant data, were completely different to those in the laboratory. The authors use this to make the claim that this single correlation can be used to predict liquid inclusions in NaCl purely as a function of crystal size, regardless of operating conditions. They go further to show that the inclusions of the other crystals that were tested (KCl, succinic acid and potassium hydrogen phthalate) could also be roughly predicted by equation (1) (Saito et al., 2000). This is questionable as in the same report the difference in the amount of inclusions between agitated and non-agitated systems is discussed. This conclusion is contrary to what was suggested by Myerson (1977) who stated that, once NaCl crystals had grown beyond the critical point to allow inclusions to occur, the amount of inclusion was dependent on process variables like agitation rate, growth rate etc, and not on crystal size at all. This sort of disagreement is common within the literature and it indicates the variability of the systems and the complexity of the events taking place.

From the 4$^{th}$ order power law in Equation (1) it can be seen that the volume of liquid inclusion per volume of crystal increases as the crystal size increases. Whether or not the actual equation

is accurate is debatable, but this is a trend commonly observed in literature. Also it was found that there exists a minimum size below which liquid inclusions do not appear. It has been shown that there is a growth rate dependent critical crystal size beyond which the crystal surface becomes unstable (Chernov, 1963). This partially serves to explain why there exists a minimum crystal size before inclusions are found. This finding is supported by a number of other sources (Slaminko and Myerson, 1981; Brooks, Horton and Ferguson, 1968; Denbigh and White, 1966).

Type 2 inclusions, as discussed earlier, are inclusions that are trapped between agglomerating particles. It is generally understood that, as the number of constituent crystals in an agglomerate increases, the amount of included liquor increases too, and subsequently the purity of the product decreases. Saito et al (2001) argue, however, that liquid in agglomerates alone cannot be used to account for the decrease in overall product purity. Conditions that favour agglomeration may also favour the production of highly pure crystals. That is to say, conditions may result in type 2 inclusions due to agglomeration, but the individual crystals might be entirely free of type 1 inclusions. Thus, despite the fact that crystals are agglomerated, the overall purity is still high because the constituent crystals of the agglomerate are very pure. Thus, it is necessary to operate at conditions that minimise both type 1 and type 2 inclusions, noting that sometimes there are trade-offs that must be made between the two.



## 4.3 Isomorphous impurities

Isomorphous impurities are mixed crystals or solid solutions that have undergone isomorphous substitution. Isomorphous substitution is characterised by the random replacement of an ion within the macro-component by an 'impurity' ion, or micro-component (Figure 5). This phenomenon can be utilised to intentionally dope substances, as has been done in the past to give zeolites a number of variable properties (Aiello et al., 2005). In many applications however, this sort of impurity uptake is undesirable. These types of inclusions are believed to be influenced by a number of factors including chemical composition, solubility, interactions between particles and solvent, symmetry and parameters of the crystal lattice (Kirkova, Djarova and Donkova, 1996; Zhang and Grant, 1999). How these factors influence isomorphous substitution has not been conclusively determined from a sound theoretical perspective. However, findings indicate that most impurities found in crystalline products are as a result of these solid solutions as opposed to liquid inclusions (Zhang and Grant, 1999). This should not be interpreted as an absolute statement that applies to all systems however, but what must be

noted is that in systems as complex and varied as industrial brines there is a significant probability that solid solutions could occur.

Solid solutions in the form of metal alloys have been investigated at length in the past, but little research into the potential for salts to form solid solutions, especially in the case of polyatomic ions, could be found. The concept of isomorphous replacement, which appears to be identical to isomorphous substitution, is used frequently in gemmology, especially to explain the differences between stones within a single family, for example garnets.

It is generally understood that crystallization is an effective purification process because of the tendency for growing crystals to reject foreign particles. This is related to the large energetic penalties incurred when the structure of the crystal lattice is disrupted (Myerson, 2002). That is to say, it is thermodynamically favourable for a growing crystal to reject particles that do not form part of the natural crystal structure. However, crystal growth, which is a molecular recognition process, is not perfect and it is possible for foreign substances to be integrated into the crystal lattice. The frequency of this occurrence can be considered to be related to the degree of energetic disturbance that a foreign body in the lattice might cause and the concentration of the foreign body in the mother liquor. If a substance crystallizes from a solution containing a high concentration of a substance similar to one of the crystallizing substances, there is likely to be a large amount of isomorphous substitution. These similarities refer to issues pertaining to molecular volume, ionic radii and steric interactions (Myerson, 2002). In a system as varied as industrial brine there is much potential for some of the dissolved substances to be similar enough to the crystallizing substances such that molecular recognition fails and foreign particles are incorporated.

When crystallizing very slowly, such that the crystal and solution are close to equilibrium, the impurity in the product crystal can be calculated from

$$x_{sol} = K x_{liq} \tag{2}$$

Where $x_{sol}$ is the concentration of impurity incorporated into the crystal and $x_{liq}$ is the concentration of impurity in the mother liquor (Burton, Prim and Slichter, 1953). $K$ is referred to as the segregation coefficient and is essentially a means of relating the solubility of the impurity in the solvent to its solubility in the solid solute. For $K$ values less than 1, purification is achieved, and for values greater than 1, concentration of the impurity in the host is achieved (Myerson, 2002). Though this equation does well to illustrate the concept, industrial crystallizers operate well away from equilibrium, and this relationship would not be applicable. Other relationships have been developed to predict the quantity of isomorphous substitution, but these require knowledge of the heat of mixing within the solid phase. These can be

computed for simple crystal structures, but for the most part can be considered to be unavailable.

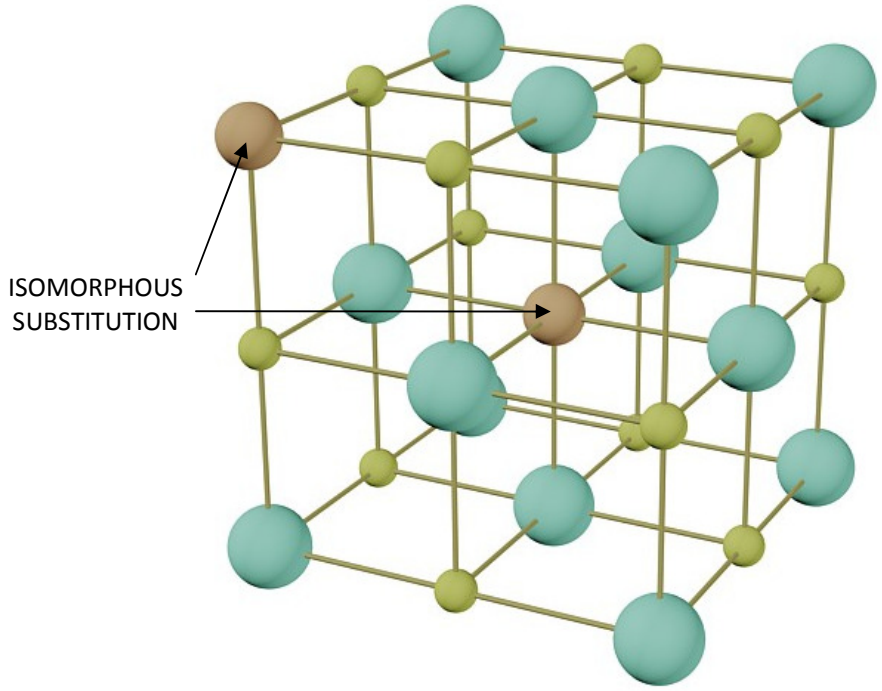


**Figure 5: Isomorphous substitution.**
**In isomorphous substitution, one ion within the crystal lattice is replaced by a different ion without disturbing the overall structure of the crystal. The substitution is random and does not represent any repeating pattern.**

### *4.3.1 Structural dependence of isomorphous inclusion*

It stands to reason that the more similar two crystalline structures are, the more likely they are to be interchangeable with one another. What is observed however is that the structure of the microcomponent adapts to suit that of the macro component (Kirkova, Djarova and Donkova, 1996). For example; $MgSO_4 \cdot 7H_2O$, $NiSO_4 \cdot 7H_2O$ and $ZnSO_4 \cdot 7H_2O$ have a rhombic structure, whereas $FeSO_4 \cdot 7H_2O$, $CoSO_4 \cdot 7H_2O$, $MnSO_4 \cdot 5H_2O$ have a monoclinic structure. Despite this however, these substances can form solid solutions by mutual substitution (Kirkova, Djarova and Donkova, 1996). It would seem that other factors are more important in determining isomorphous substitution than crystalline structure.

### *4.3.2 Temperature dependence of isomorphous inclusions*

The relative temperature dependence of the impurity's solubility in the host and the solvent is a factor when considering an impurity. The solubility of an impurity in the crystal, relative to its solubility in the mother liquor, may change with temperature. To achieve effective purification it is desirable that the impurity is freely soluble in the solvent at the operating temperature and insoluble in the host (Myerson, 2002). Given that EFC can operate over a range of temperatures within the metastable zone, this is a parameter that could potentially be utilised to influence product purity.

### *4.3.3 Effects of mass transfer on isomorphous inclusions*

The amount of isomorphous impurity found in the product crystal is, amongst other things, dependent on the concentration of the impurity in the mother liquor relative to the concentration of the host in the mother liquor. Since crystallizing ions are assimilated and foreign substances are rejected at the face of the growing crystal, a situation arises in which the concentrations of the impurities are raised locally around the crystals, see Figure 6. This increases the likelihood of impurities being incorporated into the crystal. This, however, is dependent on the width of the boundary layer around the crystals. In the case of a crystal left to grow in a non-agitated system the accumulation of impurities at the growing surface may be quite significant, resulting in measurable incorporation of impurities. In a vigorously agitated system the effects of mass transfer limitations are less likely as the impurities never accumulate at the growth surface. The effects of agitation on the system can therefore not be ignored and will have to be considered in the experimental stages. This area does pose some difficulty in that agitation in laboratory scale tests is usually much higher than that found at an industrial scale. All that can really be inferred from such tests is how sensitive a particular system is to mass transfer limitations, rather than accurate predictive correlations.

A further result of this accumulation is that there is a heterogeneous distribution of impurities in the crystal. The amount of impurity uptake by a crystal is dependent on the concentration of impurities at the growing surface. As the crystal grows, impurities are rejected and in a mass transfer limited system can accumulate around the crystal. Thus, over time, the concentration of impurities at the crystal surface increases and the concentration of impurities surrounding the crystal is constantly changing (Kirkova, Djarova and Donkova, 1996). Assuming that the impurity is being concentrated in the bulk as is the case in most crystallization processes, the concentration of the impurity within the crystal will increase radially from the centre out. However, as was discussed earlier, if the segregation coefficient, $K$, is greater than unity the

concentration of the impurity will actually decrease in the bulk and thus the concentration of the solid solution will increase towards the core of the crystal.

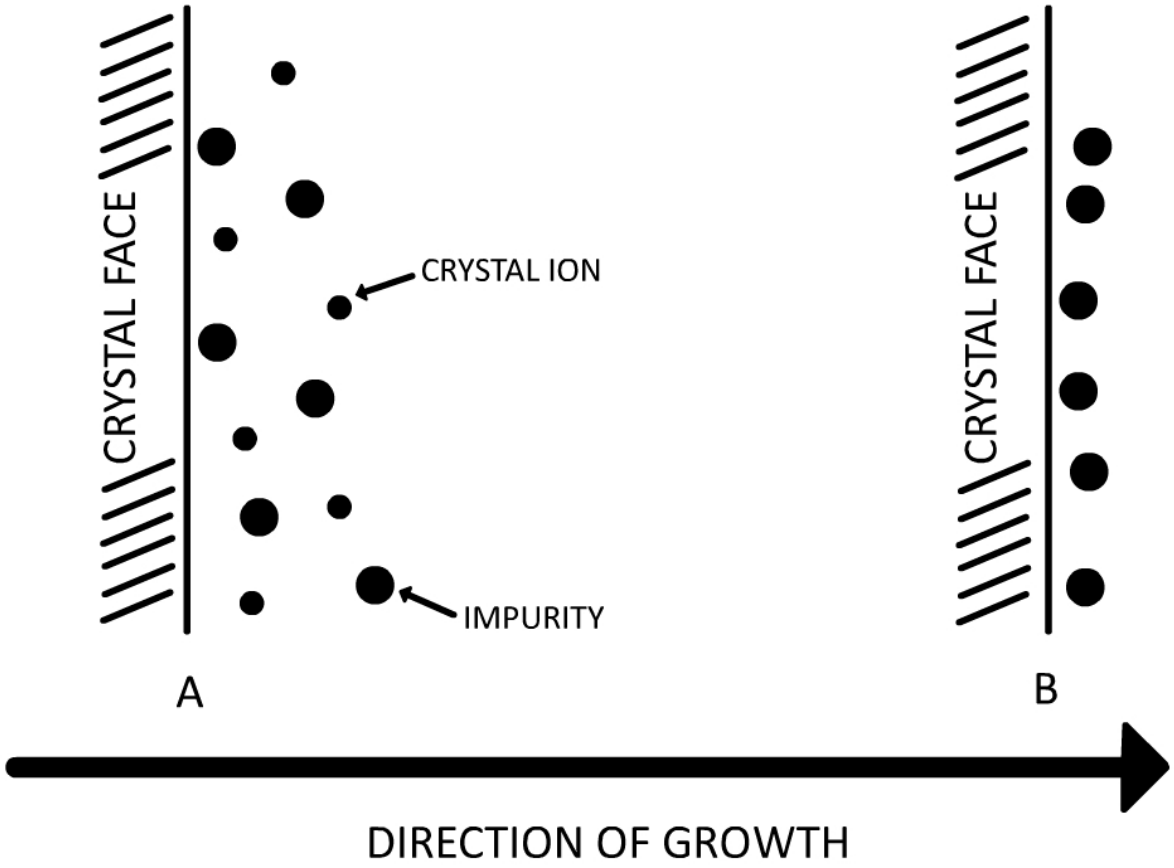


**Figure 6: Accumulation of impurities at the crystal growth face.**
**Adapted from Myerson (2002)**



### *4.3.1 Impact of growth or mass deposition rate on isomorphous inclusions*

During crystal growth, growth particles are subject to various orienting forces before being completely incorporated into the lattice (Myerson, 2002). Inorganic, ionic crystals grow under the direction of strong aligning forces and organic crystals usually grow under weaker ones. Stronger forces allow the growth unit to be more quickly oriented such that it can be properly positioned into the lattice. During rapid growth these units can be incorporated before they are properly oriented, resulting in irregularities and dislocations in the crystal. These conditions seem to provide additional sites that promote the uptake of impurities. This is in keeping with the convention that slower growth results in purer crystals.

# 5 Introduction to PGM brine

Preceding this research into impurities, a case study was done where EFC was applied to a PGM brine (Reddy and Lewis, 2009). In this work, a PGM brine was treated with EFC to produce sodium sulphate decahydrate ($Na_2SO_4 \cdot 10H_2O$). The experimental procedure and results are presented below.

## 5.1 Composition of the brine

Before the brine was treated with EFC, a compositional analysis was performed. The results are presented in Table 1.

### *5.1.1 Analytical techniques*

The following analytical techniques were used:

- The $HCO_3^-$ concentration was determined using titration (uncertainty of measurement: 7.6% to 9.3%).
- The $NO_3^-$ /$NH_4^+$ concentrations were determined using a cadmium reduction method with an AutoAnalyzer (uncertainty of measurement: 3.2% for $NO_3^-$ and 7.9% for $NH_4^+$).
- Inductively coupled plasma optical emission spectrometry (*ICP-OES*) was used in the analysis for all other the remaining ions (uncertainty of measurement ranged from 2.5% to 4.3%).

The PGM brine is both highly concentrated, and contains a large variety of dissolved components, shown in Table 1. The most prevalent ions are sodium, sulphate and chloride. This indicates that when processed through EFC, a large amount of sodium sulphate and sodium chloride are expected as products.

**Table 1: Composition of PGM brine**

| Species | mg/kg | | Species | mg/kg |
|---|---|---|---|---|
| Na | 75756 | | Si | 8 |
| Cl | 52889 | | Se | 775 |
| Ni | 14 | | Te | 2 |
| K | 256 | | Pt | 3 |
| Ca | 47 | | Pd | 0 |
| Fe | 0.2 | | Au | 0.3 |
| Cd | 0.3 | | Rh | 0.4 |
| Li | 36 | | Ru | 2 |
| $NO_3$-N | 2200 | | Ir | 0 |
| $NH_4$-N | 1008 | | Ag | 0.2 |
| $CO_3$ | 0 | | B | 0.9 |
| Mg | 27 | | As | 109 |
| $SO_4$ | 72870 | | P | 8 |
| $HCO_3$ | 3904 | | | |
| Temperature | 20˚C | | pH | 9 |



## 5.2 Application of EFC to brine

### *5.2.1 Experimental set-up*

The following is the experimental set-up as per Reddy and Lewis (2009). Batch test studies were carried out in a 1L jacketed, glass crystallizer. Agitation was achieved using an overhead stirrer connected to a 4-bladed impeller. The coolant, Kryo 45, was circulated through the jacket of the crystallizer and Wintherm Plus v2.2 was used to control the thermostat temperature and the pump flowrate. The 2000g brine solution was filtered prior to each experiment to remove any solids. The temperature of the solution contents was measured using the DataTaker DT80 Series 2 with CEM20 Channel Expansion Module connected to a temperature monitoring device, with Pt 100 thermocouples for accurate temperature readings. A Metro-ohm conductivity meter was used as an indication for salt and ice crystallisation. A 1˚C/hr cooling rate was employed.

The experiment was run in duplicate, with Experiment A only seeded with 5g $Na_2SO_4 \cdot 10H_2O$ at 14˚C. Experiment B was seeded with 5g $Na_2SO_4 \cdot 10H_2O$ seeds at 14˚C and 5g $Na_2CO_3 \cdot 10H_2O$ at

5˚C. The seeding protocol was carried out to selectively crystallise a specific salt. The experiment was run in duplicate to ensure a sufficient quantity of solution at the lower temperature ranges to produce $NaCl{\cdot}2H_2O$. However, the production of ice in the crystalliser reduced the quantity of solution to an impractical quantity at the very low temperature ranges (<-20˚C).

The salt produced was washed with a saturated solution of $Na_2SO_4$ at approximately 4°C. The ice crystals were washed with supercooled de-ionised water.

### *5.2.2 Results and discussion*

The temperature\concentration profile of the ionic species can be seen in Figure 7 and Figure 8. Between 20°C and 14°C, both figures show species changing concentration. This is not possible as no phase changes are occurring. All species should be straight, horizontal lines until the first phase change occurs at 14°C. This can only be attributed to analytical error.

Because the sample is highly concentrated in sodium sulphate, it begins to crystallize first at roughly 14°C. This is represented by the decrease in concentration of sodium and sulphate ions between 14°C and -5°C. It appears that chlorine ion concentration also decreases. Considering there are no chlorine salts produced at that temperature range. This extraction of chloride ions from the mother liquor could be attributed to chlorine adhesions onto the sodium sulphate crystals. Upon examining the washed sodium sulphate salt, the concentration of chloride ions is negligible (Figure 9). This seems to indicate that chloride was loosely bound to the surface of the salt crystals, in addition to liquid entrainment.

Below -5°C, ice begins to form. As the water is removed, as ice, the concentration of non-crystallizing ions increases. This can be seen in Figure 7 and Figure 8. Because sulphate ions are being consumed by the formation of sodium sulphate at the same rate at which ice is formed, the concentration appears to remain the same. Though sodium is also being consumed by the formation of sodium sulphate, it is present in excess, and thus is being consumed at a slower rate than that of ice formation. Thus, its concentration increases as ice is removed.

What is not expected, however, is the decrease in the concentration of selenium as sodium sulphate crystallizes, shown in Figure 8. No selenium salts are thermodynamically predicted and as such it is expected that selenium must be extracted along with the sodium sulphate somehow. This theory is further substantiated by Figure 9, where it can be seen that the selenium concentration is not affected by washing. This indicates that selenium is part of the sodium sulphate crystals.

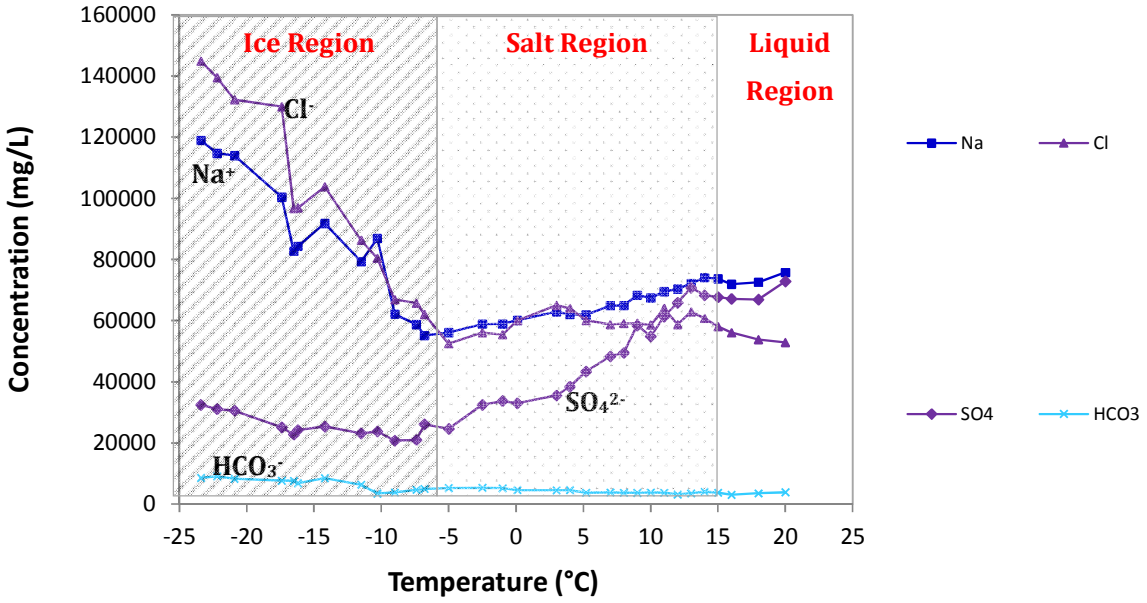


**Figure 7: Change in concentration of major ionic species with temperature for application of EFC to PGM brine**
**(Reddy and Lewis, 2009).**

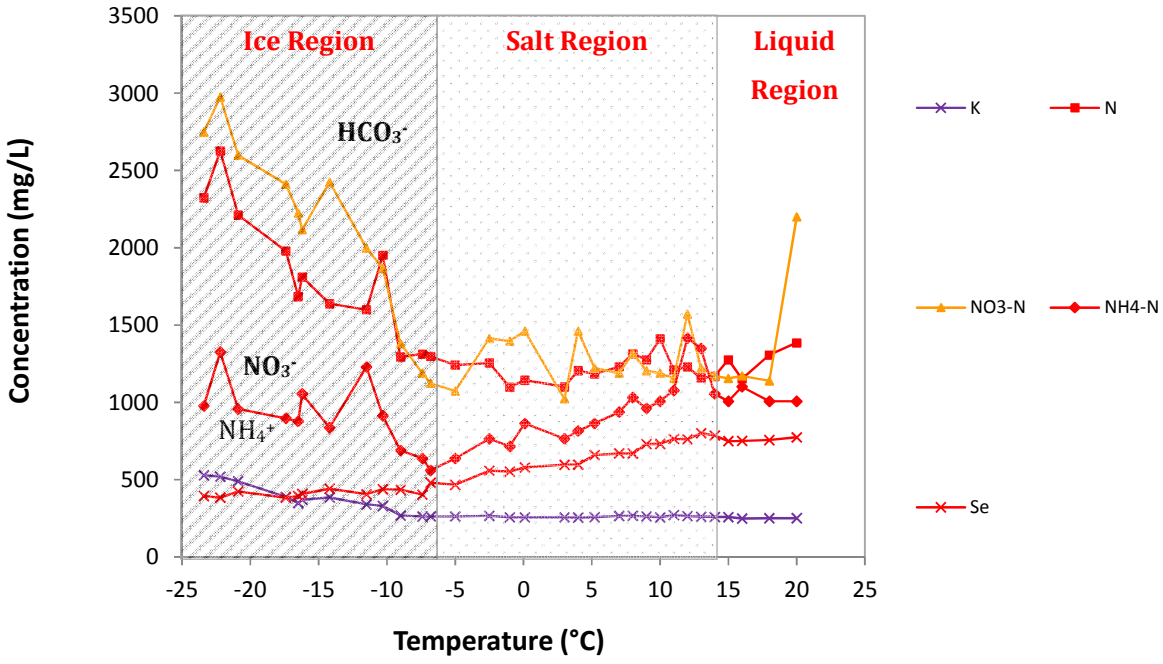


**Figure 8: Change in concentration of the minor impurities as a function of temperature for application of EFC to PGM brine**
**(Reddy and Lewis, 2009).**

A possible reason for this phenomenon included the possibility of liquid inclusions. Liquid inclusions are chambers of mother liquor within the crystal, as seen in Figure 10. This, however, cannot account for the decreasing selenium concentration in the brine as sodium sulphate is formed, or the high it's high concentration in the salt. It is thus concluded that, though liquid inclusion is a likely source of impurity, it alone cannot account for the uptake of selenium. This anomalously high selenium concentration is investigated in the following sections.

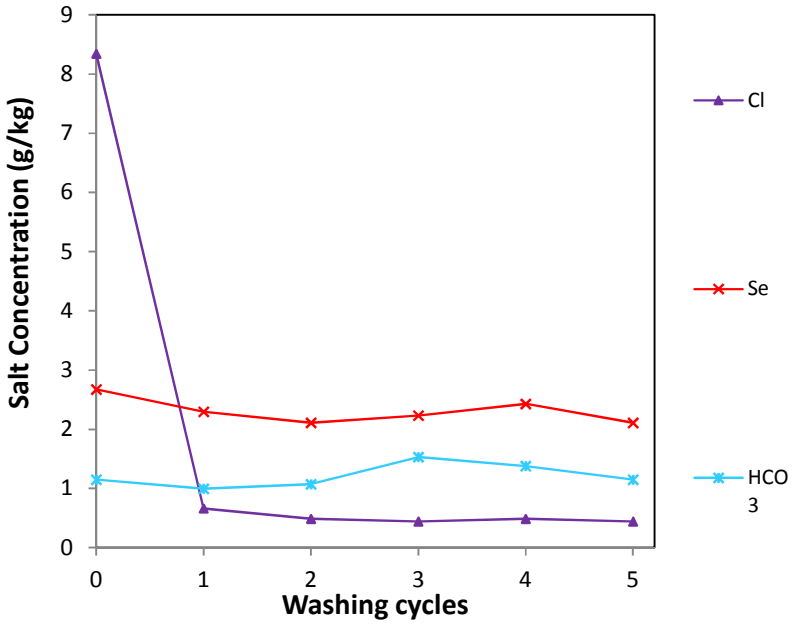


**Figure 9: Concentration of impurities on salt after successive washing (Reddy and Lewis, 2009)**

A complete overview of the impurities found in the product salt after washing can be seen in Figure 11. It is apparent that the major salt contaminations are $Cl^-$, Se, and $HCO_3^+$. Because chloride ions are present in high concentrations in the mother liquor, it is plausible that the chloride impurity can be accounted for by the presence of liquid inclusions. The bicarbonate impurity is considered to be benign in nature, and is thus will not be considered at this time. Selenium, however, could substantially limit the marketability of the sodium sulphate, and as such will be investigated further.

It does not appear that the wash solution was investigated in this study, as this information was unavailable.

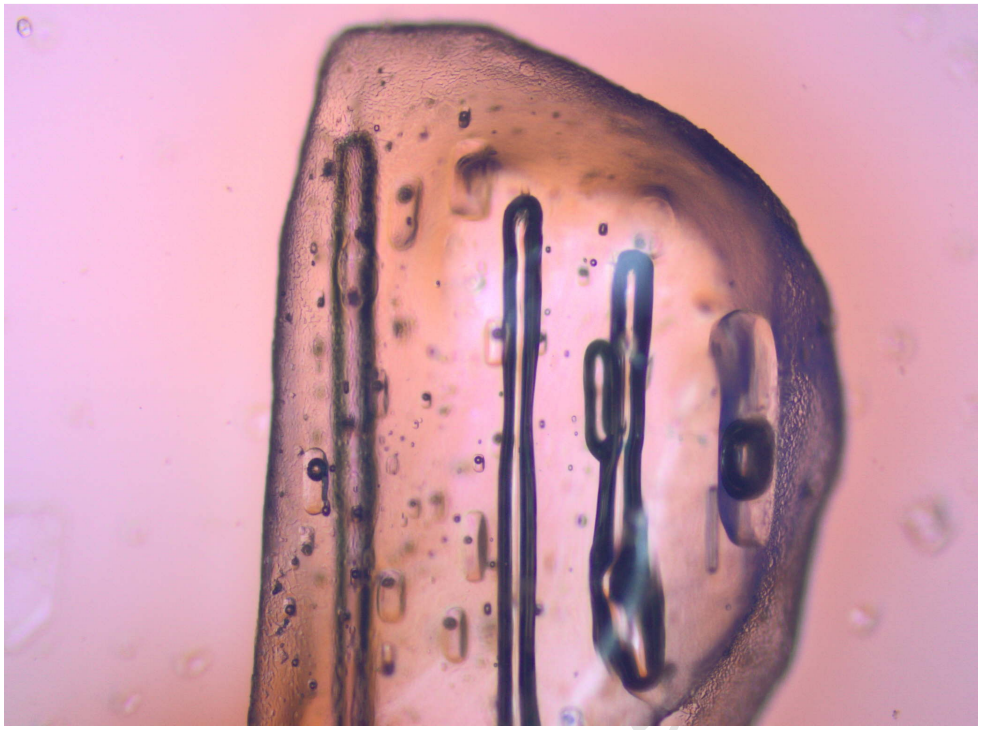

**Figure 10: Liquid inclusions inside sodium sulphate decahydrate crystal**
**For illustration purposes only. Not an actual crystal from PGM salt**

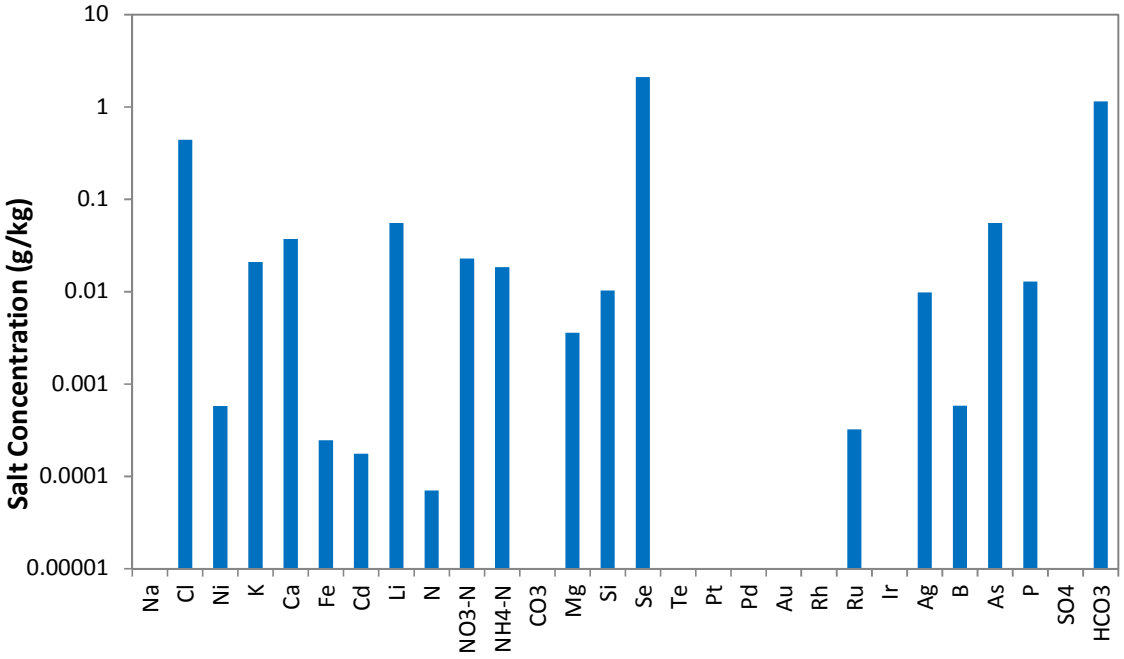


**Figure 11: Impurities present in the salt recovered at 0.1°C after 5 washes.**

(Reddy and Lewis, 2009)

## 5.3 Location of the selenium impurity

In order for liquid inclusions to be the only source of selenium impurity, the ratio of the non-crystallizing impurities relative to one another must be the same in both the mother liquor and the salt. Instead, a large amount of selenium is preferentially retained, as can been seen when Figure 12 is compared to Figure 13. This further indicates that liquid inclusions cannot be the only mechanism of impurity uptake.

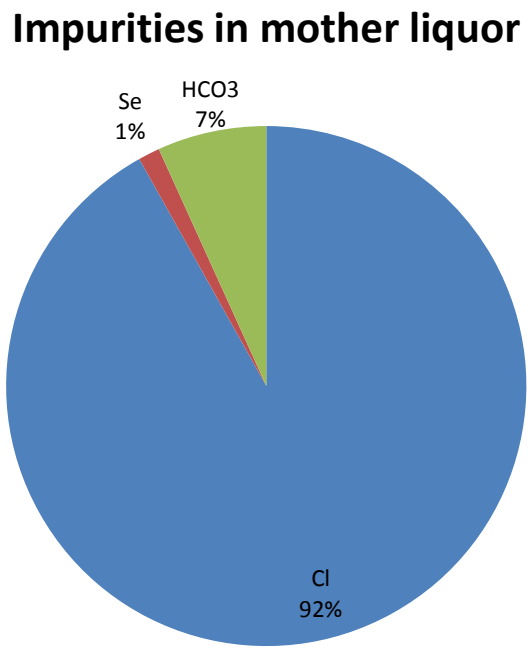


**Figure 12: Mass ratio of non-crystallizing components in PGM mother liquor. Not all brine components are included; only the most significant ones.**

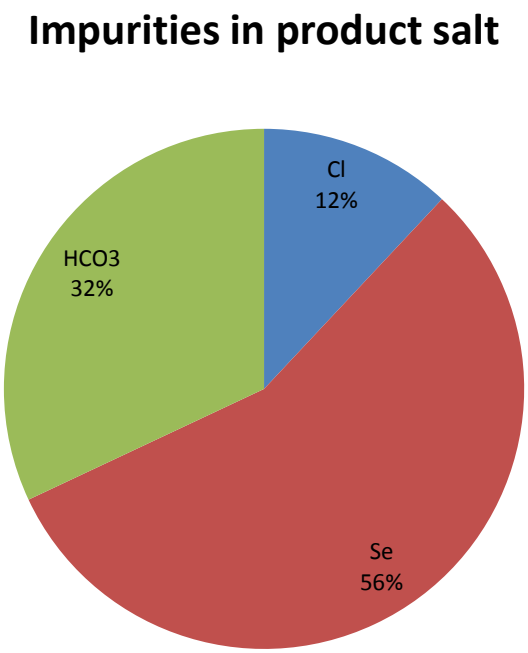


**Figure 13: Mass ratio of non-crystallizing components in PGM product salt. Not all components are included; only the most significant ones.**



Furthermore, from the analysis of the washing process in Figure 9, it can be deduced that liquid inclusions are not the most significant source of impurity uptake either. Figure 9 shows that the concentration of chloride decreases significantly after the first wash. This represents the mother liquor and being washed off the surface of the crystals. Before washing, the total amount of chloride can be assumed to be contributed by the sum of liquid entrainment and liquid inclusion. After the first wash however, the chloride level decreases noticeably and the remaining chloride is what is assumed to be contained within the liquid inclusions only. Considering that the mother liquor contains a high concentration of dissolved chloride, it is expected that it would be the most abundant impurity resulting from liquid inclusion. When considering the total impurity in the salt however, chloride is insignificant when compared to selenium. Selenium, however, has a comparatively low concentration in the brine. If liquid inclusions were the main source of impurity, the selenium concentration would have to be much less than that of chloride. Figure 12 and Figure 13 illustrate that this is not observed. From this it can be deduced that apart from not being the only source of impurity, liquid inclusions are not the most significant source of impurity either. The most likely potential source of impurity is believed to be isomorphous substitution.

## 5.4 Similarity between selenate and sulphate

From the findings in the work discussed in the previous section, it was hypothesized that selenate was isomorphously substituting for sulphate. This theory was premised on the fact that selenate and sulphate ions are very similar. The similarity between these ions is illustrated in work done for this project by Dr Gerhard Venter.

Modelling work was done using the Gaussian 03 Computational Chemistry Package (Gussian Inc, 2004).

"*Quantum chemical calculations were performed using the Gaussian 03 package. Geometries were optimised at the B3LYP/6-311+G(2df,p) level, followed by single point calculations at the CCSD(T)/aug-cc-pVTZ level. Molar volumes were calculated from the molecular volume of a single gas phase ion using the DFT charge density and a subsequent Monte-Carlo integration scheme, with a grid size of 100 points per bohr$^3$, up to an envelope size of 0.001 e/ bohr$^3$. The average over 100 evaluations was taken to minimise the error from the random integration. The two anions are compared based on their physical structure and shape as well as their electronic structure.*

*Both anions have a perfect tetrahedral shape with O-Se/S-O angles of 109.47°. Selenate has Se-O bond lengths of 1.669 Å, whereas the S-O bonds in sulphate are much shorter, 1.509 Å. The shorter bonds of the latter leads to a smaller volume of the $SO_4^{2-}$ anion, as reflected by the calculated molar volume of 58 cm$^3$/mol, versus the $SeO_4^{2-}$ volume of 63 cm$^3$/mol.*

*For sulphate, Mulliken charges are 2.000 e on the sulphur and -1.000 e on the oxygen atoms. The selenate anion has a higher positive charge on the selenium, 2.2470 e, which then leads to the oxygens having a higher negative charge of -1.062 e. The effect of this charge partitioning is reflected in the electrostatic potential, shown below, mapped to a 0.001 e/bohr$^3$ isodensity surface. The scales in both images are similar with red mapped to -0.385 au and blue to -0.335 au (and white, the midpoint, at -0.360 au). The band of highly negative potential around the S-O bonds in sulphate is likely due to the smaller size of the anion."*

– End of Dr Gerhard Venter's work

This research indicates that the molar volumes of sulphate and selenate are within 10% of each other. This is in agreement with literature values as to the acceptable tolerance for isomorphous substitution to occur. In addition to this, the model reveals that the sulphate and selenate ions are structurally very similar in that they have identical bond angles. This minimises disruption of the crystal lattice in the event that selenate is incorporated into the lattice. The less of a

disturbance that a guest molecule has on the structure of the crystal, the more likely it is to be incorporated. Though electrostatic potential is given by the model, it is not known to what tolerances electrostatic properties must fall to allow for isomorphous substitution to occur.

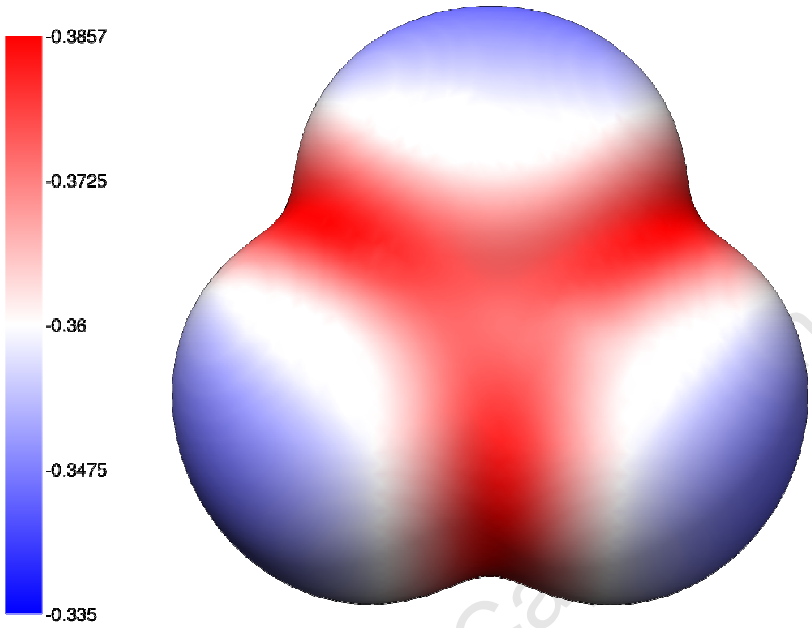


**Figure 14: Electrostatic potentials of sulphate, mapped to a 0.001 e/bohr3 isodensity surface (Dr Gerhard Venter)**

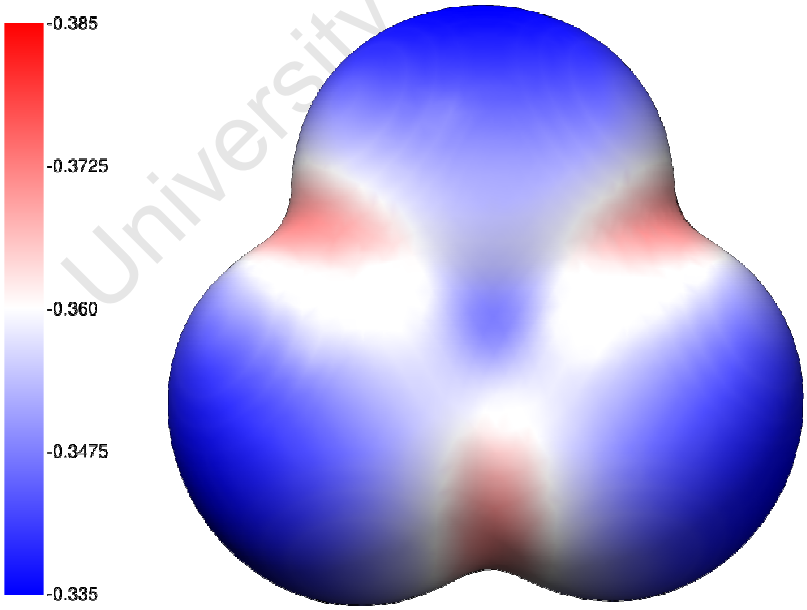


**Figure 15: Electrostatic potentials of selenate, mapped to a 0.001 e/bohr3 isodensity surface. (Dr Gerhard Venter)**

# Experimental Investigations into Impurities in EFC

## 6 Further investigation into selenium impurity of PGM brine

### 6.1 Nature of selenium impurity; selenate or selenite

The exact nature of selenium in the mother liquor must be verified. It is not clear from the previous investigation what form selenium is being incorporated as. It is unlikely that selenium is present in the brine in an unoxidised state. The two likely possibilities are that selenium is present in either selenite form (4+ oxidation state) or selenate form (6+ oxidation state). Due to the structural similarity between selenate and sulphate ions it is expected that the selenium is in selenate form. The more similar an ion is to another, the more likely it is to be incorporated as a foreign body. This would help to explain the presence of the selenium impurity in the sodium sulphate salt product. The possibility that the selenium exists as selenite cannot be ignored however, and must be investigated further. It is therefore necessary to establish the different influence that selenite and selenate have on the purity of the product salt.



#### *6.1.1 Experimental*

The experiment consisted of a number of separate beaker tests in which a standardised solution containing sodium sulphate and sodium chloride was doped with varying amounts of sodium selenate or sodium selenite. If there is a different uptake of selenium when selenate was present as opposed to when selenite was present, conclusions about the nature of the selenium impurity can be made. The concentrations of sodium chloride and sodium sulphate in the synthetic test brine were made to be the same as those in the original PGM brine. Other components in the PGM brine, at this stage of the investigation, were assumed to have a negligible impact on the product purity and were not included in the synthetic test brine.

The separate beakers were cooled in order to crystallise the sodium sulphate. The crystals were then filtered and dried in an oven and analysed by ICP-OES for concentrations and selenium. If the amount of selenium found in the salts was different for samples containing selenate compared to those containing selenite, conclusions can be made as to the nature of the selenium impurity found in the original brine.

### Solution Preparation

A standard solution containing 90 g/l NaCl and 110 g/l $Na_2SO_4$ was made. One batch was enough to supply all the individual beaker tests. Separate solutions containing 150 g/l $Na_2SeO_4$ and 150 g/l $Na_2SeO_3$ were also made. These were also enough to supply the entire experiment. All solutions were made with 18MΩ.cm water, and Merck laboratory grade chemicals.

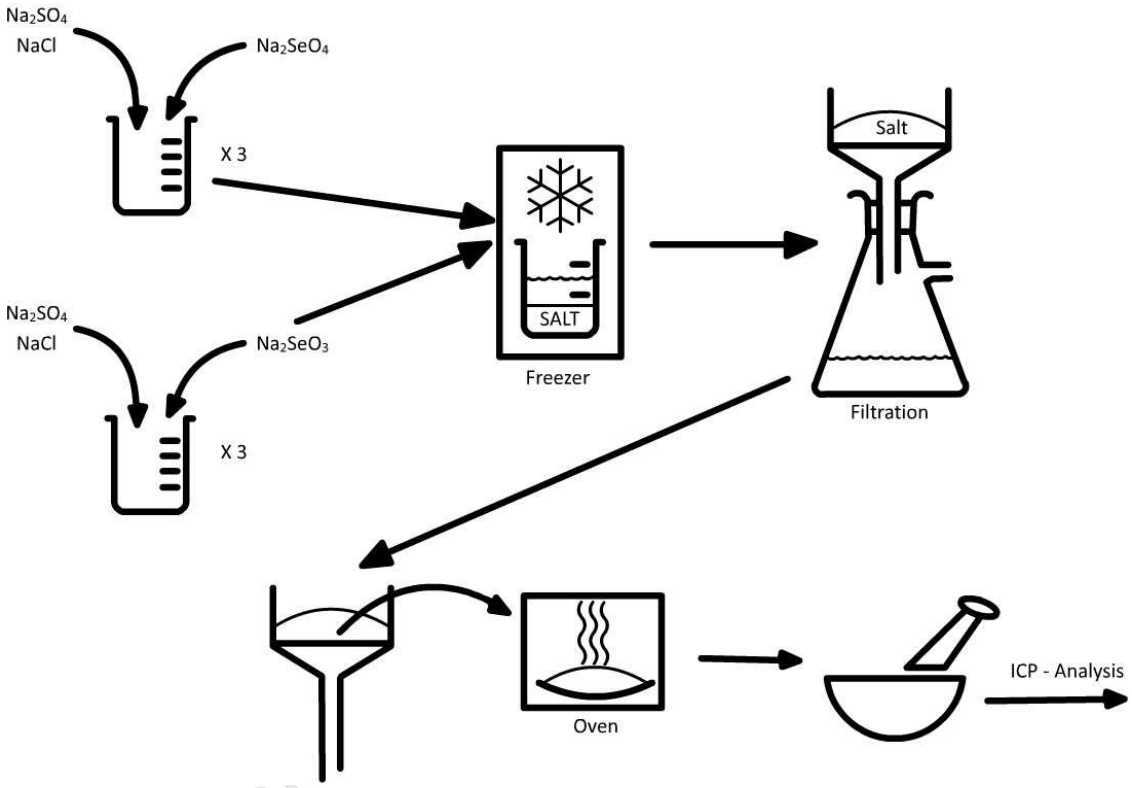


**Figure 16: Experimental procedure for determining nature of selenium in mother liquor**

**Table 2: Concentrations of sodium selenate or sodium selenite in beaker tests**

| Batch | Concentration (g/l) |
|---|---|
| 1 | 1.00 |
| 2 | 1.30 |
| 3 | 1.60 |
| 4 | 1.90 |
| 5 | 2.20 |

**Procedure (See Figure 16)**

An experimental matrix is presented in Table 8 in the appendix. A 200 ml volume of the $NaCl/Na_2SO_4$ solution was pipetted into each beaker. The necessary quantity of $Na_2SeO_4$ or $Na_2SeO_3$ was then pipetted into the beakers. The change in volume due to the addition of $Na_2SeO_4$ and $Na_2SeO_3$ was considered to be negligible. The largest volume change as a result of the addition was less than 1.5%. Each individual beaker test was repeated three times. The concentrations of $Na_2SeO_4$ and $Na_2SeO_3$ can be found in Table 2. Note that each concentration was done for both sodium selenate and sodium selenite. Thus there was a total of 10 different compositions, each repeated 3 times, for a total of 30 runs.

The experiment was randomised by swapping the beakers between different magnetic stirrers. Since each magnetic stirrer was placed at a different area in the temperature controlled room, the possibility of localised temperature differences was accounted for. Additionally, each group of three selenate containing beakers was placed in the temperature controlled room along with the corresponding selenite containing beakers. The three stirrers used for the selenate experiments in one run were then used for the selenite experiments in the next run, and vice versa. Refer to the experimental matrix in Table 8 of the appendix for details further details on how the beakers were randomised on the stirrers.

The beakers were then placed in a temperature controlled room at -3.5°C and stirred with magnetic stirrers. This temperature was chosen because at this point, most of the sodium sulphate is crystallized out of solution. For reasons of space and practicality, only six beakers were cooled at a time. The beakers were left at this temperature for 4 hours. This time was chosen as it was found to be a sufficient time for the solution to equilibrate at -3.5°C. It is important to note that temperature controlled rooms have defrost cycles. For this experiment, the scheduling of this cycle was known, and 4 hour long experiments could be fitted in between each defrost period. After 4 hours, the salt from each beaker was thoroughly filtered, but not washed, and placed in an oven to dry.

It was decided not to wash the crystals to prevent error. If the crystals were washed, the wash would be done with a saturated solution of sodium sulphate. While washing with a saturated solution it is possible, if the salt and wash solution are not at exactly the same temperature, that the sodium sulphate would crystallise on the cold crystal surface, or possibly partially melt the crystal. Because the concentration of selenium in the brine is low, surface liquid entrainment would not have resulted in a significant contribution to the selenium impurity value. It is known that by not washing, there may be entrained liquor on the surface, but this is believed to result

in a more consistent error than if washing was implemented, for the reasons discussed above. Thus, the experiments could be more effectively compared, and the trends observed.

The purpose of the drying is to prevent analytical inaccuracies caused by the unpredictable decay of the decahydrate to the anhydrate form of sodium sulphate. The oven melts the sodium sulphate decahydrate and then drives off the water. In the absence of water and at the higher temperature, all sodium sulphate recrystallises in the anhydrous form. After the drying process the crystals were ground up in a pestle and mortar and sent to be analysed externally by ICP-OES, for selenium content.

### *6.1.2 Results and discussion of selenate vs selenite*

It must be noted that beakers in a temperature controlled room are not a precise means to control temperature. In the previous work discussed in section 5.2, experiments were carried out in jacketed reactors. For this experiment it was decided that this was not necessary, because only the broad trend was desired as a result and precise temperature control would have been superfluous. It can be seen in Figure 17 that difference between selenate and selenite results is very large, and the trend is clearly visible. Additionally, unlike the experiment described in section 5.2, these experiments were not seeded. It was found, in work undocumented here, that seeding did not have a significant impact on selenium uptake by sodium sulphate. As such, seeding was not implemented here.

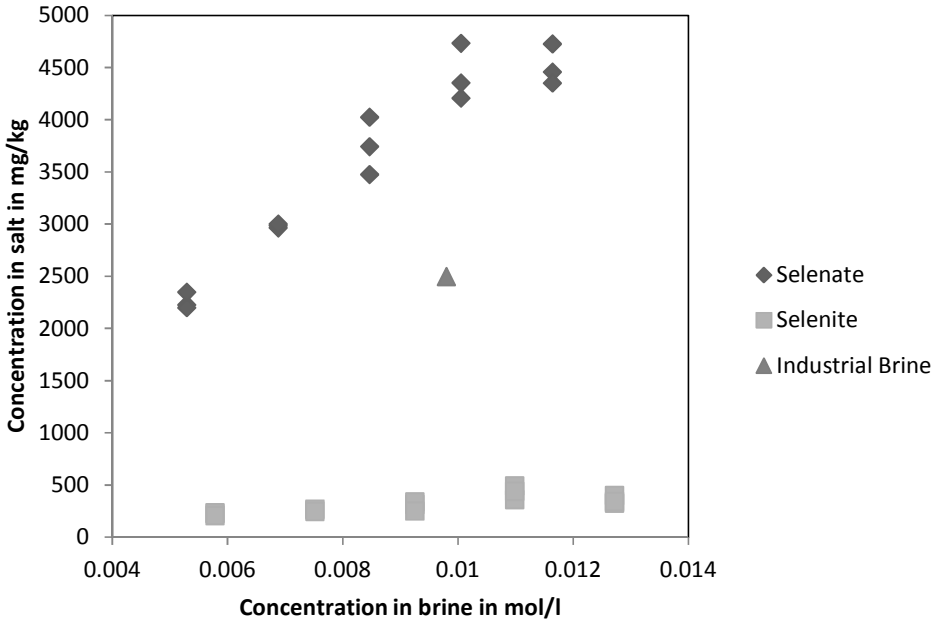


**Figure 17: Comparison between uptake of selenate and selenite by sodium sulphate (n=3) (Raw data in Table 9 and Table 10 in appendix)**

The purpose of this experiment was to verify that the selenium in the brine is in the form of selenate ions and that this is the cause of the selenium uptake. A results table can be found in Table 9 and Table 10 in section 11.1 of the appendix. Figure 17 displays that selenate is absorbed far more preferentially than selenite. Additionally, the selenate values are comparable to the results from the actual industrial brine tests, discussed in section 5.2, and shown in Figure 17. The selenite values, however, are an order of magnitude different to the results from the industrial. In the actual brine, a concentration of roughly 108 g/l of sodium sulphate, 90 g/l sodium chloride and 775 mg/l selenium produced an impurity of 2-3 g/kg of selenium in the sodium sulphate salt product. Though this result was not exactly matched in the experiment, it can be seen that the selenate values fall within the same orders of magnitude as the values found in the industrial brine.

Figure 17 displays that selenate ions are preferentially incorporated over selenite ions. When the source of selenium in the brine was selenate, far more selenium was incorporated than when the source was selenite. This supports the theory that the similar nature of selenate and sulphate ions is the main reason for the selenium inclusion. It is likely that the selenite ions were rejected to a greater degree than selenate ions because of their large difference to sulphate ions. For example, sulphate and selenate ions are tetrahedral, whereas selenite ions are pyramidal. Incorporation of selenite ions would disrupt the crystal lattice of sodium sulphate crystals far more than selenate.

Another factor to consider is that sodium sulphate and sodium selenate form decahydrates at low temperatures, whereas sodium selenite forms a pentahydrate at low temperatures. This further serves to explain the compatibility of sodium sulphate with selenate, and its incompatibility with selenite.

As can also be seen in Figure 17 that the selenium uptake in the case of the industrial brine was not exactly replicated by the experimental brines. The solution containing only selenate resulted in selenium incorporation greater than that seen in the industrial brine, and vice versa for the solution containing only selenite. Though this can possibly be attributed to the differing crystallization rates between the industrial brine and the synthetic brine, it is also possible that the industrial brine contains selenium in both the selenate and selenite forms. Both selenate and selenite contribute to the total selenium concentration reported in the brine, but only the selenate has a significant impact on the purity of the product. In this way the selenium impurity in the sodium sulphate could vary by changing the concentrations of sodium selenate and sodium selenite without changing the total selenium concentration.

Because selenate results in a much greater impurity uptake than selenite, it can be concluded that in terms of impurity inclusion, the selenate ion is of greatest interest. For this reason the selenium in the synthetic brines of further experiments will be in the form of selenate ions, contributed as sodium selenate.

### *6.1.3 Thermodynamic modelling*

In order to investigate if a separate selenium salt is being produced, it is necessary to thermodynamically model the system.

The thermodynamic modelling was carried out using OLI Stream Analyser (OLI Systems Inc, 2008) which uses the revised Helgeson-Kirkham-Flowers (HKF) model for the calculation of standard thermodynamic properties of aqueous species and the frameworks of Bromley, Zemaitis, Pitzer, Debye-Huckel, and others for the excess terms. A number of thermodynamic models are available in OLI (OLI Systems Inc, 2008), but what was selected for use was the Mixed Solvent Electrolyte (MSE) model. It uses a true speciation model capable of reproducing speciation, chemical, and phase equilibria. It is applicable to complex, multicomponent, water-organic-salt systems over a full range of concentrations and at temperatures below 0°C (OLI Systems, 2011). This makes this package the best suited for the modelling of complex industrial brines under eutectic conditions.

The MSE model makes use of the Helgeson-Kirkham-Flowers equation of state to calculate the standard Gibbs free energy of formation. This equation of state predicts thermodynamic properties as functions of seven terms. These terms are integration constants for heat capacity ($C_1$, $C_2$), volume ($a_1$, $a_2$, $a_3$, $a_4$) and temperature and pressure properties of water (ω). R and 0 represent reference and standard state properties respectively.

$\overline{H_i^0} = \overline{H_i^R} + f_{Hi}(a_1, a_2, a_3, a_4, c_1, c_2, \omega,)$.....Partial molal enthalpy

$\overline{G_i^0} = \overline{G_i^R} - \overline{S_i^R}(T - T^R) + f_{Gi}(a_1, a_2, a_3, a_4, c_1, c_2, \omega,)$.....Partial molal Gibbs free energy

$\overline{S_i^0} = \overline{S_i^R} + f_{Si}(a_1, a_2, a_3, a_4, c_1, c_2, \omega,)$.....Partial molal entropy

$\overline{Cp_i^0} = \overline{Cp_i^R} + f_{Cpi}(a_1, a_2, a_3, a_4, c_1, c_2, \omega,)$.....Partial molal heat capacity

$\overline{V_i^0} = \overline{V_i^R} + f_{Vi}(a_1, a_2, a_3, a_4, c_1, c_2, \omega,)$.....Partial molal Entropy

The standard Gibbs free energy of formation is then used to calculate the activity coefficient of each species. A complete explanation of the working of the model can be found in Liu and Papangelakis (2005)

The results from modelling the cooling of the synthetic brine are presented in Figure 18. The concentrations of the components in the modelled brine are shown in Table 3. The sodium selenate line represents zero values. Thus model illustrates that no selenium salt is predicted from the EFC of the PGM brine. Any selenium found in sodium sulphate product must then be included by a different mechanism.

**Table 3: Concentration of components in simulated brine**

| Component | Concentration (g/l) |
|---|---|
| $Na_2SO_4$ | 110.6 |
| NaCl | 87.1 |
| $Na_2SeO_4$ | 1.9 |

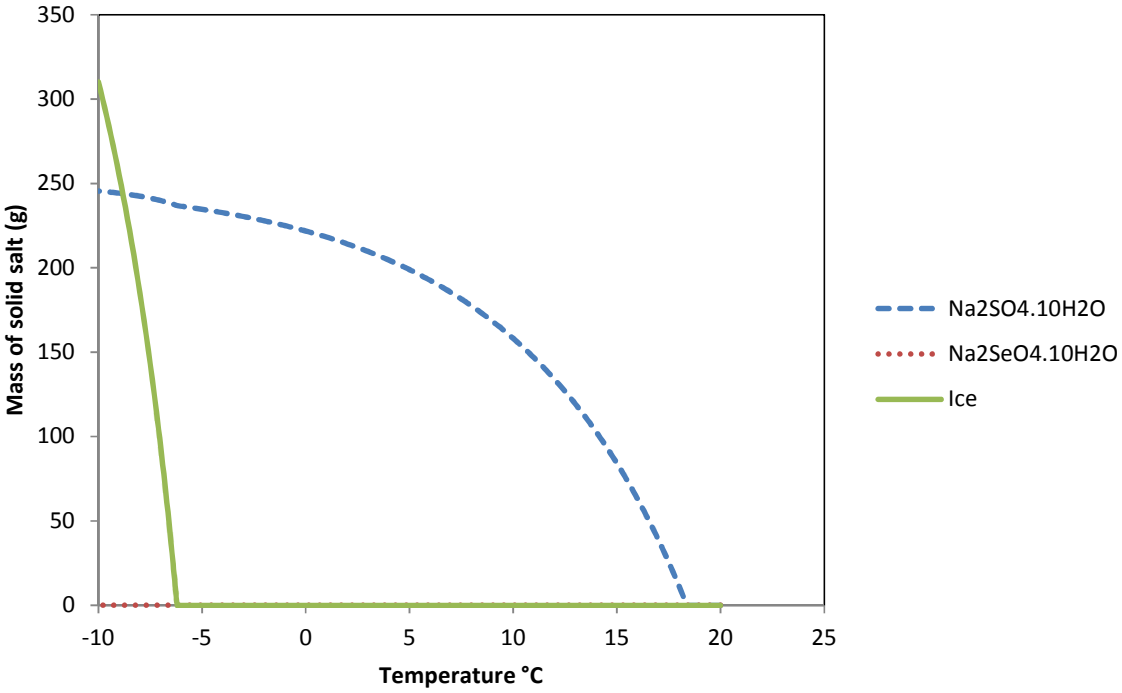


**Figure 18: Solids produced by OLI simulation of cooling of 1 litre of synthetic brine. The concentrations of the components can be found in Table 3.**

## 6.2 Relationship between NaCl, $Na_2SO_4$ and $Na_2SeO_4$ on inclusion of selenium in salt

It has been found that the presence of sodium sulphate and sodium selenate alone is not sufficient to explain the concentration of selenium in the product salt. In informal work done for

this project, but not documented, all instances where sodium sulphate decahydrate ($Na_2SO_4 \cdot 10H_2O$) was crystallized out of solutions containing only sodium sulphate and sodium selenate, the selenium impurity was far below what was detected in the salt from the PGM brine. It is therefore necessary to investigate the impact of other ions in the mother liquor on the purity of the product.

The most likely aqueous component in the industrial brine sample to have an impact on the uptake of selenium is sodium chloride. This is for two reasons; firstly, sodium chloride is the most prolific salt in the brine, on a molar basis. Additionally, it shares the common sodium ion with sodium sulphate and sodium selenate, which is likely to impact on the product salt.

### *6.2.1 Experimental*

To understand the impact of NaCl on the selenium incorporation in the product salt, an experiment was devised to explore the relationship between NaCl, $Na_2SO_4$ and $Na_2SeO_4$. This was done with a number of beaker tests, where sodium sulphate decahydrate was crystallised from solution with varying concentrations of sodium sulphate, sodium chloride and sodium selenate. The purpose of this experiment was to establish if there is a correlation between the concentration of sodium chloride and selenium uptake.



**Solution Preparation**

Standard solutions of NaCl, $Na_2SO_4$ and $Na_2SeO_4$ were made using purified water of 18MΩ.cm. The concentrations of the solution can be found in Table 4. The standard solutions were highly concentrated solutions so that the necessary concentrations could be achieved in the brine once all the solutions were combined.

**Procedure (See Figure 19)**

The required volume of each solution was pipetted into each beaker. Once all the solutions were added, each beaker was topped up with 18MΩ.cm water until the 200 ml mark was reached. For a complete list of concentrations and volumes added consult Table 11 in the appendix. All chemicals were Merck Laboratory grade.

**Table 4: Concentrations of standard solutions**

| Salt | Concentration (g/l) |
|---|---|
| $Na_2SO_4$ | 170 |
| NaCl | 300 |
| $Na_2SeO_4$ | 150 |

The 200 ml brine samples were placed in a freezer room at -3.5°C and the sodium sulphate decahydrate was allowed to crystallise. This temperature was chosen because at this point, most of the sodium sulphate is crystallized out of solution. The samples were left in the freezer for 4 hours. This time was chosen as it was found to be a sufficient time for the solution to equilibrate at -3.5°C. It is important to note that temperature controlled rooms have defrost cycles. For this experiment, the scheduling of this cycle was known, and 4 hour long experiments could be fitted in between each defrost period. For purposes of practicality only 6 brine samples were placed in the freezer at once. The crystals of each sample were filtered thoroughly, but not washed. This was to prevent error resulting from inconsistent washing from sample to sample.

It was decided not to wash the crystals to prevent error. If the crystals were washed, the wash would be done with a saturated solution of sodium sulphate. While washing with a saturated solution it is possible, if the salt and wash solution are not at exactly the same temperature, that the sodium sulphate would crystallise on the cold crystal surface, or possibly partially melt the crystal. Because the concentration selenium in the brine is low, it is believed that this would have introduced a greater error than leaving the crystals unwashed.

The filtered crystals were placed in an oven and dried at 35°C. At this temperature the sodium sulphate decahydrate melts. The water in the melt is driven off and all of the salt recrystallizes in the anhydrous form. The anhydrous salt is ground in a pestle and mortar and sent to an external laboratory for analysis by ICP-OES of selenium content.

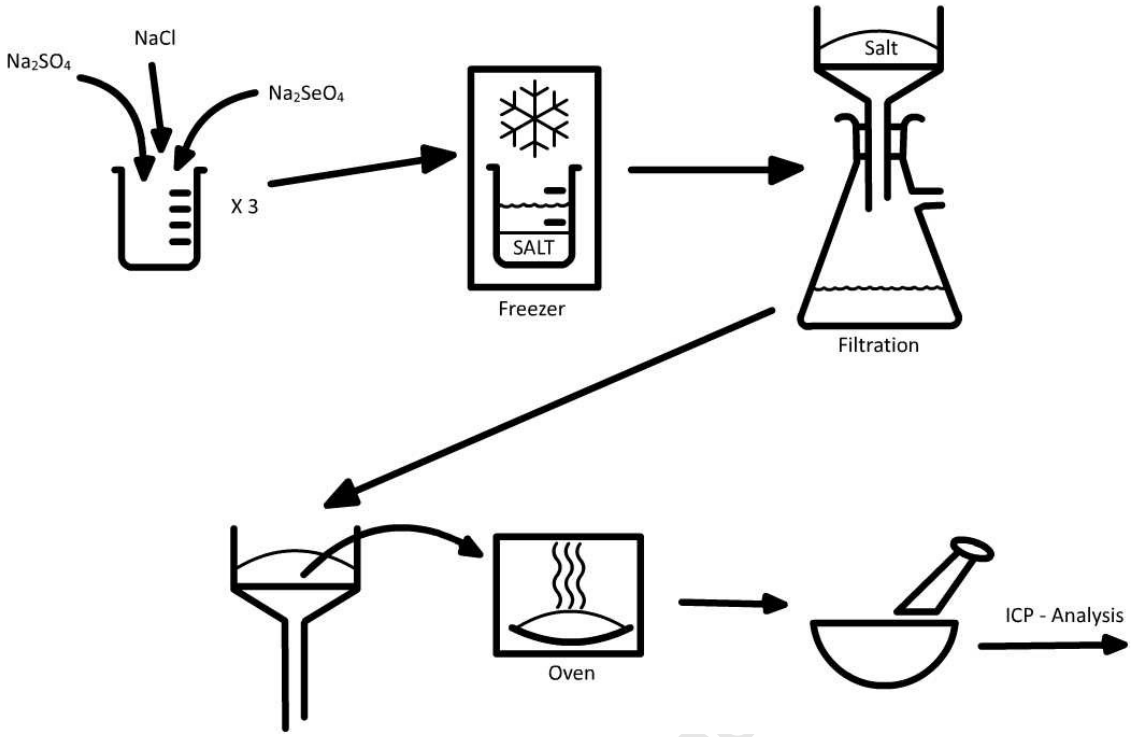


**Figure 19: Experimental procedure for the investigation into the relationship between $Na_2SO_4$, NaCl and $Na_2SeO_4$**

### *6.2.2 Experimental Results and discussion*

A table of results can be found in Table 12 in section 0 of the appendix. Figure 20 shows the impact of $Na_2SO_4$ concentration on the inclusion of selenium in the sodium sulphate salt product. The horizontal axis displays the concentration of sodium selenate in the mother liquor. The vertical axis represents the mass of selenium detected in the product salt. The legend to the right describes the concentrations of NaCl and $Na_2SO_4$ in g/l in the mother liquor. For example, the first entry reads 30 and 90. This means that the mother liquor had a sodium sulphate concentration 30 g/l and a sodium chloride concentration of 90 g/l.

Figure 20 shows that as the concentration of sodium sulphate decreases, the concentration of selenium in the product salt increases. This is because when the selenium concentration in the brine is kept constant and the concentration of sodium sulphate is decreased, it is the same as increasing the amount of selenium relative to sodium sulphate.

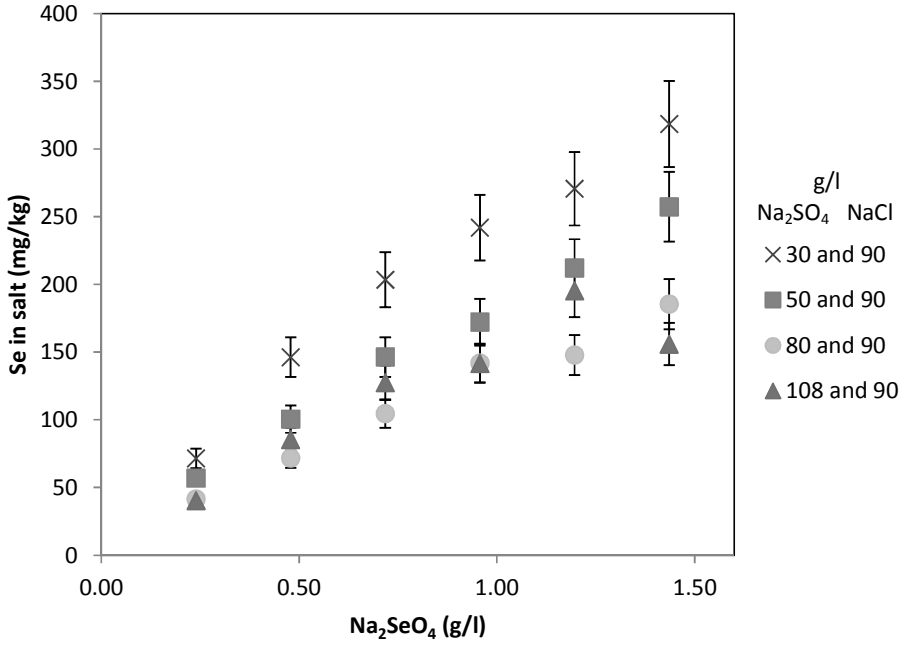


**Figure 20: Effect of varying concentration of $Na_2SO_4$ on the inclusion of Se in product sodium sulphate salt (n=1) (Raw data in Table 12 in the appendix)**

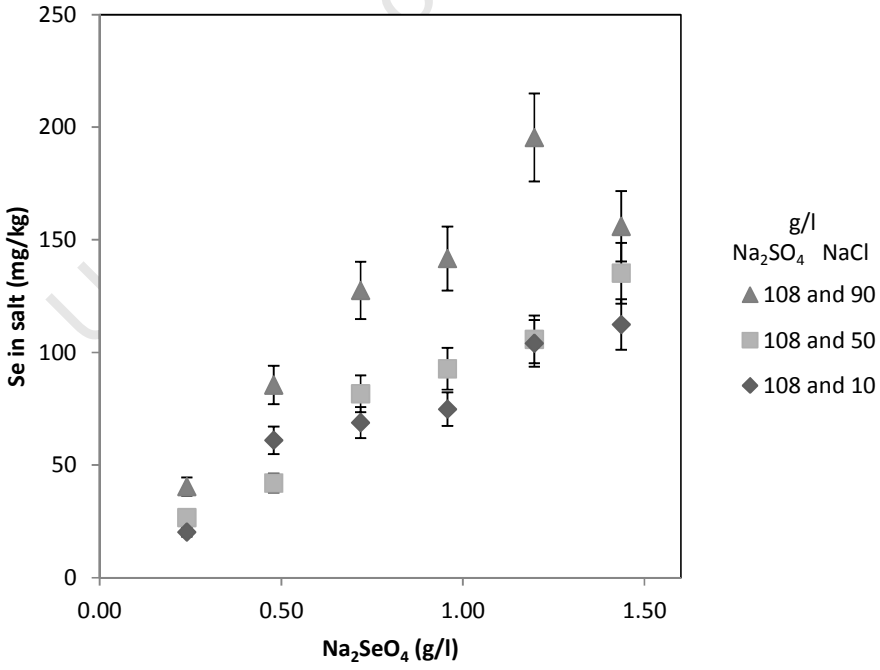


**Figure 21: Effect of varying concentration of NaCl on the inclusion of Se in product sodium sulphate salt (n=1) (Raw data Table 12 in the appendix)**

Figure 21 displays that an increase in the concentration of sodium chloride relative to sodium sulphate and sodium selenate results in an increased amount of selenium in the salt product. In this experiment, the data points are erratic, but still illustrate the trend effectively. This erratic behaviour is further discussed in section 6.3. The common sodium ion serves to decrease the solubility of sodium sulphate. Thus, for a fixed cooling rate, the rate of crystallization will increase with the addition of sodium chloride. As has already been theorised, an increased crystallization rate could result in an increased selenium uptake. This occurs because at faster crystallization rates the molecular recognition process is more prone to failure. That is to say; the growing sodium sulphate crystal is more likely to mistaken a selenate ion for a sulphate ion, under conditions of rapid growth. The impact that the common ion effect has on the solubility of sodium sulphate and sodium selenate respectively is modelled and discussed in sections 6.2.3 and 6.2.1. The effect that an increased growth or mass deposition rate has on the uptake of selenium is considered in section 6.4.

The results in both Figure 20 and Figure 21 indicate that the relationship between selenium in the mother liquor and selenium in the salt product is linear for each brine composition. This is expected since it is probable that an increase in the concentration of a substance in the mother liquor will correspondingly result in an increased presence of that substance in the salt product. The trends are consistent except for the data point corresponding to 108 g/l $Na_2SO_4$, 90 g/l NaCl and 1.44 g/l $Na_2SeO_4$. This point is substantially lower than expected, but this is most likely due to analytical error. The trends show that if the sodium sulphate and sodium selenate ratios are kept constant while the sodium chloride concentration is increased, the selenium impurity in the product salt increases. This is potentially due to the increased concentration of sodium ions promoting the uptake of selenium in the sodium sulphate salt.

It is also possible that the selenium is crystallizing in small amounts along with the sodium sulphate in the form of sodium selenate. If this is the case, the increased presence of sodium ions from the sodium chloride could result in the common ion effect playing a role in the selenium inclusion. In this case, one salt might be slightly more affected by the presence of the common ion more than the other. In order to examine this further it is necessary to model the impact of sodium chloride on the solubility of both salts, which is investigated in 6.2.3.

Another possible reason for the increased incorporation of selenium is the altered ionic strength of the mother liquor. As sodium chloride is added, not only is the concentration of sodium ions increasing, but the ionic strength of the solution is also increasing. This may impact on the solubility of sodium sulphate and sodium selenate in such a way as to promote the uptake of selenium. The issue of ionic strength is considered in section 6.3.

The error is given by a 10% analytical error expected from ICP analysis. That is why the error increases at higher concentrations. The source of this errors is due to the dilution of the salt, and inaccuracies in the equipment.

### *6.2.3 Modelling impact of common Na ion on solubility of $Na_2SO_4$ and $Na_2SeO_4$*

A binary salt dissociates according to the formula

$A_\alpha B_\beta \rightarrow \alpha A + \beta B$,

and the solubility product in pure water is expressed as

$$k_{sp} = [A]^\alpha [B]^\beta$$

where $k_{sp}$ is the solubility product in mol/l, and A and B are the concentrations in mol/l.

Extending this to the sodium sulphate and sodium selenate and within the system in question, the solubility is described as follows:

$$k_{sp} = [Na^+_{NaCl} + Na^+_{Na_2SeO_4} + Na^+_{Na_2SO_4}]^2[SO_4^{2-}]$$

$$k_{sp} = [Na^+_{NaCl} + Na^+_{Na_2SeO_4} + Na^+_{Na_2SeO_4}]^2[SeO_4^{2-}]$$

Where $k_{sp}$ refers to the solubility of either sodium sulphate or sodium selenate. The subscripts attached to $Na^+$ indicate the salt that is donating the ions. That is to say, the total sodium concentration in solution is the sum total of the sodium ions from the dissolved sodium chloride, sodium sulphate and sodium selenate.

Upon simplification, the formula to solve for the solubility of sodium sulphate and sodium selenate is the same

$$k_{sp} = Na^+_{NaCl} + Na^+_{Other} + 2x]^2[x]$$

In this equation, $Na^+_{Other}$ indicates the sodium contributed by the other salt in question. In other words, if the solubility of sodium sulphate is what is being solved for, then $Na^+_{Other}$ is the sodium contributed by sodium selenate, and vice versa. $x$ represents the concentration of either selenate or sulphate, depending on which solubility is being solved for. The $2x$ derives from the fact that there are two sodium ions in solution for every sulphate or selenate ion.

A model was made to solve for $x$ over a range of sodium chloride concentrations, from a temperature range of 0-100°C.

### *6.2.1 Modelling results and discussion*

The graphs below show the impact that the presence of excess sodium has on the solubility of sodium sulphate and sodium selenate. The y-axis represents the resulting solubility of sodium sulphate under varying temperatures, z-axis, and in the presence of differing NaCl concentrations, x-axis. The presence of NaCl affects the total concentration of the common Na ion.

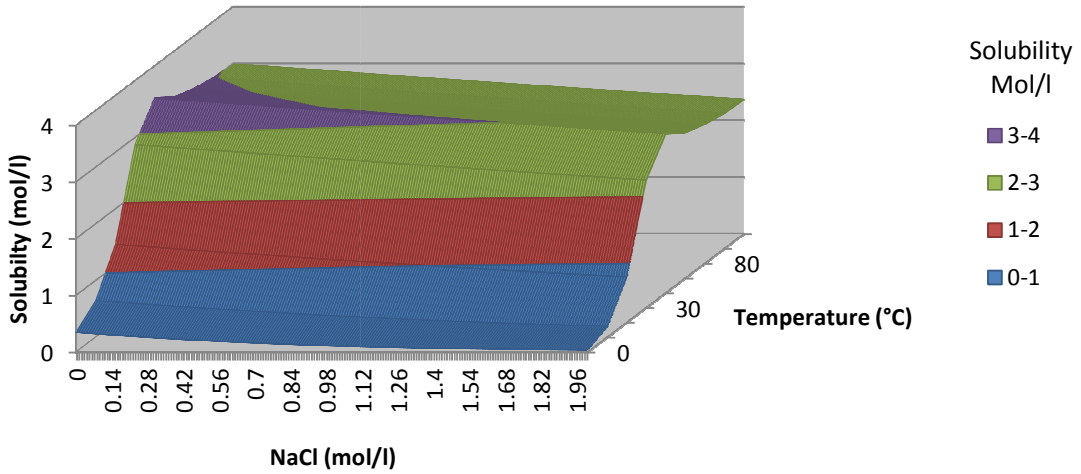


**Figure 22: Change in solubility of sodium sulphate due to the presence of NaCl and sodium sulphate over a range of temperatures**

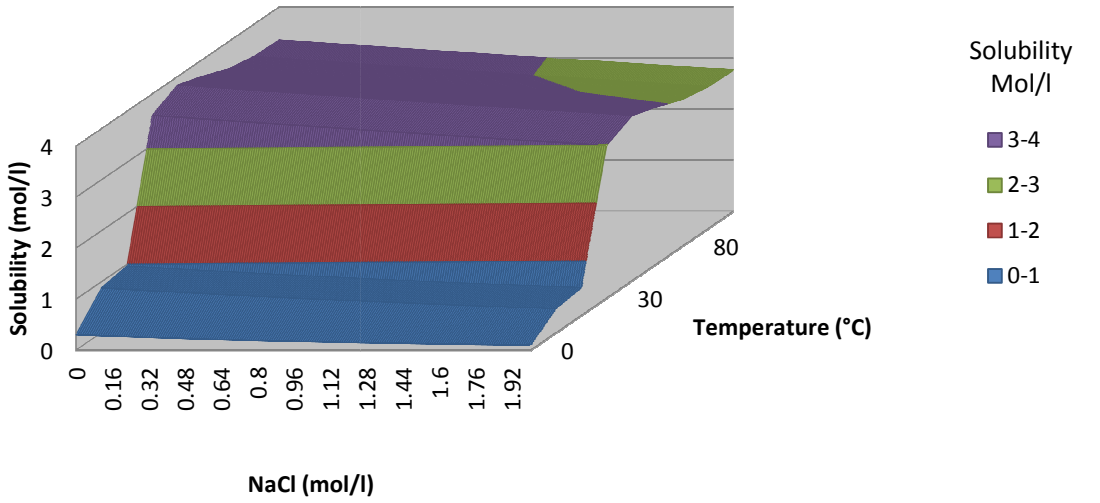


**Figure 23: Change in solubility of sodium selenate due to the presence of NaCl and sodium sulphate over a range of temperatures**



The similarity between the two graphs indicates that both sodium sulphate and sodium selenate are similarly affected by the presence of sodium chloride. Both Figure 22 and Figure 23 display that an increase in the concentration of dissolved sodium chloride becomes marginally more pronounced with an in temperature.

It would be illuminating to compare an isotherm of sodium sulphate directly to one of sodium selenate because it allows for the direct comparison between the changing solubilities. Since the crystallization process under investigation occurs at low temperatures, the 0°C isotherm for the two salts will be compared (Figure 24).

Figure 24 displays how the solubility of the two salts vary with respect to one another at 0°C. The solubility of sodium sulphate decreases as a result of increased sodium ions more significantly than the solubility sodium selenate. This relationship in itself does not serve to explain the increased uptake of selenium at higher sodium chloride concentrations. However, the decreased solubility of the sodium sulphate would result in an increased crystallization rate, for a given rate of cooling. A faster crystallization rate results in the increased likelihood of the selenate ion being incorporated into the lattice accidentally.

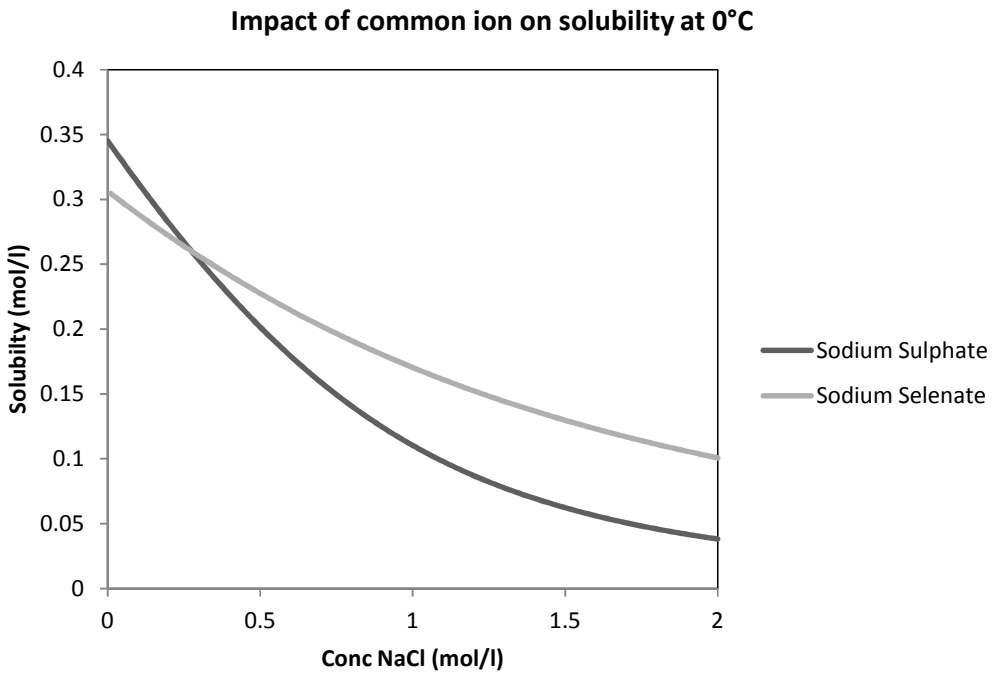


**Figure 24: Solubility of sodium sulphate and sodium selenate in the presence of varying sodium chloride concentration**



## 6.3 Impact of ionic strength on uptake of selenium by sodium selenate

It was clear from previous experiments that the presence of sodium chloride noticeably increased the uptake of selenium in the product. It was initially thought that the common ion effect was causing the decreased solubility of sodium selenate. Results in the previous section, however, indicate the opposite. It is also not likely that the crystallization of a separate sodium selenate salt is being promoted, as was found in section 6.1.3. Therefore, an investigation into the ionic strength of the solution was performed, to see if it could have an impact on selenium uptake. This investigation further illustrated if it is specifically the additional sodium provided by the dissolved NaCl that promoted the uptake of selenium.

An experiment was conducted whereby the ionic strength of the mother liquor was altered and the resulting selenium impurity in the sodium sulphate salt product was measured. The ionic strength of the solution was increased by adding potassium chloride to a standard solution containing the same concentrations of sodium sulphate and sodium selenate as the original industrial brine. Potassium chloride was used so that the ionic strength of the solution could be adjusted without directly impacting on the solubility of sodium sulphate through the common ion effect.

In parallel to the above experiment, an identical experiment was performed whereby the ionic strength was increased by the addition of sodium chloride. In this way a direct comparison could be made between the solutions containing sodium chloride and potassium chloride.

### *6.3.1 Experimental*

**Solution preparation**

A standard solution containing of 3.36 g/l $Na_2SeO_4$ and 220 g/l $Na_2SO_4$ was made up. To maximise repeatability, one batch was enough to supply all individual beaker tests. Separate solutions containing 200 g/l NaCl and 200 g/l KCl were also made. These too were enough to supply the entire experiment. All solutions were made with 18MΩ.cm water and Merck laboratory grade chemicals.

**Experimental procedure (See Figure 25)**

100 ml of the $Na_2SO_4$ /$Na_2SeO_4$ was pipetted into each 250 ml beaker. Then the necessary quantity of KCl or NaCl was pipetted into the beakers. 18MΩ.cm water was used to top up each beaker to 200 ml. Each individual beaker test was repeated three times. The concentrations of NaCl and KCl can be found in Table 5. Note that each concentration was done for both KCl and NaCl. Thus there was a total of 8 different compositions, each repeated 3 times, for a total of 24 runs. Further information on the exact volumes used for each run can be found in the appendix, in Table 13.

These concentrations were chosen to investigate the impact of ionic strength at and around the ionic strength levels found in the industrial brine. These concentrations are well below the saturation level of either salt, at -3.5° C, and thus it is not believed that the salts will crystallize out of solution.

**Table 5: Concentrations of NaCl or KCl in mother liquor**

| Batch | Concentration (g/l) |
|---|---|
| 1 | 70.00 |
| 2 | 80.00 |
| 3 | 90.00 |
| 4 | 100.00 |

After the samples were prepared they were then placed in a freezer room at -3.5°C and stirred with magnetic stirrers. This temperature was chosen because at this point, most of the sodium sulphate is crystallized out of solution. For reasons of space and practicality, only six beakers were cooled at a time. The beakers were left at this temperature for 4 hours. This time was chosen as it was found to be a sufficient time for the solution to equilibrate at -3.5°C. It is important to note that temperature controlled rooms have defrost cycles. For this experiment, the scheduling of this cycle was known, and 4 hour long experiments could be fitted in between each defrost period. After 4 hours, the salt from each beaker was filtered, and placed in an oven to dry. The purpose of the drying was to prevent analytical inaccuracies caused by the unpredictable decay of the decahydrate to the anhydrate form of sodium sulphate. The oven melts the sodium sulphate decahydrate and then drives off the water. In the absence of water and at the higher temperature, all the sodium sulphate recrystallizes in the anhydrous form. After the drying process the crystals are ground up in a pestle and mortar and sent to be analysed externally by ICP-OES for concentration of selenium.

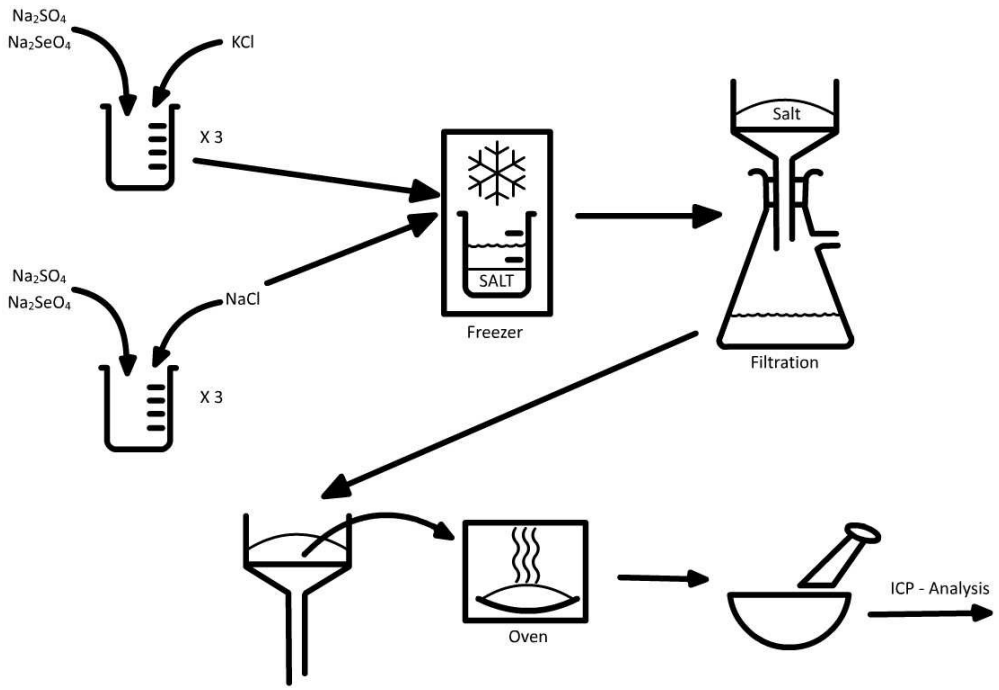


**Figure 25: Experimental setup for comparison between impact of NaCl and KCl on incorporation of selenium**

### *6.3.2 Experimental results and discussion*

The results from this experiment can be found in Table 14 in section 11.3 of the appendix. Figure 26 displays the impact that ionic strength has on the uptake of selenium. The data points on the top represent the selenium impurity when the ionic strength was altered with NaCl. The bottom set of data points represent the selenium impurity when the ionic strength was altered with KCl.

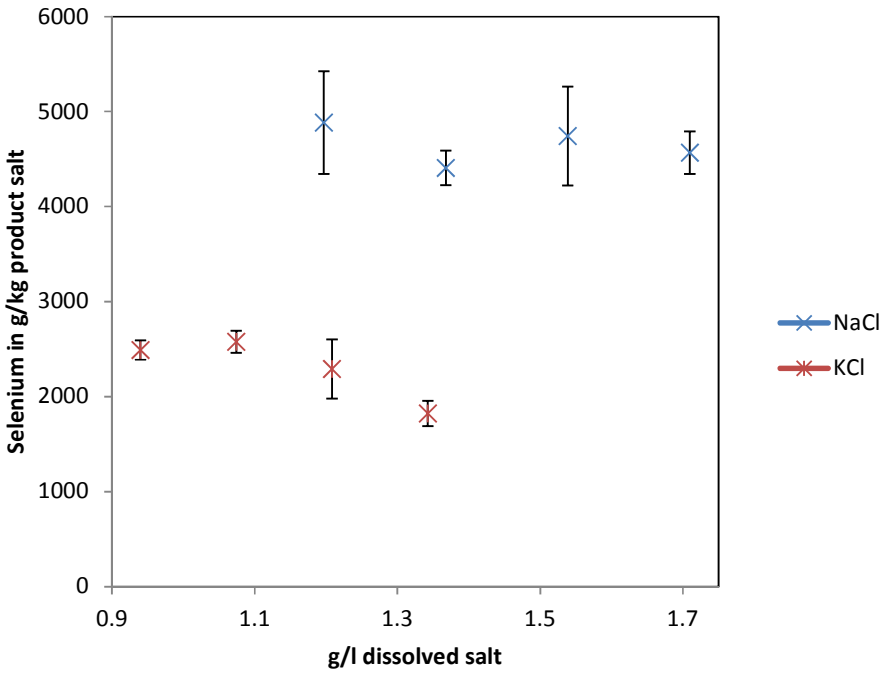


**Figure 26: Impact of ionic strength on uptake of selenium by sodium sulphate (n=3) (Raw data in Table 14 in the appendix)**

The error here represents the standard deviation between the three repeat experiments at each concentration. Because these experiments were analysed by ICP, there is an accepted 10% error. This is especially relevant when analysing very low concentration substances, like the selenium, in a very concentrated medium, like the sodium sulphate. This error then compounds any experimental error. Though the error is seen here is large, the trend that sodium chloride results in a much higher selenium uptake is still clearly visible.

It can be seen in Figure 26 that an increasing ionic strength does not have a significant impact on the uptake of selenium. This is illustrated in both cases, NaCl and KCl. It is possible that over a broader range of sodium chloride or potassium chloride concentrations, a change in the detected concentration of selenium in the sodium sulphate product might be noticed.

It can also be seen that the uptake of selenium is significantly increased by the presence of sodium chloride as opposed to potassium chloride. This indicates that it is specifically the presence of extra sodium that influences the degree to which selenium is taken up. From section 6.2.1 it would appear unlikely that it is the common ion's effect on relative solubilities that is promoting the uptake of selenium. Another possibility is that the rate of mass deposition is being affected by the common sodium ion. This is discussed in 6.4.

It is possible that the results from this experiment serve to corroborate the findings in section 6.2. The results in section 6.2 were found to be erratic, particularly with regard to measurements done at the lower sodium chloride concentrations. It is possible that any quantity of sodium chloride is enough to impact on the uptake of selenium, but beyond a certain critical concentration, additional sodium chloride has a diminishing effect.

There was a jump in the uptake of selenium between the concentrations of 50 g/l and 90 g/l sodium chloride (Figure 21). In this ionic strength experiment, all sodium chloride concentrations were well above 50 g/l. The lowest concentration investigated is 70 g/l. This would indicate that the impact of sodium chloride on the selenium impurity is not linear. This would serve to explain why the uptake of selenium, in Figure 26, did not increase as the concentration of NaCl was increased. This theory would require far more experimental testing to be validated, and cannot be confirmed here.

## 6.4 Impact of mass deposition rate on the uptake of selenium

From sections 6.2 and 6.3 it is apparent that the presence of excess sodium has an influence on the uptake of selenium. It is believed that this phenomenon is in some way related to the common ion effect.

Modelling indicates that the solubility of sodium selenate is not changed relative to sodium sulphate in the presence of excess sodium ions. It is however possible that the mass deposition rate of sodium sulphate for a given cooling rate is increased by the common ion effect. In section 4.3.1 it was discussed how growth or mass deposition rate may have an impact on the inclusion of isomorphous impurities. At higher mass deposition rates, it is more likely that foreign substances are accidently incorporated into the crystal lattice.

The following experiment aims to determine the degree to which mass deposition rate influences the purity of the product. This is related to the rate at which supersaturation is generated and consumed by the system.



### *6.4.1 Experimental*

In this experiment, sodium sulphate/sodium chloride brine samples containing varying amounts of sodium selenate were cooled at different rates. The rate of mass deposition of sodium sulphate was calculated, as was the resulting selenium impurity for each run. In this way, it could be seen if there is a correlation between mass deposition rate and selenium uptake.

**Solution Preparation**

Synthetic brine was made to simulate the major components of the PGM brine, 90 g/l NaCl, and 108 g/l $Na_2SO_4$. To minimise variance within the experiment, one batch of synthetic brine was made to supply all individual runs. The brine was made with 18MΩ.cm water and Merck laboratory grade chemicals.

**Experimental Procedure (See Figure 27)**

3 separate runs were performed. In the first run, three brine samples containing 1.0 g/l, 1.6 g/l, and 2.2 g/l of sodium selenate, respectively, were cooled between 20°C to -3°C over 24 hours. A complete table of the experiment can be found in the appendix in section 11.4. The samples were cooled in 200 ml glass jacketed crystallizers. The brines were well agitated to prevent mass transfer limitations. Every two hours, the temperature was measured and a sample of the

supernatant liquid was taken. Once the brine was cooled for the full duration, the formed salt was filtered. To prevent inconsistencies resulting from incomplete washing, none of the samples were washed.

It was decided not to wash the crystals to prevent error. If the crystals were washed, the wash would be done with a saturated solution of sodium sulphate. While washing with a saturated solution it is possible, if the salt and wash solution are not at exactly the same temperature, that the sodium sulphate would crystallise on the cold crystal surface, or possibly partially melt the crystal. Because the concentration selenium in the brine is low, it is believed that this would have introduced a greater error than leaving the crystals unwashed.

After filtration, the salts were placed in an oven to dry. The purpose of the drying is to prevent analytical inaccuracies caused by the unpredictable decay of the decahydrate to the anhydrate forms of sodium sulphate. The oven melts the sodium sulphate decahydrate and then drives off the water. In the absence of water and at the higher temperature, all the sodium sulphate recrystallises in the anhydrous form. After the drying process the crystals are ground up in a pestle and mortar and sent to be analysed externally by ICP-OES for selenium concentration. The second and third runs are identical to the first, except that they are cooled over 12 hours and 6 hours respectively.

The different cooling rates were selected to exhibit 2 extremes, 6 hours and 24 hours, and a point in the middle. 12 hours was chosen because it is half the cooling rate of 6 hours, and twice the cooling rate of 24 hours. In this way it was believed that any obvious dependencies on mass deposition rate would become apparent.

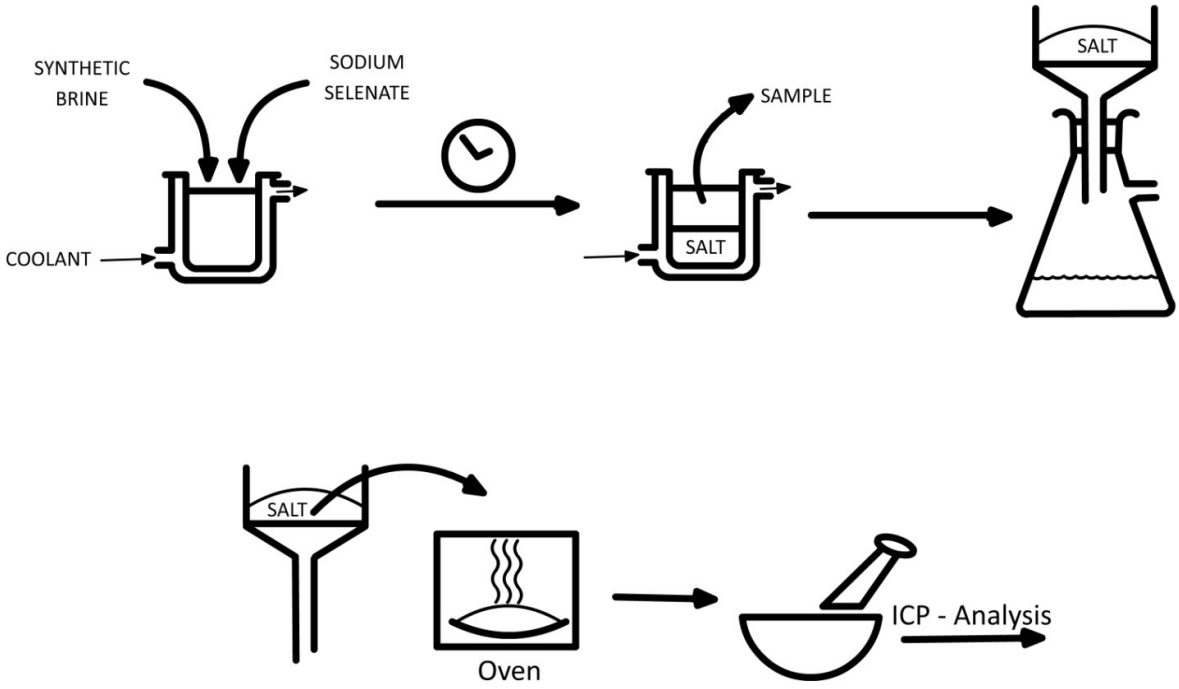


**Figure 27: Experimental procedure for mass deposition rate experiment**



### *6.4.2 Results and discussion from mass deposition experiment*

Tables of results for this experiment can be found in section 11.4 of the appendix. Figure 28, Figure 29 and Figure 30 display the differing mass deposition rates for different sodium selenate concentrations and cooling rates. The units of the mass deposition rate are arbitrary. They are meant to compare the rate at which sodium sulphate is leaving solution and depositing on the salt. It must be noted that the temperature is a linear function of time. Each temperature increment can also be represented by an appropriate time increment. The time readings and how they correspond to the temperature readings can be found in the appendix in section 11.4.

For all experiments the mass deposition rate is relatively constant for each cooling rate over the length of the experiment. The average mass deposition rate for each experiment is summarised in Table 6. In the following graphs, dm/dt is calculated by

$$\frac{dm}{dt} = \frac{(\%Na_2SO_4)_{n-1} - (\%Na_2SO_4)_n}{t_n - t_{n-1}}$$

Where $\%Na_2SO_4$ is the mass percentage of sodium sulphate dissolved in the brine, and $t$ is time in minutes. The $n$ subscript refers to the data point. That is to s, if $n$ is a random data point, $(n-1)$ refers to the data point that precedes is.

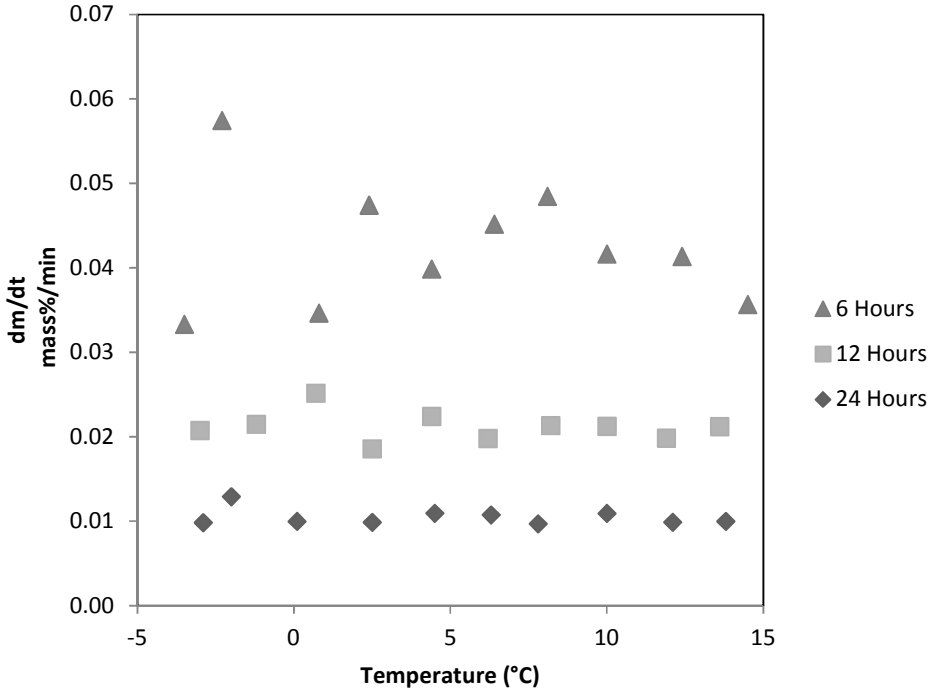


**Figure 28: Mass deposition rate of 1.0 g/l sodium selenate brine samples at differing cooling rates (Raw data in Table 15, Table 16 and Table 17 in the appendix)**

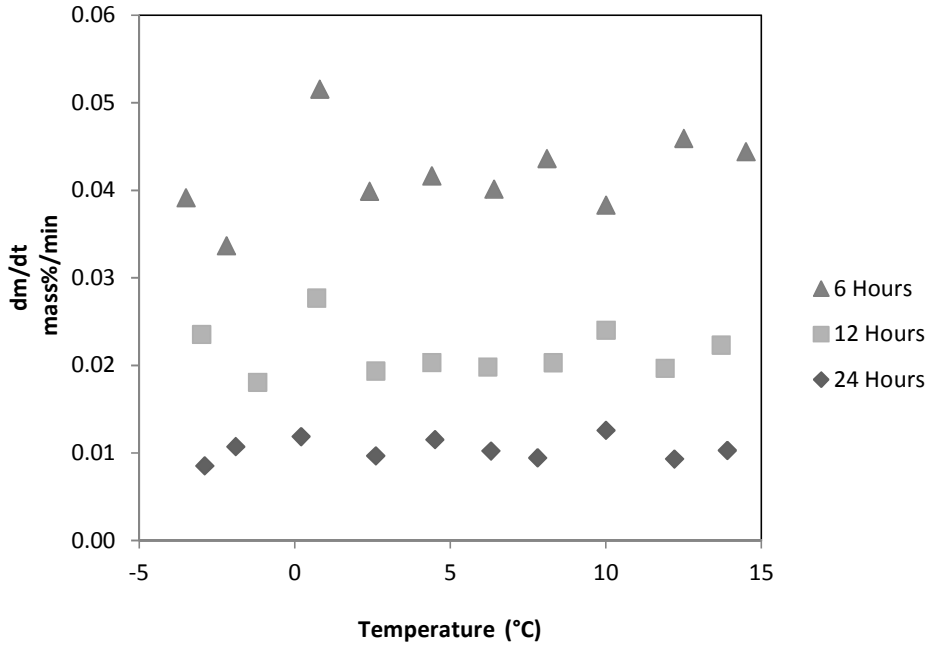


**Figure 29: Mass deposition rate of 1.6 g/l sodium selenate brine samples at differing cooling rates (Raw data in Table 18, Table 19 and Table 20 in the appendix)**

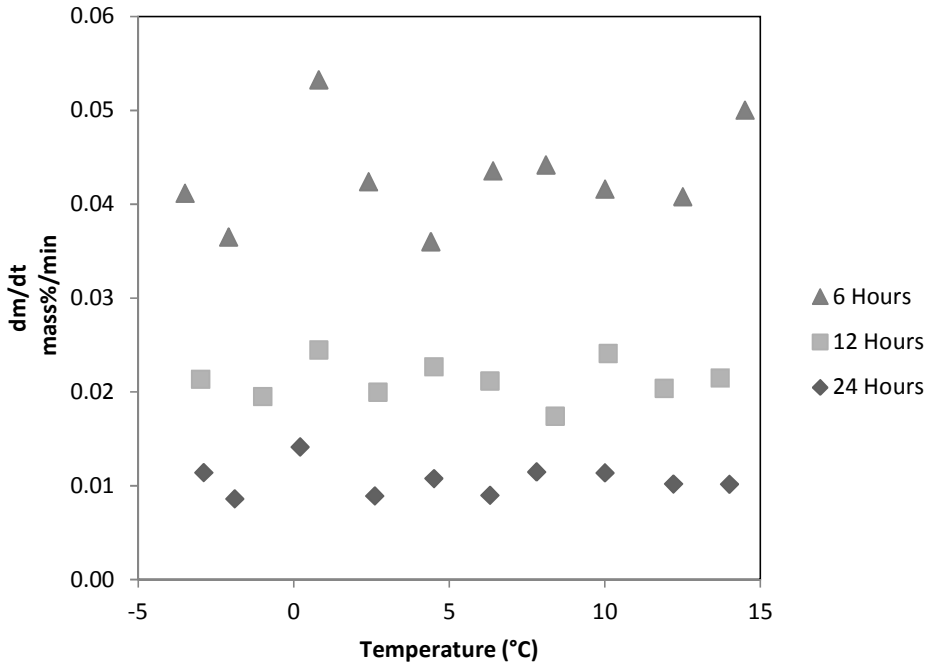


**Figure 30: Mass deposition rate of 2.2 g/l sodium selenate brine samples at differing cooling rates (Raw data in Table 21, Table 22 and Table 23 in the appendix)**

**Table 6: Mass deposition rate for different cooling rates and sodium selenate concentrations in mass%/min**

| Sodium selenate g/l in brine | 1.0 | 1.6 | 2.2 |
|---|---|---|---|
| Cooling rate | | | |
| 1°C/hour | 0.010 | 0.010 | 0.011 |
| 2°C/hour | 0.021 | 0.022 | 0.021 |
| 4°C/hour | 0.042 | 0.043 | 0.042 |

In addition to the mass deposition rates being constant throughout each experiment, they were also consistent between the experiments. What can be inferred from this is that for each experiment, the rate at which sodium sulphate is being deposited is constant throughout the experiment, and is comparable between analogous experiments.

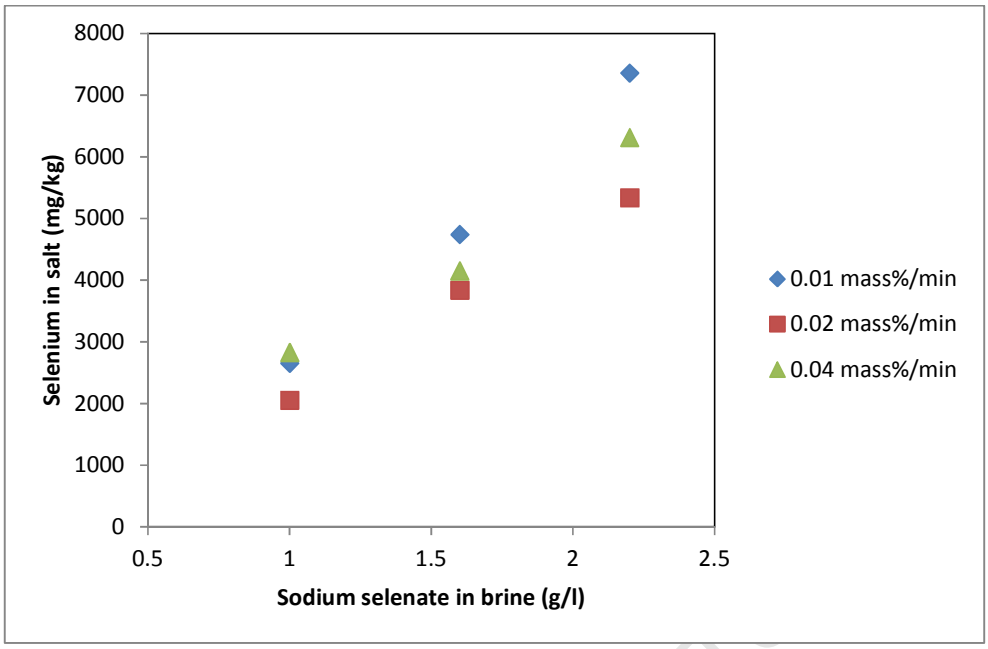


**Figure 31: Uptake of selenium by sodium sulphate at differing mass deposition rate (n=1)**

Figure 31 shows the results for the uptake of selenium at differing mass deposition rates. Once again, it can be seen that there is a linear relationship between the concentration of sodium selenate in the brine and the selenium in the product sodium sulphate.

From this data it cannot be said that mass deposition rate has a noticeable effect on the uptake of selenium. In the 1 g/l experiments, the fastest deposition rate led to the greatest uptake of selenium, but it was only slightly more than the uptake at the slowest deposition rate. Overall, the second fastest deposition consistently resulted in the lowest uptake of selenium.

This could be attributed to the strong orienting forces that ionic crystal units species are subjected to. The stronger these forces are, the more rapidly the depositing ions can be correctly positioned to be incorporated into the lattice, as was discussed in section 4.3.1. For the mass deposition rate to influence the uptake of impurity, deposition must be more rapid than the rate at which the ions can be correctly oriented and positioned.

It is possible that rapid enough mass deposition to cause this to happen was not achieved. It is not likely, however, that the solution could be cooled more rapidly without substantial scaling of ice occurring. Industrial scale crystallization should occur at mass deposition rates below those that would promote the uptake of this kind of impurity.

The systems were well agitated and it is assumed that mass transfer limitations were not in effect. This cannot however be conclusively validated. The impact of agitation with regard to mass transfer limiting effects needs to be investigated in future work.

No correlation between mass deposition rate and selenium uptake could be seen, at the cooling rates investigated. If the experiments were conducted at a wider range of rates a more noticeable relationship might appear. However, much slower mass deposition rates would make the process uneconomical on an industrial scale. It is unlikely that slower mass deposition rates are a feasible means to reduce the selenium impurity.

## 6.5 Summary of findings

A more extensive summary and discussion of conclusions can be found in section 8. A brief overview of the findings is provided below.

- Selenium is not significantly incorporated as a liquid inclusion.
- It is specifically the similar structure of sulphate and selenate that allows it to be incorporated into the sodium sulphate crystal. This lends strong evidence to the fact that isomorphous substitution is the dominant mechanism of impurity uptake
- The selenium uptake was promoted by the presence of extra sodium ions
- Ionic strength does not have a noticeable impact on the uptake of selenium
- Mass deposition rate was not found to have an appreciable impact on the uptake of selenium.

# 7 Introduction to coal power plant brine

The coal power plant brine represents a blend of waste effluent from a colliery and a coal power plant cooling tower effluent. This blend is passed through a reverse osmosis plant. Some of the retentate is sprayed on the power plant ash heap, and the rest is returned to the colliery where it is pumped into mined caverns. Neither of these disposal regimes is sustainable, and serves as another example of how South Africa's waste disposal practices need to be revised with new technologies.

This brine contains mostly sodium sulphate and sodium chloride. It also contains appreciable amounts of calcium, potassium and magnesium. The brine composition can be found in Table 7. Brine analysis is very difficult and is still not perfect. There is an excess of negatively charged ions reported in the brine. This is most likely due to an incorrect analysis of either sulphate or sodium. Errors in sodium analysis are common in brine analysis, and a subsequent analysis on the same brine has illustrated this. The brine was re-analysed by ICP-OES and while all other species matched the existing analysis, sodium deviated quite substantially. For modelling purposes, it has been assumed that there is enough sodium to balance the excess sulphate ions. This imbalance only influences the modelling of the brine, and does not compromise the integrity of the experimental findings.

In contrast to the PGM brine, the coal power plant sample is dilute, and must be concentrated before any salt will form. In order to crystallize the sodium sulphate, the brine must be concentrated by a factor of about 4.5 times in order to reach its saturation point at its predicted eutectic point of -2.01°C.

Unlike the PGM brine, the results from this investigation will not be subject to further investigation beyond the initial application of EFC. The work done on this brine serves to illustrate additional impurities that can be encountered when crystallizing salts out of complex brines.

**Table 7: Composition of coal power plant brine**

| Major elements (mg/L) | | | Minor elements (mg/L) | |
|---|---|---|---|---|
| **Species** | **mg/L** | | **Species** | **mg/L** |
| B | 2.24±0.02 | | Al | 0.045±0.006 |
| Ca | 106.99±1.69 | | As | 0.0068±0.0001 |
| K | 106.2±0.9 | | Ba | 0.057±0.002 |
| Mg | 163.36±0.85 | | Cd | 0.00017±0.00001 |
| Na | 4804.88±2.72 | | Co | 0.014±0.0004 |
| Si | 13.11±0.08 | | Cr | 0.014±0.001 |
| Cl | 2424±16 | | Cu | 0.26±0.09 |
| SO4 | 8858±86 | | Fe | 0.24±0.20 |
| Sr | 3.055±0.010 | | Mn | 0.0017±0.0001 |
| | | | Mo | 0.039±0.001 |
| pH | 7.75±0.03 | | Ni | 0.12±0.01 |
| | | | P | 0.82±0.03 |
| EC (mS/cm) | 16.69±0.50 | | Pb | 0.0039±0.0036 |
| TDS | 15400±282 | | Se | 0.0049±0.0001 |
| | | | Ti | 0.00069±0.00055 |
| | | | V | 0.019±0.001 |
| | | | Zn | 0.13±0.01 |

**Brine analysis obtained from the University of the Western Cape, from Ojo Olanrewaju Fatoba**

## 7.1 Application of EFC to coal power plant brine

### *7.1.1 Experimental set-up and procedure*

The experimental procedure for the investigation of the coal power plant brine was different to that of the PGM brine. From the previous experiments it became apparent that for the purposes of investigating the product salt, numerous temperature readings and very frequent brine composition analysis is both costly and unnecessary. Additionally, the purity of the salt cannot be analysed at different stages of the experiment. This is because the amount of salt produced at each stage is impractically small for collection and analysis. Instead of repeating the procedure used for the PGM brine, a different experimental process was devised.

It is understood that this experimental procedure cannot be repeated exactly. This procedure was chosen to be informal in order to acquire as much rough information as possible with the limited time available. From the results, areas of greatest concern can be focused on in future studies, and less pressing issues can be discarded.

Sodium sulphate decahydrate salt was crystallized from the coal brine in stages by cooling. At each stage the salt was removed from the system and filtered. The filtrate was returned to the brine and subjected to further cooling. At each stage, a sample of the brine was taken for analysis. In this way it could be established if there were any noteworthy correlations between the changing concentration of the impurities in the brine and the purity of the salt.

The raw coal power plant brine was first concentrated in a semi-continuous process in two 3L stirred beakers. The brine was agitated in the 3L beakers by 4 bladed impellers at 240 rpm in an ice room maintained at -17°C. This was the coldest temperature that the ice room could maintain. This low temperature was desired to facilitate the rapid removal of ice. The selection of the impeller speed was chosen to be fast enough to prevent ice agglomeration and build up, but slow enough not to prevent spillage. Once enough ice had formed, the contents of the beakers were filtered to remove ice. The ice was discarded. Ice was not analysed because the scope of this investigation is focused on the impurity in the salt. The concentrated filtrate was then topped up with more raw coal power plant brine and the process repeated. This was continued until all the raw coal power plant brine had been depleted. The remaining concentrate was then further reduced through removal of ice, in successively smaller containment vessels until the first traces of salt formation were noticed. At this point the concentrating of the brine was ceased. This point was found to be when concentrated brine was 20% of the volume of the original brine. A diagrammatic representation of this process can be found in Figure 32.

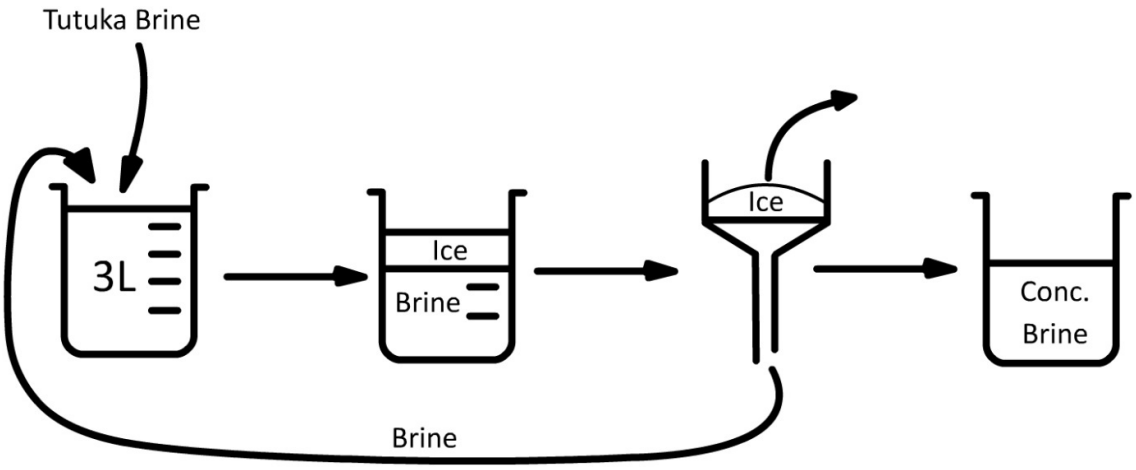


**Figure 32: Concentrating of coal power plant brine**

Once the brine had been concentrated to the saturation point of sodium sulphate, the brine was moved to three, 200 ml jacketed crystallizers. The purpose of moving the brine to these crystallizers is because they have a higher height to volume ratio than the 3L beakers. This creates a larger vertical space between the ice and salt when the contents are allowed to settle and aids in the separation of ice and salt. The coolant used was glycol and was circulated through the crystallizers at -4°C. The crystallizers were agitated with magnetic stirrers. Because the volume of concentrated brine was greater than that of the crystallizers, the brine in the crystallizers was topped up as ice and salt were removed. Each time that ice was to be removed the agitation of the crystallizers was ceased and the contents were allowed to settle. When the contents of the crystallizers had settled into a clearly defined ice, liquor and salt regions, the ice region was gently agitated with a spoon to dislodge entrapped salt crystals. It is important to note that only the ice was agitated, to prevent the re-suspension of the settled salt. After the first salt sample was taken, evidence of primary nucleation was detected, as the solution had become cloudy. This was likely because the saturation point of calcium sulphate had been reached due to the continued removal of ice. It was decided to continue the experiment without removing the calcium sulphate so that its impact on the purity of the product could be analysed.

Salt was not removed every time that ice was removed. If this was done the salt samples would have been too small to handle effectively. Instead, the salt was allowed to accumulate before being extracted. Periodically, throughout the experiment, all the salt was removed. This was done so that a number of separate salt samples existed from different stages of the experiment. In this way the purity of the salt could be examined throughout the experiment. When the salt was removed from the process, liquid samples were also taken. The impurity concentrations of the salt could then be directly compared to the impurity concentrations in the brine at the time.

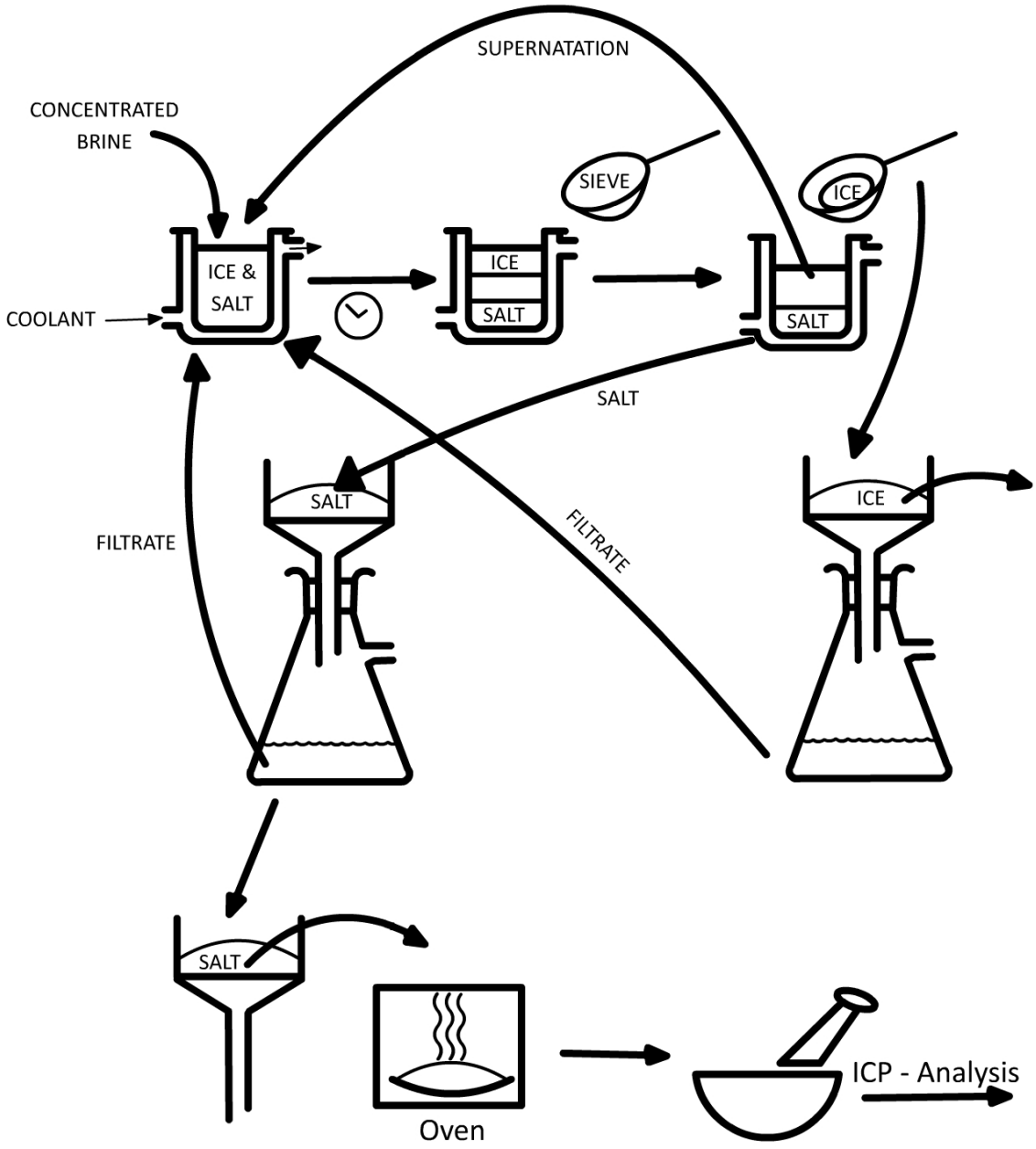


**Figure 33: Experimental procedure for removal of sodium sulphate salt from coal power plant brine**

After each sample of salt was removed it was filtered. Half the sample was removed from the filter and placed in the oven for drying. The remaining quantity of the sample was washed with a saturated solution of sodium sulphate before being placed in the oven. The reason half the sample is washed is to draw be able to make a comparison between washed and unwashed samples, specifically with reference to the possible calcium sulphate impurity. All samples were placed in an oven to drive off excess water, and convert the sodium sulphate decahydrate to

anhydrous sodium sulphate. This step cannot be overlooked. As soon as the decahydrate is removed from solution it begins to decay to the anhydrous form of sodium sulphate. Any water in the sample that is unaccounted for corrupts the analysis by affecting the mass concentration of the impurities. It is therefore necessary to completely remove all traces of moisture from the sample, both entrained and bonded as waters of crystallization.

Temperature readings were not taken due to the fact that it was not believed that specific temperature readings would have provided useful information about the trends observed. It was not overlooked that temperature is an important factor in the process, but understanding that the temperature decreases with each stage was sufficient. This is confirmed in the results, as no specific temperature related factors could have been identified.

Because the sodium sulphate decomposes at 32°C, the salt samples melt in the oven. This could be regarded as the salt dissolving in its own waters of hydration. As the water is driven from the salt recrystallizes in the anhydrous form. In case the impurities were not homogenously redistributed during the recrystallization process, the anhydrous salt is crushed and mixed before being sent for ICP-OES analysis.



### *7.1.2 Results of coal power plant salt and liquid analysis*

Tables of all the results presented here can be found in the appendix in section 11.5 of the appendix.

**Salt Analysis**

The impurities found in the sodium sulphate salt are shown below in Figure 34, Figure 35 and Figure 36. The salts are denoted by TS, referring to coal power plant Salt. The significance of each stage of the experiment is described below.

1 ➔ First salt taken. This salt was taken before any calcium sulphate precipitate formed.

2 ➔ Salt taken as soon as calcium sulphate formation was visually detected. Unwashed

3 ➔ Salt taken, calcium sulphate present. Unwashed

4 ➔ Washed fraction of 3.

5 ➔ Salt taken, calcium sulphate present. Unwashed

6 ➔ Washed fraction of 5

The complete analysis can be seen in Figure 34, but it is more illuminating to disregard sodium and sulphate concentrations and focus on impurities only. The major impurities are shown more clearly in Figure 35, and the minor impurities in Figure 36.

The error in this analysis is related to the estimated 10% analytical error involved in the dilution of the salts and analysis by ICP.

Additional sources of error are the potential liquid entrainment in the unwashed salts. However, as can been seen from the results in Figure 35 and Figure 36, there is no significant difference between washed and unwashed samples. It, therefore, does not appear liquid entrainment contributes significantly to the error of the analysis.

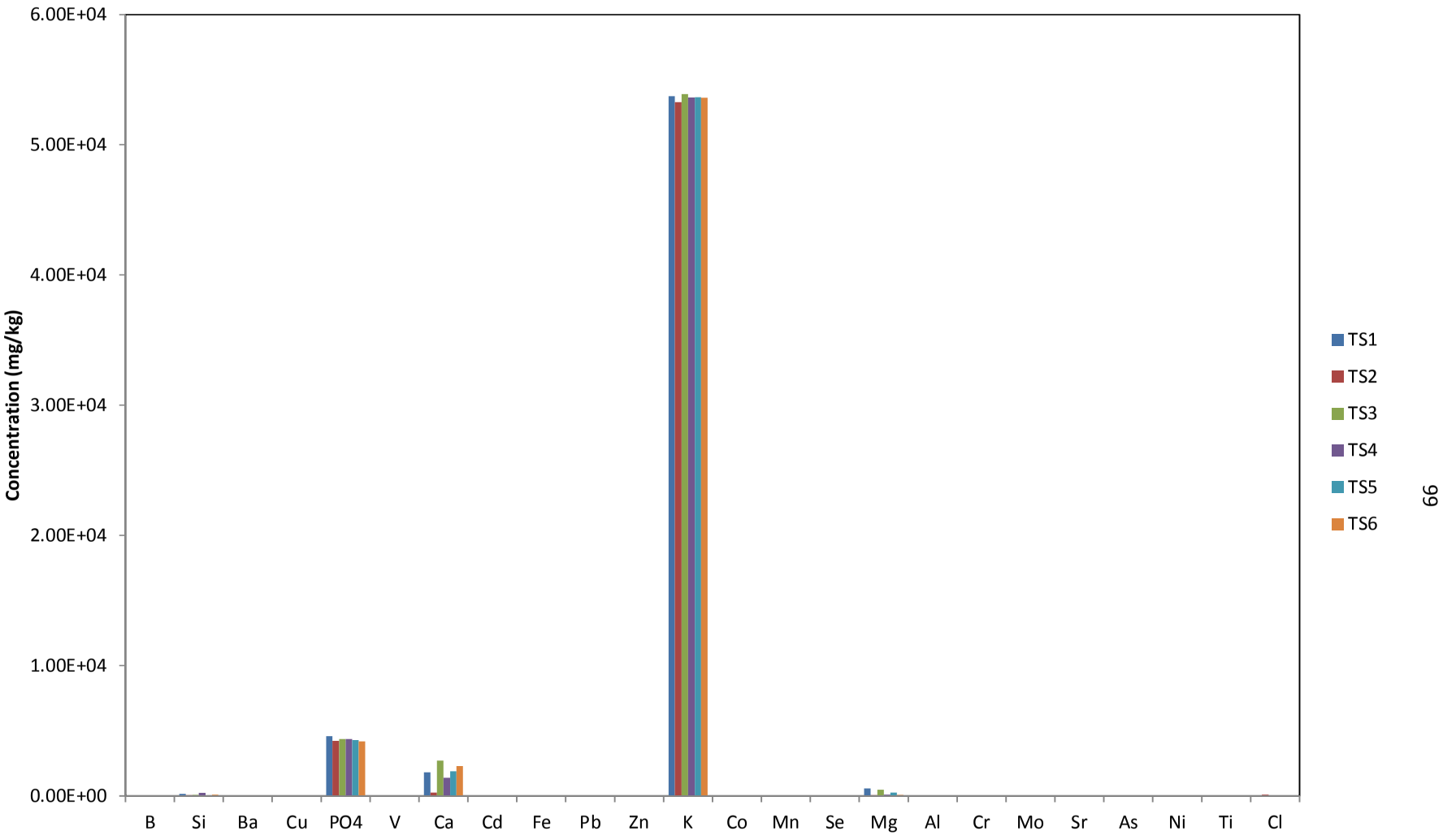


**Figure 34: Impurities in sodium sulphate recovered from coal power plant brine (Raw data in Table 25)**

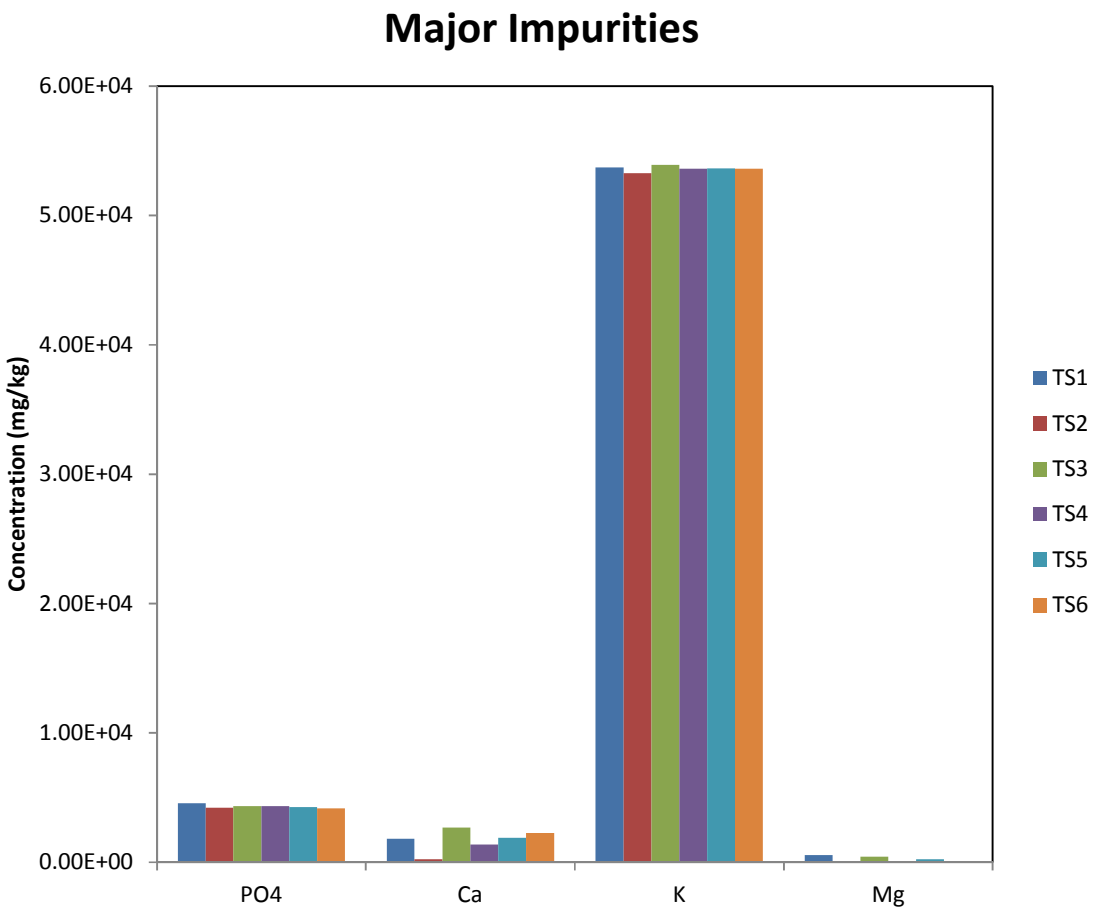


**Figure 35: Major impurities in sodium sulphate recovered from coal power plant brine (Raw data in Table 25)**



The most significant impurities are potassium, calcium, magnesium and phosphate

The phosphate accounts for approximately 0.45% of the total mass. Calcium and magnesium peak at about 0.25% and 0.06% respectively. Potassium content is significant at approximately 5.5%. This limits overall salt purity to approximately 94%.

Though these major impurities represent the most immediate interest, there are also a number of minor impurities that were also detected.

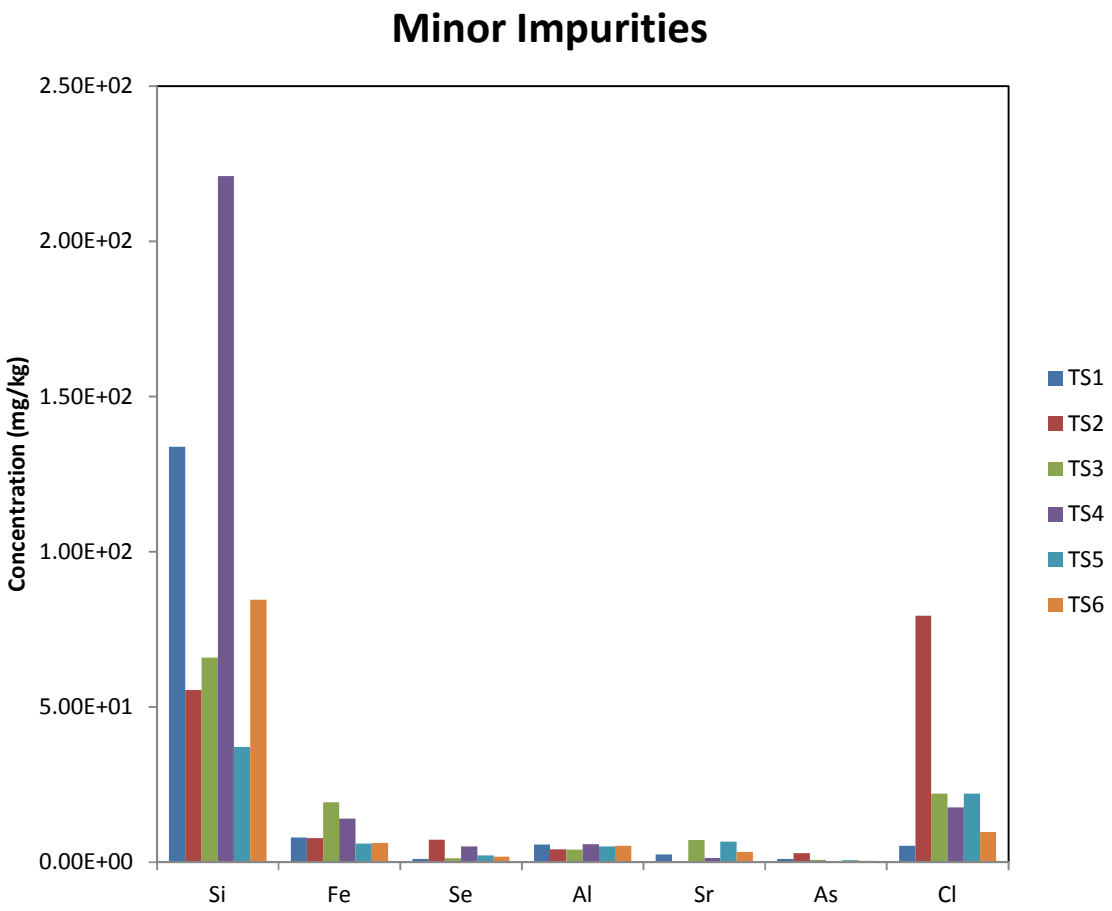


**Figure 36: Minor impurities in sodium sulphate recovered from coal power plant brine (Raw data in Table 25)**



The minor impurities are insignificant in concentration when compared to the major impurities. Silicon peaks in one sample at 0.025 wt% or 250ppm. All impurities detected at less than 1mg/kg (1ppm) were disregarded entirely and are not shown here. None of the impurities shown here are of immediate interest and, within the scope of this work, do not provide any discussion points. The very low concentration of $Cl^-$ in the salt compared to its high concentration in the brine is indicative that liquid inclusion did not have a significant impact on the purity.

**Liquid Analysis**

Liquid samples were analysed at each point at which a salt sample was taken. The different liquid samples correspond to the salt samples as follows.

Raw ➔ This is the unprocessed coal power plant brine before any concentrating or salt removal had been performed. This is also represented by Table 7.

Concentrate ➔ This is the brine after ice had been removed and crystallization of sodium sulphate was about to occur.

#1 ➔ Corresponds to salt sample TS1

#2 ➔ Corresponds to salt sample TS2

#3 ➔ Corresponds to salt samples TS3 and TS4

#4 ➔ Corresponds to salt samples TS5 and TS6

It is important to note that the sodium analysis is not accurate. As mentioned in section 7.1, there is an imbalance between the negatively and positively charged ions. The negative and positive charges within the brine should be equal, and it is believed all $Na^+$ readings are at least half what they should be. Throughout the entire project sodium analysis has been problematic. The fact that subsequent analysis for the same brine have deviated substantially for sodium illustrates this fact. For the purposes of this research the incorrect sodium readings can be tolerated because the sulphate concentrations can be used to calculate impurities in the brine and the salt relative to each other.

The results from the liquid analysis can be found in Figure 38, Figure 39 and Figure 40.

A potential source of error in this analysis is the 10% estimated error from ICP analysis, which includes the errors associated with dilution the of brine, before analysis. The sodium analysis has already been identified to be problematic, and it has been explained how this error can be tolerated within the scope of this investigated.

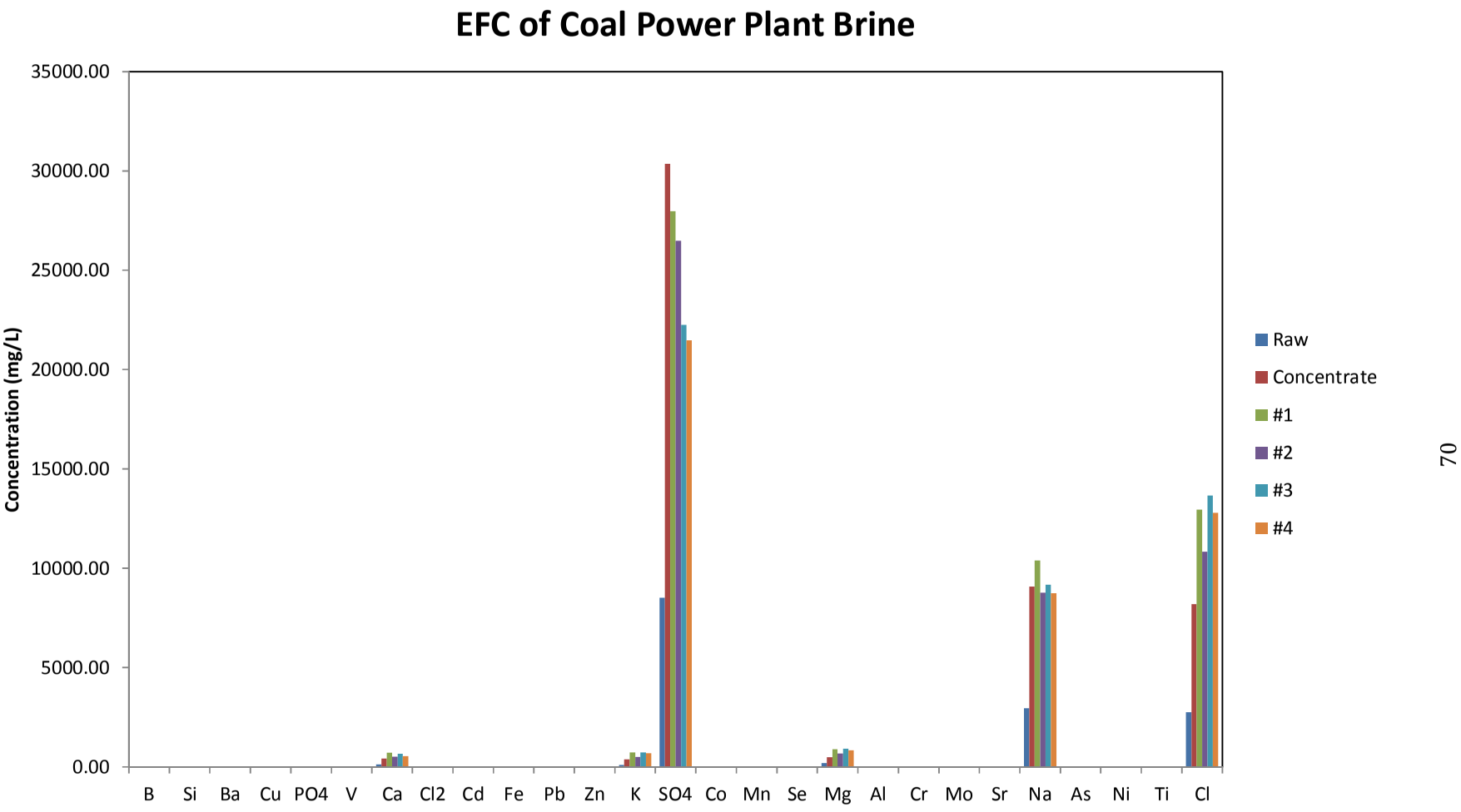


**Figure 37: Composition of coal power plant brine throughout salt removal experiment (Raw data in Table 26)**

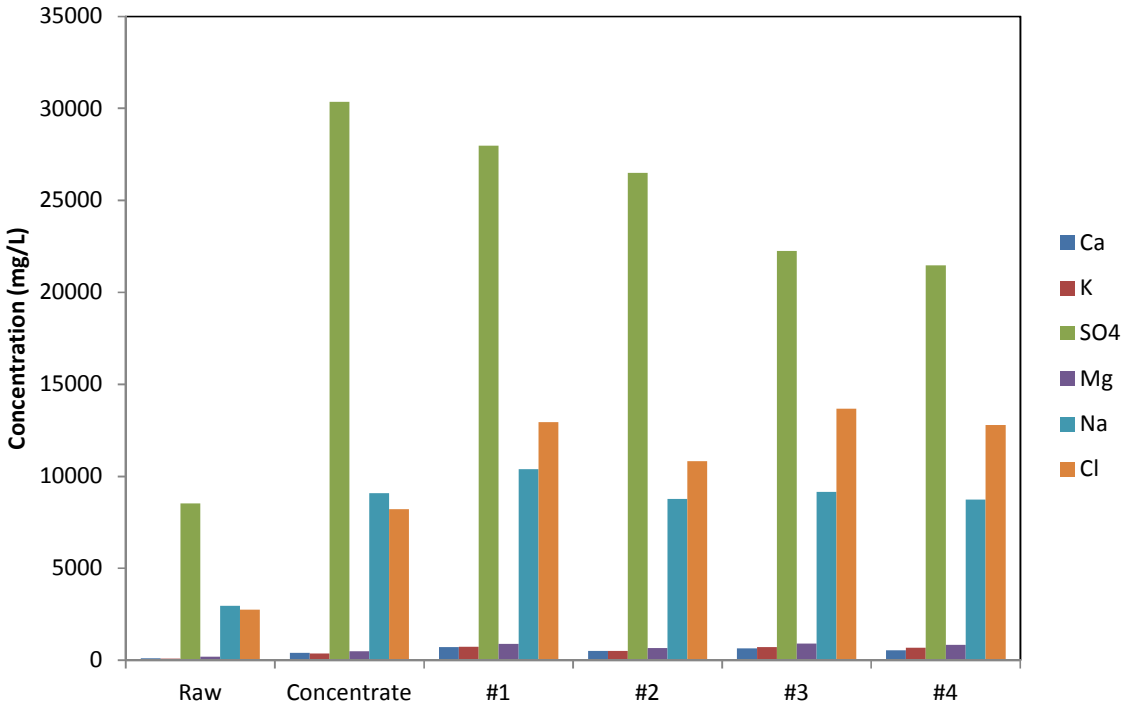


**Figure 38: Major dissolved ions in coal power plant brine throughout preconcentration and salt removal (Raw data in Table 26)**

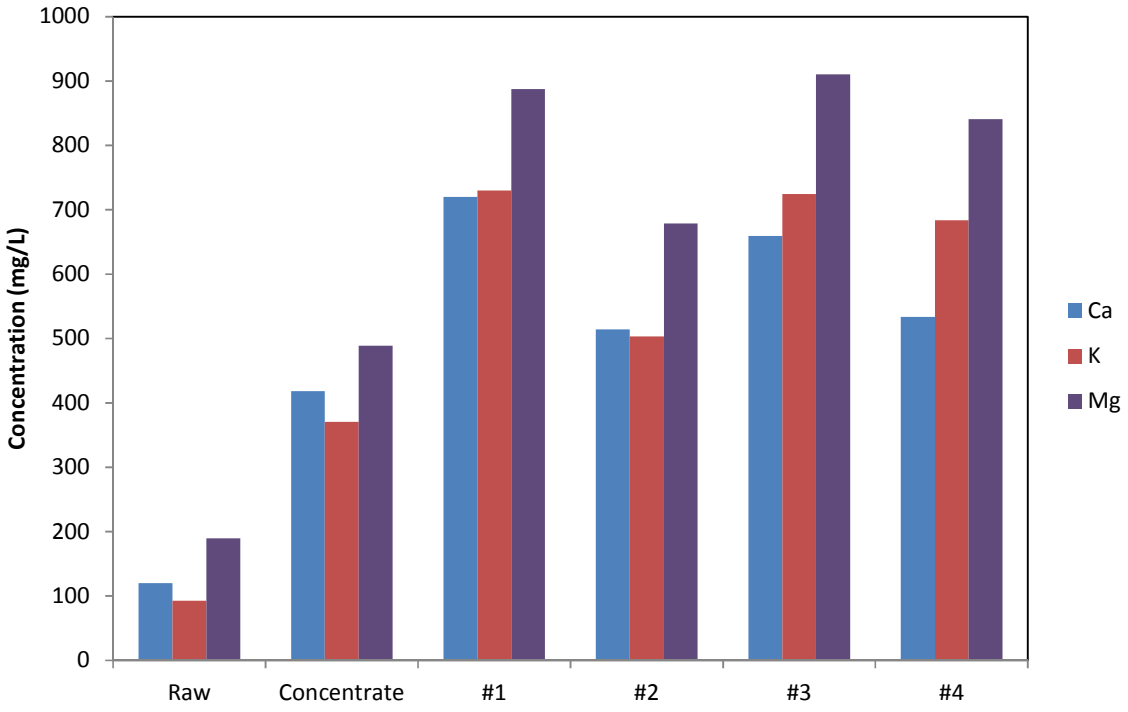


**Figure 39: Major impurities in coal power plant brine throughout preconcentration and salt removal $Cl^-$ not shown. (Raw data in Table 26)**

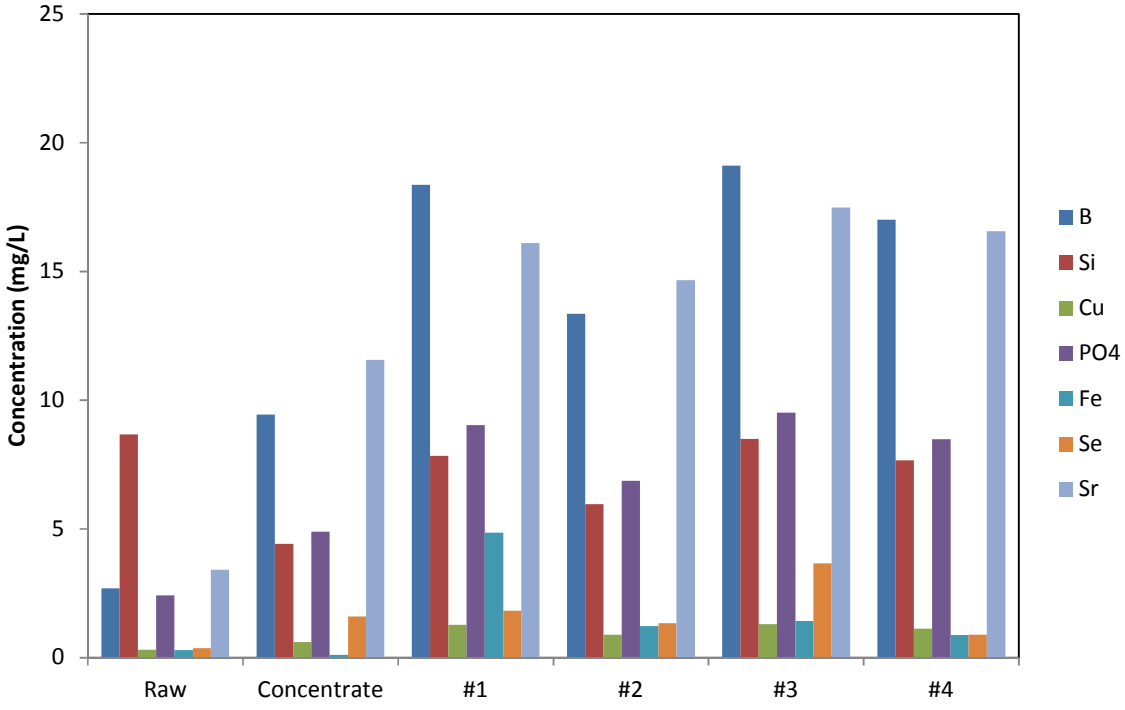


**Figure 40: Minor impurities in coal power plant brine throughout preconcentration and salt removal (Raw data in Table 26)**

All figures display the expected trend of ions increasing in concentration from the raw brine to the concentrate. In Figure 38 it can be seen that sulphate is at its highest concentration in the concentrate stream, just before salt crystallization occurs. At subsequent points, the concentration of sulphate decreases. This is to be expected, because, though ice and salt are removed from solution simultaneously, other ions are gradually concentrated. This is best illustrated by the chloride ions in Figure 38. This increased concentration of ions results in a freezing point depression. Thus, ice forms at lower and lower temperatures. As this ice crystallization temperature decreases, EFC operates at a lower and lower temperature. At these lower temperatures, the solubility of sodium sulphate is also decreased. Thus, sodium sulphate crystallizes out of solution and the sulphate concentration decreases.

It is interesting to note that for all non-crystallizing components, there is a decrease in concentration from sample #1 to sample #2. Sample #2 is the first sample taken after the crystallization of sodium sulphate begins. It is it is possible that during nucleation, between points #1 and #2, the crystallization process is less ordered and controlled than during growth. During this nucleation, foreign impurities are thus more likely to be accidentally incorporated then during the more ordered and controlled growth period. After nucleation, however, steady

growth of the sodium sulphate, between points #2 to #4, begins to reject foreign impurities more effectively. Thus, they begin to be concentrated in the brine once again.

### *7.1.3 Modelling of EFC of coal power plant brine*

OLI Stream Analyser (OLI Systems Inc, 2008) was used to predict the formation of salt in the EFC of a coal power plant brine. Because of the large difference in the amount of solid product for each substance, all substances cannot effectively be displayed in one graphic. Figure 41 shows all solid products from the EFC of the brine, but the large amount of ice formed hides the other substances. For this reason, each graphic concentrates on only one substance, by ignoring solid products that exist in larger amounts. In **Error! Reference source not found.**, however, alcium sulphate is represented on the same graphic as sodium sulphate to illustrate how they form at the same temperatures. The results are referred to and discussed in the overall discussion of results in 7.1.4.

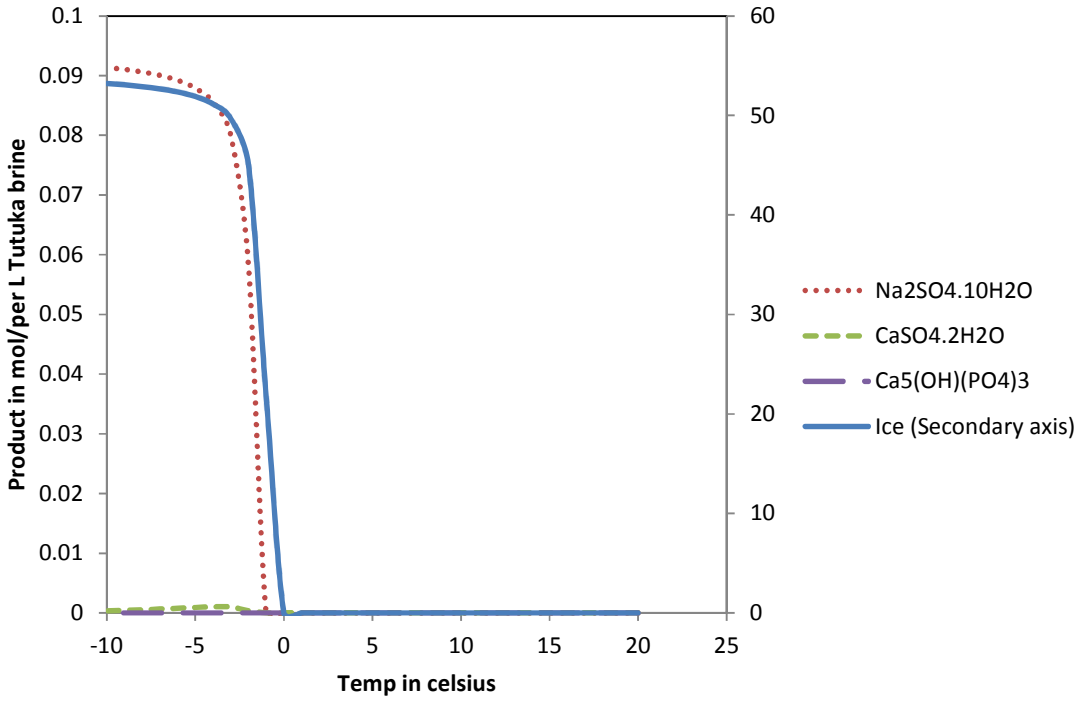


**Figure 41: Thermodynamic modelling of EFC of coal power plant brine**

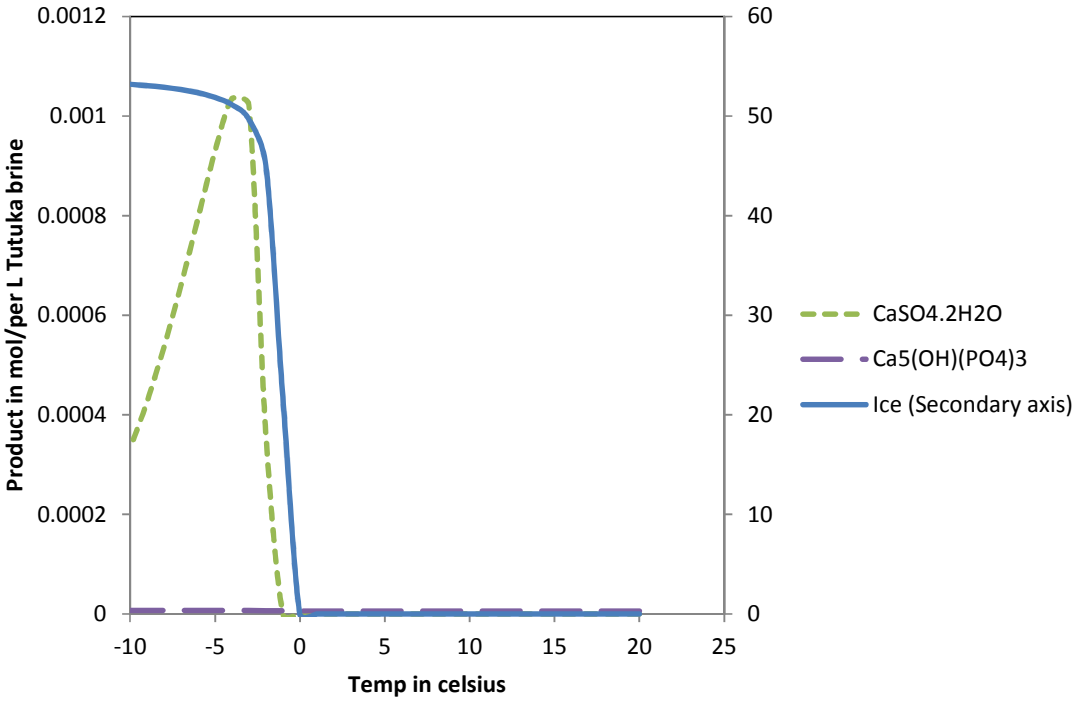


**Figure 42: Thermodynamic modelling of EFC of coal power plant brine (Ice and sodium sulphate not shown)**

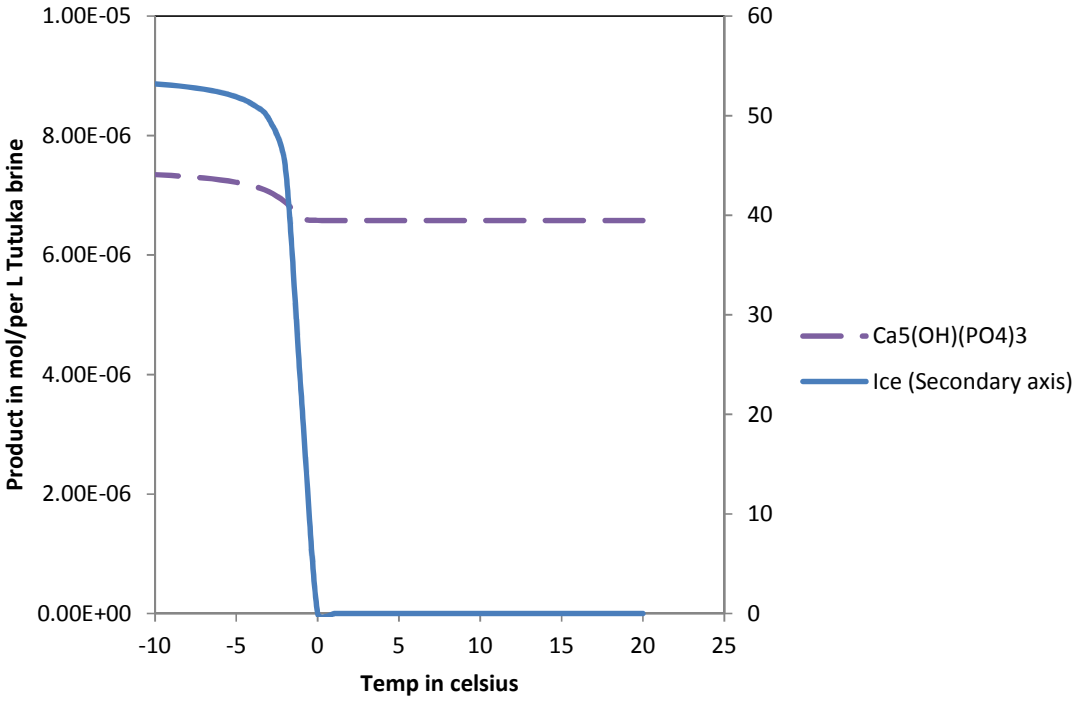


**Figure 43: Thermodynamic modelling of EFC of coal power plant brine (Calcium hydroxide phosphate only)**

### *7.1.4 Discussion of results from salt and liquid analysis of coal power plant brine*

**Phosphate ($PO_4^{3-}$)**

Despite phosphate ($PO_4^{3-}$) only being a minor impurity in the mother liquor, it is present in the salt as a major impurity. Relative to the sulphate concentration in the brine, the phosphate increases by a factor of three.

*In mother liquor; $PO_4^{3-}/SO_4^{2-}$ = 0.23*

*In salt, $PO_4^{3-}/SO_4^{2-}$= 0.75*

Sulphate is the limiting species in the formation of sodium sulphate, and is thus a good basis for the degree to which $PO_4^{3-}$ is being concentrated in the salt. Sodium sulphate cannot be used in the comparison for two reasons. Primarily, the sodium analysis is not believed to be accurate. Additionally, because sodium chloride is present as well as sodium sulphate, the concentration of dissolved sodium will change relative to all other species as sodium sulphate is removed. That is to say, in the brine, there is more sodium present relative to the sulphate than there is in the sodium sulphate salt and it is thus not a suitable frame of reference for other impurities.

It can thus be seen that phosphate is being concentrated in the salt and effective separation is not taking place. Even once ice has been removed from the raw brine the phosphate concentration in the concentrated brine is still low at approximately 4.9 mg/l. All other impurities in the brine at low concentrations do not feature in the salt at all, yet phosphate is quite prolific. It is unclear as to whether the phosphate is being isomorphously included in the sodium sulphate or is precipitating out as a separate salt. Though OLI predicts the formation of a phosphate salt, Figure 43, it is not believed that this suitably explains the presence of phosphate. Because the salt predicted by OLI is a calcium salt, this is further discussed under the calcium heading on the following page.

**Potassium ($K^+$)**

Unlike phosphate, potassium is a major impurity in the mother liquor and it is expected that the sodium sulphate product will suffer some potassium contamination. What is not expected, however, is the degree to which it is being concentrated in the salt. It increases relative to sulphate by a factor of 16.

*In mother liquor $K^+/SO_4^{2-}$ = 0.01*

*In salt* $K^+ / SO_4^{2-} = 0.16$

It is plausible that potassium is present as some form of substitution. It is not understood at this point if this substitution is random or as an ordered and defined salt mixed with pure sodium sulphate. OLI Stream Analyzer (OLI Systems Inc, 2008) does not predict the formation of any potassium salt, as is shown in Figure 41 to Figure 43. This increases the likelihood of sodium being isomorphously substituted for potassium.

**Calcium ($Ca^{2+}$)**

The presence of calcium in the salt analysis, Figure 35, suggests the formation of calcium sulphate ($CaSO_4$). There does not appear to be an appreciable impact of washing, which is to be expected. Once the calcium sulphate forms it cannot redissolve, and thus washing is not sufficient to remove it from the crystal sample. That is only the case in this particular experimental set-up however. The filter paper used in the filtration of sodium sulphate was too fine to allow the calcium sulphate precipitate to pass through. If a larger mesh was used, calcium sulphate could be washed from the sodium sulphate sample and would be allowed to pass through. Despite the prevention of the removal of calcium sulphate, calcium is not a significant impurity in the recovered coal power plant sodium sulphate. Because the calcium sulphate does not appear to have an enormous impact on the purity of the product and it is believed that it could be washed from the product, it is not of immediate concern. It is possible that calcium sulphate could get trapped between agglomerating sodium sulphate crystals, or be trapped between crystals on the filter medium. In this case, calcium sulphate could not easily be washed of the crystal surface, but this would need to be validated by further test work.

At this point the presence of phosphate cannot conclusively be explained. Calcium phosphate, $Ca_3(PO_4)_2$, is highly insoluble with a solubility 0.002 g/100 ml, and was initially thought to be the source of both the calcium and phosphate. OLI (OLI Systems Inc, 2008) predicts the precipitation of pentacalcium hydroxide phosphate, $Ca_5HO(PO_4)_3$ (Figure 43). This seems an unlikely explanation as calcium results would have to be much higher to support this. In the salt, there is approximately 45.5mmol/kg of phosphate, and about 43mmol/kg of $Ca^{2+}$. There is thus not enough calcium present to support either theory.

Despite the questionable sodium analysis previously mentioned, calcium analysis has not shown any reason to be unreliable. As such, the calcium values are trusted.

**Magnesium ($Mg^{2+}$)**

OLI Stream Analyzer (OLI Systems Inc, 2008) does not predict any magnesium salt formation and the cause of the magnesium is as yet unknown. Present at a concentration of only 0.06wt% however, it can be disregarded as an impurity for most applications.

It is important to note that the concentration of an impurity is not the only factor when considering if a salt can be considered impure or not. One can only say that a salt is impure in the context of its application. While the PGM brine has a lower concentration of impurities compared to the coal power plant brine, the most significant impurity is selenium. Selenium is toxic, and sodium selenate is especially so. This might greatly limit its potential application for health and environmental reasons. The coal power plant salt on the other hand, while less pure overall than the PGM salt, is likely to only contain potassium and phosphate, which can be regarded as being benign and non-toxic in far more applications.

**Other impurities**

Though noticeable concentrations of potentially toxic elements Boron and Strontium were detected in the brine, they were not found in appreciable quantities in the salt product. It is likely that these substances were successfully rejected by the crystallizing sodium sulphate, and does not appear they are of immediate interest for future study.

# 8 Conclusions and recommendations

## 8.1 PGM brine

It was found that highly pure sodium sulphate (99.5%) could be recovered from the PGM brine. The unpredicted presence of selenium was also found however, and this prompted further investigation.

The results in sections 5 and 5.3 indicate quite conclusively that selenium is not present as a liquid inclusion. Due the fact that chloride, which is the most concentrated non-crystallizing species present in the brine, is not a major contaminant, it can be concluded that liquid inclusion is not a significant contributor to the uptake of impurities in this system.

In section 6.1 it can be determined that selenium is present in the form of selenate, and that selenate's similar structure and properties to sulphate allowed it to be isomorphously included in the sodium sulphate crystals. It is possible that selenium is present in other forms as well, but it is specifically the selenate form that manifests as an impurity. This serves to further substantiate the theory that selenium is included as an isomorphous substitution. Modelling work done in 5.3 gives evidence of the structural and electrostatic similarities between selenate and sulphate that allow selenate to be incorporated in place of sulphate.

Section 6.2 investigated the impact that other dissolved components have on the uptake of impurities. It was found that the high concentration of sodium chloride in the brine promoted the uptake of selenate. This was shown in both sections 6.2.2 and 6.3. It was theorised that the impact of sodium chloride was due to the effect of the common sodium ion. It was believed that the common ion effect between sodium sulphate, sodium selenate and sodium chloride might have an impact on the solubility of sodium selenate relative to sodium sulphate. This proved not to be the case however. In section 6.2.1, a theoretical analysis of this was performed with a simple model, and it illustrated that while the solubility of sodium sulphate is affected by the presence of sodium chloride, both sodium sulphate and sodium selenate are similarly affected, and the solubility of one does not change relative to the other.

In addition to further illustrating the impact of excess sodium on the uptake of selenium, section 6.3 investigated if it was the increased ionic strength of the solution that caused the increased uptake of selenium. Here it was found that there was no correlation between increasing ionic strength and the amount of impurity uptake. This, in addition to the fact that sodium chloride had a far greater impact on the uptake of selenium than potassium chloride, led to the

conclusion that it was specifically the presence of the excess sodium ions that were promoting the uptake of the selenium impurity.

The impact of mass deposition rate on the uptake of selenium by sodium sulphate was investigated in section 6.4. It was believed that at higher mass deposition rates there is an increased probability that selenate is accidentally incorporated into the growing sodium sulphate crystals. Experiments were conducted where sodium sulphate/sodium chloride solutions with varying sodium selenate concentrations were cooled at different rates. Despite the experiments achieving consistent mass deposition rates, there did not appear to be a correlation between deposition rate and impurity uptake.

It is unlikely that the selenium impurity can be significantly decreased by process by decreasing the cooling rate, because the uptake is not greatly affected by mass deposition rates. The impurity is facilitated by the similarity between selenate and selenite. To decrease the uptake of selenium, the concentration of selenate ions in the brine must be reduced.

Though investigation shows that the PGM brine can produce a high purity product salt of at least 99.5%, it must be noted however that the presence of selenium might severely limit the saleability of the salt. Because selenium is considered both toxic and environmentally unfriendly, it is likely that many potential customers will be unable to accept it. Purity constraints are however subject to the requirements of its intended use, and the small amount of selenium need not necessarily render the sodium sulphate completely without use.



## 8.2 Coal power plant brine

This study showed that both potassium and phosphorus from the coal power plant brine are being concentrated in the product sodium sulphate. It is possible that potassium is included as either an isomorphous substitution, or as separate double salt. Regardless of the nature of the impurity, it can be seen that the amount of potassium contamination is substantial, accounting for 5.5% of the total mass of the salt. It is unlikely that potassium contamination is a result of the formation of a separate salt. The mechanism of the phosphorous impurity is unknown.

It appears as though the formation of calcium sulphate ($CaSO_4$) along with sodium sulphate is unavoidable, leading to a small amount of salt contamination. This is not anticipated to be of immediate concern because of the small impact on purity. In addition to this, calcium sulphate forms an insoluble precipitate. It is believed that that it can be rinsed off the surface of the sodium sulphate crystals in a suitable washing process.

All other impurities were found to be in low enough concentrations to be ignored. Though the overall impurity of the sodium sulphate salt is low, it might still find application because the impurities can be considered to be non-toxic, and relatively benign. The usefulness of this salt will have to be investigated further, as will the specific nature of the impurities.

## 8.3 Recommendations

### *8.3.1 Recommendations for further investigation into salt impurities*

- Improve brine and salt analysis techniques. Throughout this project, accurate brine and salt analysis represented a continual area of concern. Before further work is continued in the area of salt impurity, it is necessary that consistent and reliable brine and salt analysis techniques are perfected.
- Investigate the impact of seeding on the uptake of isomorphous impurities. This work has not yet investigated if seeding could have an impact on the uptake of impurities.
- Investigate the impact of agitation on the uptake of isomorphous impurity. Throughout this work it was assumed that sufficient agitation was achieved to prevent mass transfer limitations to impact on the outcome of the experiment. It is still necessary however, to investigate how much of an impact agitation can have on the uptake of isomorphous impurities.
- Investigate the temperature dependence on the uptake of impurities. As was previously mentioned, impurity uptake is dependent on how soluble one substance is in another. Because solubility can be temperature dependent, it is necessary to investigate if impurity uptake can be controlled by manipulating the temperature at which crystallization occurs.

### *8.3.2 Recommendations for further investigation into coal power plant salt*

- Investigate nature of potassium uptake. The exact nature of the potassium uptake has not been confirmed. It is not yet know if the potassium is present as an isomorphous substitution, or some sort of double salt, or as a separate potassium salt.
- Investigate nature of phosphorous uptake. In addition to potassium, phosphorous is also present in quantities significant enough to justify further investigation.
- Investigate if calcium sulphate can be washed from the salt. It was predicted that calcium sulphate could be washed from the sodium sulphate, but this is yet to be validated.

# 9 Summary

The essence of this thesis was to establish and present the most important factors impacting on the purity of salts crystallised out of industrial brine.

The most significant finding in this work has been that isomorphous substitution is, by a large margin, the most significant mechanism by which impurities are taken up in the EFC of industrial brines. Liquid inclusions and entrainment are not important factors when compared to isomorphous substitution. While they possibly do contribute to impurity uptake, the primary area of interest is with isomorphous substitution.

This finding serves to focus further research into the issue of impurities in crystals formed by Eutectic Freeze Crystallization. Future studies can therefore, within the framework of isomorphous substitution, investigate in greater detail the issues that were touched on in the project.

# 10 Works Cited


Aiello, R., Nagy, J., Girodano, G., Katavic, A. and Testa, F. (2005) 'Isomorphous Substitution in Zeolites', *ChemInform*, vol. 36, no. 33.

Belyustin, A. and Fridman, S. (1968) 'Trapping of Solution by a Growing Crystal', *Soviet Physics - Crystallography Vol 13, No. 2*, vol. 13, no. 2, March, pp. 363-365.

Bohm, J. (1985) 'The Early History of Crystallization', *Acta Physica Hungarica*, vol. 57, no. 3-4, pp. 161-178.

Brooks, R., Horton, A. and Ferguson, J. (1968) 'Occlusion of Mother Liquor in Solution Grown Crystal', *J. Cryst. Growth*, vol. 2, p. 279.

Burton, J., Prim, R. and Slichter, P. (1953) *J. Chem. Phys*, vol. 21, no. 11, pp. 1987-1996.

Chernov, A. (1963) *Soviet Phys. Cryst.*, vol. 8, p. 63.

Denbigh, K. and White, E. (1966) 'Studies of liquid inclusions in crystals', *Chem. Eng. Sci.*, vol. 21, p. 739.

Edie, D. and Kirwan, D. (1973) 'Impurity trapping during crystallization from melts ', *Ind. Eng. Chem. Fund.*, vol. 12, p. 100.

Gaussian 03, Revision 03, Frisch, M. J.; Trucks, G. W.; Schlegel, H. B.; Scuseria, G. E.; Robb, M. A.; Cheeseman, J. R.; Montgomery, Jr., J. A.; Vreven, T.; Kudin, K. N.; Burant, J. C.; Millam, J. M.; Iyengar, S. S.; Tomasi, J.; Barone, V.; Mennucci, B. (2004) 'Gussian 03', *Gaussian Inc., Wallingford CT*.

Kirkova, E., Djarova, M. and Donkova, B. (1996) 'Inclusion of Isomorphous Impurities During Crystallization from Solutions', *Prog. Crystal Growth and Charact.*, vol. 32, pp. 111-134.

Lewis, A., Nathoo, J., Thomsen, K., Kramer, H., Witkamp, G., Reddy, S. and Randall, D. (2010) 'Design of Eutectic Freeze Crystallization Procees for Multicomponent Wastewater Stream', *Chem Eng Res Des*, vol. 88, pp. 1290-1296.

Liu, H. and Papangelakis, V.G. (2005) 'Chemical modeling of high temperature aqueous processes', *Hydrometallurgy*, vol. 79, no. 1-2, September, pp. 48-61.

Myerson, A. (2002) 'Handbook of Industrial Crystallization', pp. 67-100.

Myerson, A. and Kirwan, D. (1977) 'Impurity capture during crystal growth', *Ind. Chem. Ind. Fundam*, vol. 16, no. 4, pp. 414-420.

OLI Systems (2011) 'http://www.olisystems.com', Available: http://www.olisystems.com/mixedSolventElec.htm [9 September 2011].

OLI Systems Inc (2008) 'Oli Stream analyser, Version 2.0.57', Morris plains (New Jersey, USA).

Reddy, S. and Lewis, A. (2009) 'Waste minimisation through recovery of salt and water from a hypersaline brine', Mine Water and Innovative thinking, Wolkersdorfer, 179-183.

Reddy, S., Lewis, A., Witkamp, G., Kramer, H. and van Spronsen, J. (2010) 'Recovery of Na2SO4·10H2O from a reverse osmosis retentate by eutectic freeze crystallisation technology', *Chem Eng Res Des*, vol. 88, no. 9, September, pp. 1153-1157.

Saito, N., Yakota, M., Akira, S. and Noriaki, S. (1999) 'Growth Enhancement and Liquid-Inclusion Formation by Contacts on NaCl Crystal', *AIChE Journal*, vol. 45, no. 5, pp. 1153-1156.

Saito, N., Yakota, M., Fujiwara, T. and Kubota, N. (2001) 'A note of the purity of crystals produced in batch crystallization', *Chemical Engineering Journal 84*, pp. 573-575.

Saito, N., Yokota, M., Fujiwara, T. and Kubota, N. (2000) 'Liquid inclusions in crystals produced in suspension crystallization', *Chemical Engineering Journal*, vol. 79, pp. 53-59.

Slaminko, P. and Myerson, A. (1981) 'The effect of crystal size on occlusion formation during crystallization from solution', *AiChe Journal*, vol. 27, no. 6, pp. 1029-1031.

van der Ham, F., Witkamp, G., de Graauw, J. and van Rosmalen, G. (1997) 'Eutectic Freeze Crystallization: Application to process streams and waste water management', *Chemical Engineering and Processing*, vol. 37, October, pp. 207-213.

van der Ham, F., Witkamp, G., de Graauw, J. and van Rosmalen, G. (1999) 'Eutectic freeze crystallization simultaneous formation and separation of two solid phases', *Journal of Crystal Growth*, vol. 198/199, pp. 744-748.

Wilcox, R. (1968) 'Removing inclusions from crystals by gradient techniques', *Ind. Eng. Chem.*, vol. 60, no. 3, March, pp. 12-23.

Zerfoss, S. and Slawson, S. (1956) 'Origin of Authigenic Inclusions in Synthetic Crystals', *American Mineroligist*, vol. 46, no. 7.

Zhang, G. and Grant, D. (1999) 'Incorporation mechanism of guest molecules in crystals: solid solution or inclusion', *International journal of pharmaceutics*, vol. 181, pp. 61-70.

# 11 Appendix

## 11.1 Data for selenate vs selenite experiment

**Table 8: Experimental matrix for selenate vs selenite experiment**

| | Vol of prepared solutions added (ml) | | | | Stirrer |
|---|---|---|---|---|---|
| Sample | $Na_2SeO_4$ | $Na_2SeO_4$ | $Na_2SO_4$ | NaCl | |
| | 150 g/l | 150 g/l | 108 g/l | 90 g/l | |
| 1 | 1.33 | - | | 200 | A |
| 2 | 1.33 | - | | 200 | A |
| 3 | 1.33 | - | | 200 | A |
| 4 | - | 1.33 | | 200 | B |
| 5 | - | 1.33 | | 200 | B |
| 6 | - | 1.33 | | 200 | B |
| 7 | 1.73 | - | | 200 | B |
| 8 | 1.73 | - | | 200 | B |
| 9 | 1.73 | - | | 200 | B |
| 10 | - | 1.73 | | 200 | A |
| 11 | - | 1.73 | | 200 | A |
| 12 | - | 1.73 | | 200 | A |
| 13 | 2.13 | - | | 200 | A |
| 14 | 2.13 | - | | 200 | A |
| 15 | 2.13 | - | | 200 | A |
| 16 | - | 2.13 | | 200 | B |
| 17 | - | 2.13 | | 200 | B |
| 18 | - | 2.13 | | 200 | B |
| 19 | 2.53 | - | | 200 | B |
| 20 | 2.53 | - | | 200 | B |
| 21 | 2.53 | - | | 200 | B |
| 22 | - | 2.53 | | 200 | A |
| 23 | - | 2.53 | | 200 | A |
| 24 | - | 2.53 | | 200 | A |
| 25 | 2.93 | - | | 200 | A |
| 26 | 2.93 | - | | 200 | A |
| 27 | 2.93 | - | | 200 | A |
| 28 | - | 2.93 | | 200 | B |
| 29 | - | 2.93 | | 200 | B |
| 30 | - | 2.93 | | 200 | B |

The table to the left represents the experimental matrix described in section 6.1.1 on pg 32.

The "volume of prepared solutions added" represents the required volume of prepared solutions that were added to achieve the concentrations describe in Table 9. The prepared standard solutions had the following concentrations.

$Na_2SeO_4$ = 150 g/l

$Na_2SeO_3$ = 150 g/l

The stirrer column refers to which group of stirrers was used. There were six stirrers used. Three of them were referred to as group A, and the other three were group B. Between each experiment, the beakers containing selenite and selenate were swapped between group A and B.

**Table 9: Selenium in sodium sulphate salt as a result of sodium selenate in brine**

| Sample | Conc in brine (g/l) | | | Se in salt (mg/kg) |
|---|---|---|---|---|
| | $Na_2SeO_4$ | $Na_2SO_4$ | NaCl | |
| **1** | 1.00 | 108.00 | 90.00 | 2228.3 |
| **2** | 1.00 | 108.00 | 90.00 | 2200.6 |
| **3** | 1.00 | 108.00 | 90.00 | 2350.0 |
| **4** | 1.30 | 108.00 | 90.00 | 2965.2 |
| **5** | 1.30 | 108.00 | 90.00 | 2987.6 |
| **6** | 1.30 | 108.00 | 90.00 | 3003.1 |
| **7** | 1.60 | 108.00 | 90.00 | 3477.1 |
| **8** | 1.60 | 108.00 | 90.00 | 4025.8 |
| **9** | 1.60 | 108.00 | 90.00 | 3744.9 |
| **10** | 1.90 | 108.00 | 90.00 | 4735.4 |
| **11** | 1.90 | 108.00 | 90.00 | 4208.6 |
| **12** | 1.90 | 108.00 | 90.00 | 4355.6 |
| **13** | 2.20 | 108.00 | 90.00 | 4459.1 |
| **14** | 2.20 | 108.00 | 90.00 | 4353.8 |
| **15** | 2.20 | 108.00 | 90.00 | 4728.0 |

The table to the left represents the experiment described in section 6.1.1 on pg 32.

The 'Conc. in brine' columns refer to the concentrations of dissolved salts in the mother liquor. The 'Se in salt' column indicates the resulting selenium concentration in the produced sodium sulphate salt.

**Table 10: Selenium in sodium sulphate salt as a result of sodium selenite in brine**

| Sample | Conc in brine (g/l) | | | Se in salt (mg/kg) |
|---|---|---|---|---|
| | $Na_2SeO_3$ | $Na_2SO_4$ | NaCl | |
| **1** | 1.00 | 108.00 | 90.00 | 226.9 |
| **2** | 1.00 | 108.00 | 90.00 | 235.0 |
| **3** | 1.00 | 108.00 | 90.00 | 209.1 |
| **4** | 1.30 | 108.00 | 90.00 | 263.1 |
| **5** | 1.30 | 108.00 | 90.00 | 271.3 |
| **6** | 1.30 | 108.00 | 90.00 | 248.2 |
| **7** | 1.60 | 108.00 | 90.00 | 315.4 |
| **8** | 1.60 | 108.00 | 90.00 | 341.0 |
| **9** | 1.60 | 108.00 | 90.00 | 252.5 |
| **10** | 1.90 | 108.00 | 90.00 | 492.7 |
| **11** | 1.90 | 108.00 | 90.00 | 360.7 |
| **12** | 1.90 | 108.00 | 90.00 | 440.6 |
| **13** | 2.20 | 108.00 | 90.00 | 328.0 |
| **14** | 2.20 | 108.00 | 90.00 | 401.0 |
| **15** | 2.20 | 108.00 | 90.00 | 343.2 |

The table to the left represents the experiment described in section 6.1.1 on pg 32.

The 'Conc. in brine' columns refer to the concentrations of dissolved salts in the mother liquor. The 'Se in salt' column indicates the resulting selenium concentration in the produced sodium sulphate salt.

## 11.2 Data for impact of NaCl on uptake of selenium by sodium sulphate

**Table 11: Volume of standard solutions added to 200 ml samples**

| Sample | g/l | | | | ml standard added to 200 ml sample | | |
|---|---|---|---|---|---|---|---|
| | $Na_2SeO_4$ | $Na_2SO_4$ | NaCl | | $Na_2SeO_4$ | $Na_2SO_4$ | NaCl |
| **1** | 1.20 | 108.00 | 10.00 | | 1.59 | 127 | 7 |
| **2** | 2.39 | 108.00 | 10.00 | | 3.19 | 127 | 7 |
| **3** | 3.59 | 108.00 | 10.00 | | 4.78 | 127 | 7 |
| **4** | 4.78 | 108.00 | 10.00 | | 6.38 | 127 | 7 |
| **5** | 5.98 | 108.00 | 10.00 | | 7.97 | 127 | 7 |
| **6** | 7.18 | 108.00 | 10.00 | | 9.57 | 127 | 7 |
| **7** | 1.20 | 108.00 | 50.00 | | 1.59 | 127 | 33 |
| **8** | 2.39 | 108.00 | 50.00 | | 3.19 | 127 | 33 |
| **9** | 3.59 | 108.00 | 50.00 | | 4.78 | 127 | 33 |
| **10** | 4.78 | 108.00 | 50.00 | | 6.38 | 127 | 33 |
| **11** | 5.98 | 108.00 | 50.00 | | 7.97 | 127 | 33 |
| **12** | 7.18 | 108.00 | 50.00 | | 9.57 | 127 | 33 |
| **13** | 1.20 | 108.00 | 90.00 | | 1.59 | 127 | 60 |
| **14** | 2.39 | 108.00 | 90.00 | | 3.19 | 127 | 60 |
| **15** | 3.59 | 108.00 | 90.00 | | 4.78 | 127 | 60 |
| **16** | 4.78 | 108.00 | 90.00 | | 6.38 | 127 | 60 |
| **17** | 5.98 | 108.00 | 90.00 | | 7.97 | 127 | 60 |
| **18** | 7.18 | 108.00 | 90.00 | | 9.57 | 127 | 60 |
| **19** | 1.20 | 30.00 | 90.00 | | 1.59 | 35 | 60 |
| **20** | 2.39 | 30.00 | 90.00 | | 3.19 | 35 | 60 |
| **21** | 3.59 | 30.00 | 90.00 | | 4.78 | 35 | 60 |
| **22** | 4.78 | 30.00 | 90.00 | | 6.38 | 35 | 60 |
| **23** | 5.98 | 30.00 | 90.00 | | 7.97 | 35 | 60 |
| **24** | 7.18 | 30.00 | 90.00 | | 9.57 | 35 | 60 |
| **25** | 1.20 | 50.00 | 90.00 | | 1.59 | 59 | 60 |
| **26** | 2.39 | 50.00 | 90.00 | | 3.19 | 59 | 60 |
| **27** | 3.59 | 50.00 | 90.00 | | 4.78 | 59 | 60 |
| **28** | 4.78 | 50.00 | 90.00 | | 6.38 | 59 | 60 |
| **29** | 5.98 | 50.00 | 90.00 | | 7.97 | 59 | 60 |
| **30** | 7.18 | 50.00 | 90.00 | | 9.57 | 59 | 60 |
| **31** | 1.20 | 80.00 | 90.00 | | 1.59 | 94 | 60 |
| **32** | 2.39 | 80.00 | 90.00 | | 3.19 | 94 | 60 |
| **33** | 3.59 | 80.00 | 90.00 | | 4.78 | 94 | 60 |
| **34** | 4.78 | 80.00 | 90.00 | | 6.38 | 94 | 60 |
| **35** | 5.98 | 80.00 | 90.00 | | 7.97 | 94 | 60 |
| **36** | 7.18 | 80.00 | 90.00 | | 9.57 | 94 | 60 |

The table to the left represents the experiment described in section 6.2 on pg 38. The values in the 'g/l' column are the final concentrations of the salts in each synthetic brine sample. The values in the 'ml standard added to 200 ml sample' represent the volumes of standard solution added to each beaker to achieve the concentrations required in the 'g/l' column. The standard solutions were

NaCl – 300 g/l

$Na_2SO_4$ – 170 g/l

$Na_2SeO_4$ – 150 g/l

**Table 12: Results from investigation into impact of NaCl on uptake of selenium by sodium sulphate**

| Sample | NaCl in brine (g/l) | $Na_2SO_4$ in brine (g/l) | $Na_2SeO_4$ in brine (g/l) | Se in salt (mg/kg) |
|---|---|---|---|---|
| **1** | 2.00 | 21.60 | 0.24 | 20.2 |
| **2** | 2.00 | 21.60 | 0.48 | 61.0 |
| **3** | 2.00 | 21.60 | 0.72 | 68.8 |
| **4** | 2.00 | 21.60 | 0.96 | 74.8 |
| **5** | 2.00 | 21.60 | 1.20 | 104.0 |
| **6** | 2.00 | 21.60 | 1.44 | 112.3 |
| **7** | 10.00 | 21.60 | 0.24 | 26.6 |
| **8** | 10.00 | 21.60 | 0.48 | 42.0 |
| **9** | 10.00 | 21.60 | 0.72 | 81.6 |
| **10** | 10.00 | 21.60 | 0.96 | 92.8 |
| **11** | 10.00 | 21.60 | 1.20 | 105.8 |
| **12** | 10.00 | 21.60 | 1.44 | 135.1 |
| **13** | 18.00 | 21.60 | 0.24 | 40.4 |
| **14** | 18.00 | 21.60 | 0.48 | 85.5 |
| **15** | 18.00 | 21.60 | 0.72 | 127.5 |
| **16** | 18.00 | 21.60 | 0.96 | 141.7 |
| **17** | 18.00 | 21.60 | 1.20 | 195.4 |
| **18** | 18.00 | 21.60 | 1.44 | 156.0 |
| **19** | 18.00 | 6.00 | 0.24 | 71.6 |
| **20** | 18.00 | 6.00 | 0.48 | 146.3 |
| **21** | 18.00 | 6.00 | 0.72 | 203.5 |
| **22** | 18.00 | 6.00 | 0.96 | 242.0 |
| **23** | 18.00 | 6.00 | 1.20 | 270.6 |
| **24** | 18.00 | 6.00 | 1.44 | 318.5 |
| **25** | 18.00 | 10.00 | 0.24 | 57.0 |
| **26** | 18.00 | 10.00 | 0.48 | 100.5 |
| **27** | 18.00 | 10.00 | 0.72 | 146.4 |
| **28** | 18.00 | 10.00 | 0.96 | 172.2 |
| **29** | 18.00 | 10.00 | 1.20 | 212.2 |
| **30** | 18.00 | 10.00 | 1.44 | 257.3 |
| **31** | 18.00 | 16.00 | 0.24 | 41.6 |
| **32** | 18.00 | 16.00 | 0.48 | 71.8 |
| **33** | 18.00 | 16.00 | 0.72 | 104.6 |
| **34** | 18.00 | 16.00 | 0.96 | 142.0 |
| **35** | 18.00 | 16.00 | 1.20 | 147.9 |
| **36** | 18.00 | 16.00 | 1.44 | 185.5 |

The table to the left represents the results from the experiment described in section 6.2 on page 38.

The first column represents the sample number, and the following three columns represent the various concentrations of the dissolved salts. The final column shows the resulting detected selenium impurity in the product sodium sulphate salt. This data is represent in the report in Figure 20 and Figure 21.

## 11.3 Data for investigation into impact of ionic strength on uptake of selenium by sodium sulphate

**Table 13: Volume of standard solutions added to 200 ml samples**

| Sample | g/l | | | | | ml standard added to 200 ml sample | | |
|---|---|---|---|---|---|---|---|---|
| | $Na_2SeO_4$ | $Na_2SO_4$ | NaCl | KCl | | Syn Brine | NaCl | KCl |
| **1** | 110 | 1.68 | 70 | 0 | | 100 | 70 | 0 |
| **2** | 110 | 1.68 | 70 | 0 | | 100 | 70 | 0 |
| **3** | 110 | 1.68 | 70 | 0 | | 100 | 70 | 0 |
| **4** | 110 | 1.68 | 80 | 0 | | 100 | 80 | 0 |
| **5** | 110 | 1.68 | 80 | 0 | | 100 | 80 | 0 |
| **6** | 110 | 1.68 | 80 | 0 | | 100 | 80 | 0 |
| **7** | 110 | 1.68 | 90 | 0 | | 100 | 90 | 0 |
| **8** | 110 | 1.68 | 90 | 0 | | 100 | 90 | 0 |
| **9** | 110 | 1.68 | 90 | 0 | | 100 | 90 | 0 |
| **10** | 110 | 1.68 | 100 | 0 | | 100 | 100 | 0 |
| **11** | 110 | 1.68 | 100 | 0 | | 100 | 100 | 0 |
| **12** | 110 | 1.68 | 100 | 0 | | 100 | 100 | 0 |
| **13** | 110 | 1.68 | 0 | 70 | | 100 | 0 | 70 |
| **14** | 110 | 1.68 | 0 | 70 | | 100 | 0 | 70 |
| **15** | 110 | 1.68 | 0 | 70 | | 100 | 0 | 70 |
| **16** | 110 | 1.68 | 0 | 80 | | 100 | 0 | 80 |
| **17** | 110 | 1.68 | 0 | 80 | | 100 | 0 | 80 |
| **18** | 110 | 1.68 | 0 | 80 | | 100 | 0 | 80 |
| **19** | 110 | 1.68 | 0 | 90 | | 100 | 0 | 90 |
| **20** | 110 | 1.68 | 0 | 90 | | 100 | 0 | 90 |
| **21** | 110 | 1.68 | 0 | 90 | | 100 | 0 | 90 |
| **22** | 110 | 1.68 | 0 | 100 | | 100 | 0 | 100 |
| **23** | 110 | 1.68 | 0 | 100 | | 100 | 0 | 100 |
| **24** | 110 | 1.68 | 0 | 100 | | 100 | 0 | 100 |

The table to the left represents the experiment described in section 6.3 on page 47. The values in the 'g/l' column are the final concentrations of the salts in each brine sample. The values in the 'ml standard added to 200 ml sample' represent the volumes of standard solution added to each beaker to achieve the concentrations required in the 'g/l' column. The standard solutions were

NaCl – 200 g/l

KCl – 200 g/l

Syn Brine refers to a synthetic brine containing both sodium sulphate and sodium selenate.

$Na_2SO_4$ – 220 g/l

$Na_2SeO_4$ – 3.36 g/l

**Table 14: Results from investigation into impact of ionic strength on impurity uptake**

| Sample | g/l | | | | Se in salt (mg/kg) | |
|---|---|---|---|---|---|---|
| | $Na_2SeO_4$ | $Na_2SO_4$ | NaCl | KCl | | Avg |
| **1** | 110 | 1.68 | 70 | 0 | 5473.0 | |
| **2** | 110 | 1.68 | 70 | 0 | 4768.0 | |
| **3** | 110 | 1.68 | 70 | 0 | 4409.7 | 4883.5 |
| **4** | 110 | 1.68 | 80 | 0 | 4614.9 | |
| **5** | 110 | 1.68 | 80 | 0 | 4286.5 | |
| **6** | 110 | 1.68 | 80 | 0 | 4319.2 | 4406.8 |
| **7** | 110 | 1.68 | 90 | 0 | 5340.9 | |
| **8** | 110 | 1.68 | 90 | 0 | 4497.8 | |
| **9** | 110 | 1.68 | 90 | 0 | 4388.8 | 4742.5 |
| **10** | 110 | 1.68 | 100 | 0 | 4444.9 | |
| **11** | 110 | 1.68 | 100 | 0 | 4428.9 | |
| **12** | 110 | 1.68 | 100 | 0 | 4824.9 | 4566.2 |
| **13** | 110 | 1.68 | 0 | 70 | 2604.8 | |
| **14** | 110 | 1.68 | 0 | 70 | 2458.1 | |
| **15** | 110 | 1.68 | 0 | 70 | 2408.4 | 2490.4 |
| **16** | 110 | 1.68 | 0 | 80 | 2442.2 | |
| **17** | 110 | 1.68 | 0 | 80 | 2636.6 | |
| **18** | 110 | 1.68 | 0 | 80 | 2650.2 | 2576.3 |
| **19** | 110 | 1.68 | 0 | 90 | 1930.4 | |
| **20** | 110 | 1.68 | 0 | 90 | 2445.8 | |
| **21** | 110 | 1.68 | 0 | 90 | 2495.1 | 2290.4 |
| **22** | 110 | 1.68 | 0 | 100 | 1803.9 | |
| **23** | 110 | 1.68 | 0 | 100 | 1698.2 | |
| **24** | 110 | 1.68 | 0 | 100 | 1962.3 | 1821.4 |

The table to the left represents the results from the experiment described in section 6.3 on page 47.

The first column represents the sample number, and the following four columns represent the various concentrations of the dissolved salts. The final column shows the resulting detected selenium impurity in the product sodium sulphate salt. This data is represented in the report in Figure 26.

## 11.4 Raw data for impact of mass deposition rate on the uptake of selenium

The following tables represent the raw data from the investigation into the impact of mass deposition rate on the uptake of selenium by sodium sulphate.

**Table 15: Results from cooling of 1.0 g/l sodium selenate brine at 1°C/hr**

| **Selenium in brine** | **1.0 g/l** | **NaCl $Na_2SO_4$** | **90 g/l 108 g/l** | **Cooling rate** | **1°C/hr** |
|---|---|---|---|---|---|
| **Time** | Temp | | $Na_2SO_4$ mass% of brine | | dm/dt |
| **Minutes** | °C | $SO_4$ % | c | c* | mass%/min |
| **0** | 20 | 7.77 | 11.17 | 10.60 | |
| **240** | 15.9 | 6.36 | 9.14 | 7.30 | |
| **360** | 13.8 | 5.3 | 7.62 | 5.97 | 0.01 |
| **480** | 12.1 | 4.46 | 6.41 | 5.04 | 0.01 |
| **600** | 10 | 3.4 | 4.89 | 4.08 | 0.01 |
| **720** | 7.8 | 2.92 | 4.20 | 3.24 | 0.01 |
| **840** | 6.3 | 2.26 | 3.25 | 2.77 | 0.01 |
| **960** | 4.5 | 1.72 | 2.47 | 2.29 | 0.01 |
| **1080** | 2.5 | 1.45 | 2.08 | 1.85 | 0.01 |
| **1200** | 0.1 | 1.21 | 1.74 | 1.43 | 0.01 |
| **1320** | -2 | 0.78 | 1.12 | 1.13 | 0.01 |
| **1440** | -2.9 | 0.66 | 0.95 | 1.01 | 0.01 |
| **Avg** | | | | | 0.01 |

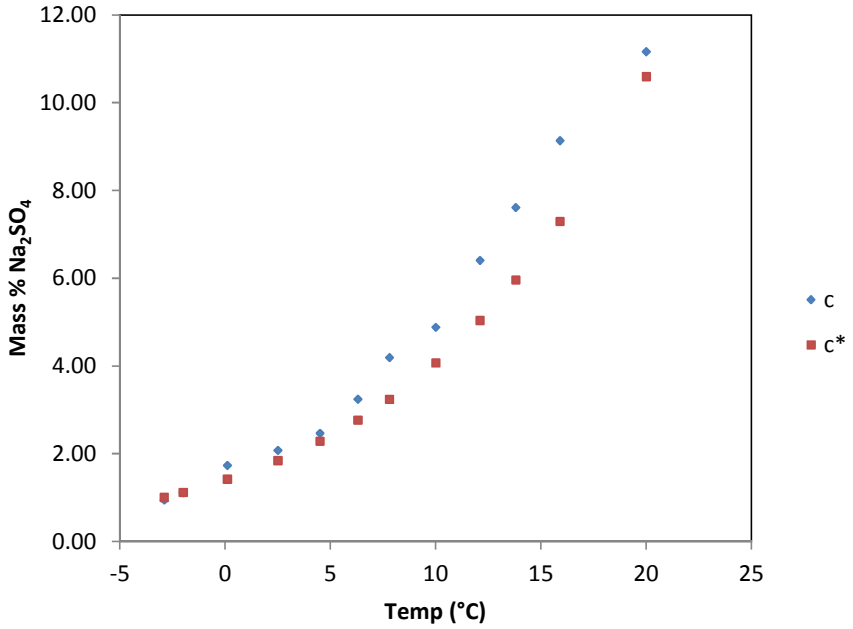


**Figure 44: Sodium sulphate concentration and saturation concentration for 1 g/l $Na_2SeO_4$ and cooling rate of 1°C/hr**

**Table 16: Results from cooling of 1.0 g/l sodium selenate brine at 2°C/hr**

| Selenium in brine | 1.0 g/l | NaCl $Na_2SO_4$ | 90 g/l 108 g/l | Cooling rate | 2°C/hr |
|---|---|---|---|---|---|
| **Time** | Temp | | $Na_2SO_4$ mass% of brine | | dm/dt |
| **Minutes** | °C | $SO_4$ % | c | c* | mass%/min |
| **0** | 20 | 7.91 | 11.37 | 10.60 | |
| **120** | 15.9 | 6.53 | 9.39 | 7.30 | |
| **180** | 13.6 | 5.13 | 7.37 | 5.85 | 0.02 |
| **240** | 11.9 | 4.31 | 6.20 | 4.94 | 0.02 |
| **300** | 10 | 3.38 | 4.86 | 4.08 | 0.02 |
| **360** | 8.2 | 2.64 | 3.80 | 3.38 | 0.02 |
| **420** | 6.2 | 2.22 | 3.19 | 2.74 | 0.02 |
| **480** | 4.4 | 1.65 | 2.37 | 2.27 | 0.02 |
| **540** | 2.5 | 1.48 | 2.13 | 1.85 | 0.02 |
| **600** | 0.7 | 0.98 | 1.41 | 1.52 | 0.03 |
| **660** | -1.2 | 0.76 | 1.09 | 1.23 | 0.02 |
| **720** | -3 | 0.61 | 0.88 | 1.00 | 0.02 |
| **Avg** | | | | | 0.02 |

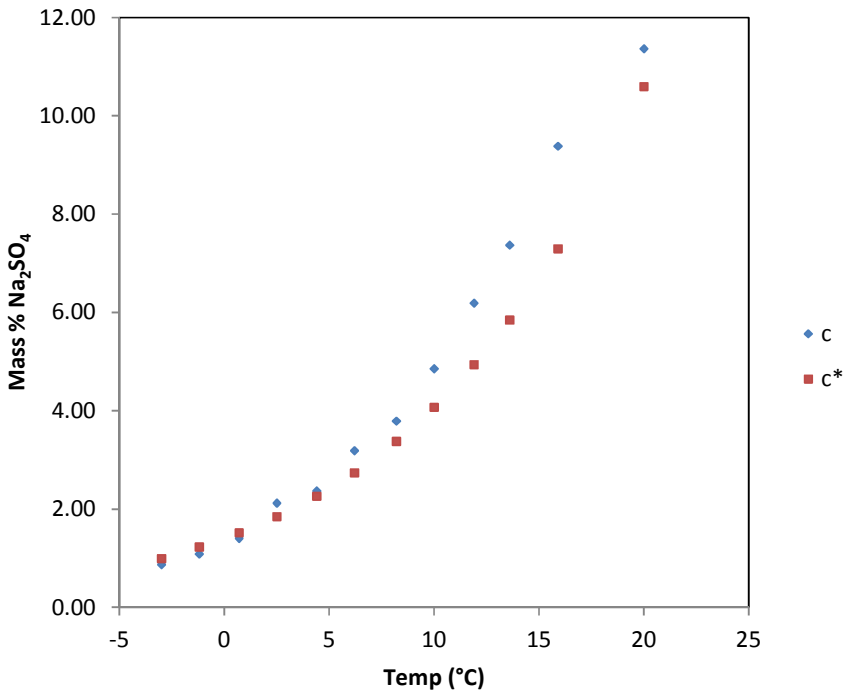


**Figure 45: Sodium sulphate concentration and saturation concentration for 1 g/l $Na_2SeO_4$ and cooling rate of 2°C/hr**

**Table 17: Results from cooling of 1.0 g/l sodium selenate brine at 4°C/hr**

| Selenium in brine | 1.0 g/l | NaCl $Na_2SO_4$ | 90 g/l 108 g/l | Cooling rate | 4°C/hr |
|---|---|---|---|---|---|
| **Time** | Temp | | $Na_2SO_4$ mass% of brine | | dm/dt |
| **Minutes** | °C | $SO_4$ % | c | c* | mass%/min |
| **0** | 20 | 8.31 | 11.95 | 10.60 | |
| **60** | 16 | 5.79 | 8.32 | 7.37 | |
| **90** | 14.5 | 5.41 | 7.78 | 6.39 | 0.04 |
| **120** | 12.4 | 4.36 | 6.27 | 5.20 | 0.04 |
| **150** | 10 | 3.49 | 5.02 | 4.08 | 0.04 |
| **180** | 8.1 | 2.4 | 3.45 | 3.35 | 0.05 |
| **210** | 6.4 | 1.77 | 2.54 | 2.80 | 0.05 |
| **240** | 4.4 | 1.48 | 2.13 | 2.27 | 0.04 |
| **270** | 2.4 | 1.04 | 1.50 | 1.83 | 0.05 |
| **300** | 0.8 | 1 | 1.44 | 1.54 | 0.03 |
| **330** | -2.3 | 0.58 | 0.83 | 1.09 | 0.06 |
| **360** | -3.5 | 0.58 | 0.83 | 0.94 | 0.03 |
| **Avg** | | | | | 0.04 |

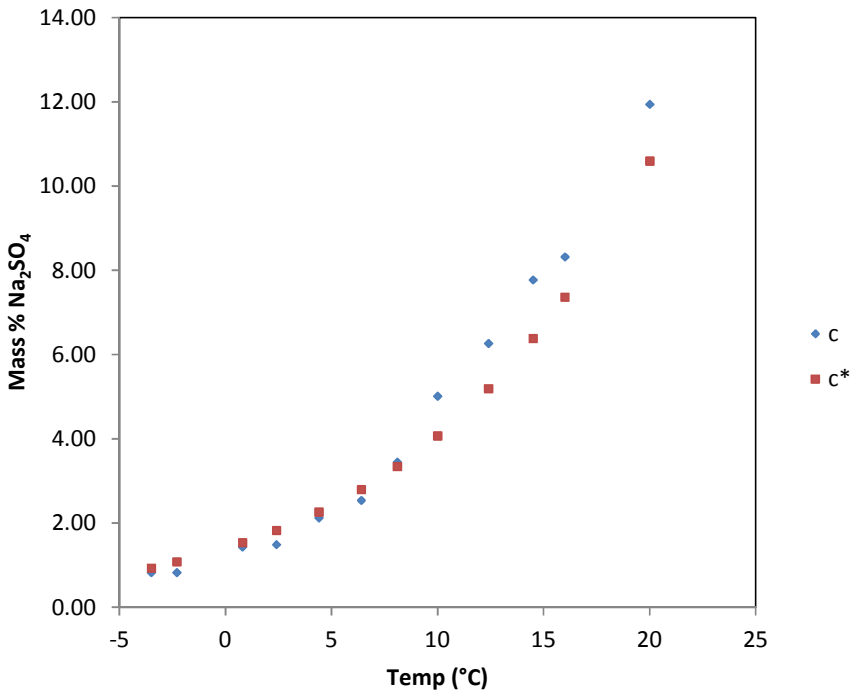


**Figure 46: Sodium sulphate concentration and saturation concentration for 1 g/l $Na_2SeO_4$ and cooling rate of 4°C/hr**

**Table 18: Results from cooling of 1.6 g/l sodium selenate brine at 1°C/hr**

| Selenium in brine | 1.6 g/l | NaCl $Na_2SO_4$ | 90 g/l 108 g/l | Cooling rate | 1°C/hr |
|---|---|---|---|---|---|
| **Time** | Temp | | $Na_2SO_4$ mass% of brine | | dm/dt |
| **Minutes** | °C | $SO_4$ % | c | c* | mass%/min |
| **0** | 20 | 8.35 | 12.00 | 10.60 | |
| **240** | 15.9 | 6.64 | 9.55 | 7.30 | |
| **360** | 13.9 | 5.36 | 7.71 | 6.02 | 0.01 |
| **480** | 12.2 | 4.78 | 6.87 | 5.09 | 0.01 |
| **600** | 10 | 3.16 | 4.54 | 4.08 | 0.01 |
| **720** | 7.8 | 2.78 | 4.00 | 3.24 | 0.01 |
| **840** | 6.3 | 2.26 | 3.25 | 2.77 | 0.01 |
| **960** | 4.5 | 1.63 | 2.34 | 2.29 | 0.01 |
| **1080** | 2.6 | 1.4 | 2.01 | 1.87 | 0.01 |
| **1200** | 0.2 | 0.98 | 1.41 | 1.44 | 0.01 |
| **1320** | -1.9 | 0.76 | 1.09 | 1.14 | 0.01 |
| **1440** | -2.9 | 0.74 | 1.06 | 1.01 | 0.01 |
| **Avg** | | | | | 0.01 |

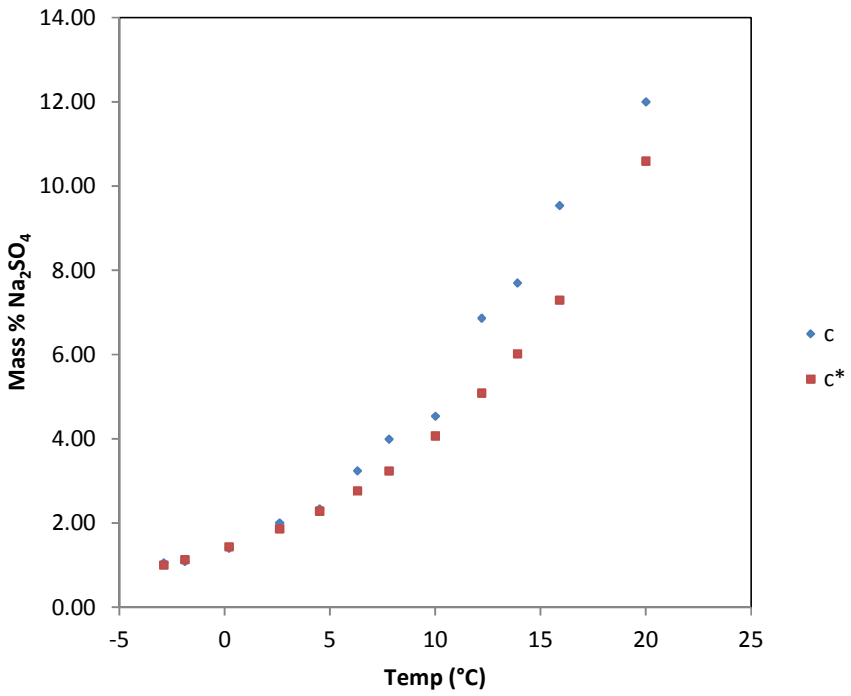


**Figure 47: Sodium sulphate concentration and saturation concentration for 1.6 g/l $Na_2SeO_4$ and cooling rate of 1°C/hr**

**Table 19: Results from cooling of 1.6 g/l sodium selenate brine at 2°C/hr**

| Selenium in brine | 1.6g/l | NaCl $Na_2SO_4$ | 90 g/l 108 g/l | Cooling rate | 2°C/hr |
|---|---|---|---|---|---|
| **Time** | Temp | | $Na_2SO_4$ mass% of brine | | dm/dt |
| **Minutes** | °C | $SO_4$ % | c | c* | mass%/min |
| **0** | 20 | 7.95 | 11.43 | 10.60 | |
| **120** | 16.2 | 6.97 | 10.02 | 7.51 | |
| **180** | 13.7 | 5.2 | 7.48 | 5.91 | 0.02 |
| **240** | 11.9 | 4.4 | 6.33 | 4.94 | 0.02 |
| **300** | 10 | 3.05 | 4.38 | 4.08 | 0.02 |
| **360** | 8.3 | 2.5 | 3.59 | 3.42 | 0.02 |
| **420** | 6.2 | 2.1 | 3.02 | 2.74 | 0.02 |
| **480** | 4.4 | 1.72 | 2.47 | 2.27 | 0.02 |
| **540** | 2.6 | 1.48 | 2.13 | 1.87 | 0.02 |
| **600** | 0.7 | 0.89 | 1.28 | 1.52 | 0.03 |
| **660** | -1.2 | 0.82 | 1.18 | 1.23 | 0.02 |
| **720** | -3 | 0.58 | 0.83 | 1.00 | 0.02 |
| **Avg** | | | | | 0.02 |

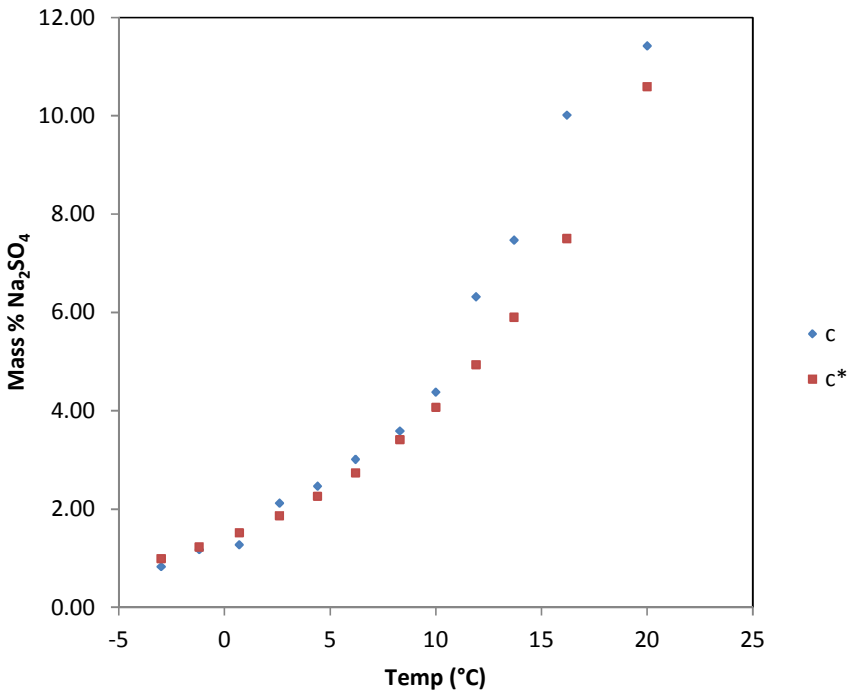


**Figure 48: Sodium sulphate concentration and saturation concentration for 1.6 g/l $Na_2SeO_4$ and cooling rate of 2°C/hr**

**Table 20: Results from cooling of 1.6 g/l sodium selenate brine at 4°C/hr**

| Selenium in brine | 1.6 g/l | NaCl $Na_2SO_4$ | 90 g/l 108 g/l | Cooling rate | 4°C/hr |
|---|---|---|---|---|---|
| **Time** | Temp | | $Na_2SO_4$ mass% of brine | | dm/dt |
| **Minutes** | °C | $SO_4$ % | c | c* | mass%/min |
| **0** | 20 | 8.11 | 11.66 | 10.60 | |
| **60** | 16.8 | 7.33 | 10.54 | 7.94 | |
| **90** | 14.5 | 5.5 | 7.91 | 6.39 | 0.04 |
| **120** | 12.5 | 3.99 | 5.74 | 5.25 | 0.05 |
| **150** | 10 | 3.47 | 4.99 | 4.08 | 0.04 |
| **180** | 8.1 | 2.65 | 3.81 | 3.35 | 0.04 |
| **210** | 6.4 | 2.2 | 3.16 | 2.80 | 0.04 |
| **240** | 4.4 | 1.76 | 2.53 | 2.27 | 0.04 |
| **270** | 2.4 | 1.47 | 2.11 | 1.83 | 0.04 |
| **300** | 0.8 | 0.95 | 1.37 | 1.54 | 0.05 |
| **330** | -2.2 | 0.94 | 1.35 | 1.10 | 0.03 |
| **360** | -3.5 | 0.8 | 1.15 | 0.94 | 0.04 |
| **Avg** | | | | | 0.04 |

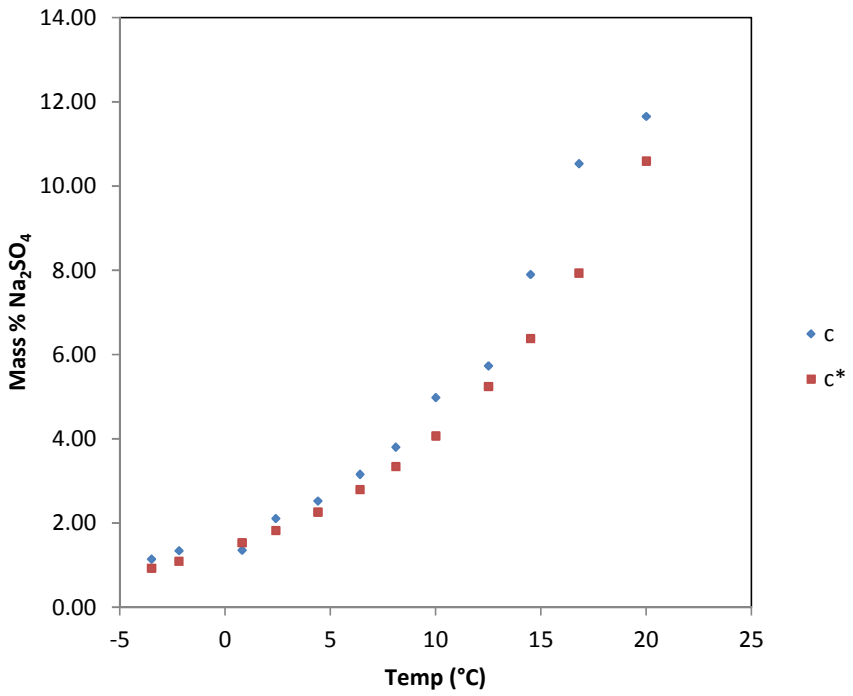


**Figure 49: Sodium sulphate concentration and saturation concentration for 1.6 g/l $Na_2SeO_4$ and cooling rate of 4°C/hr**

**Table 21: Results from cooling of 2.2 g/l sodium selenate brine at 1°C/hr**

| Selenium in brine | 2.2 g/l | NaCl $Na_2SO_4$ | 90 g/l 108 g/l | Cooling rate | 1°C/hr |
|---|---|---|---|---|---|
| **Time** | Temp | | $Na_2SO_4$ mass% of brine | | dm/dt |
| **Minutes** | °C | $SO_4$ % | c | c* | mass%/min |
| **0** | 20 | 7.8 | 11.21 | 10.60 | |
| **240** | 16 | 6.54 | 9.40 | 7.37 | |
| **360** | 14 | 5.36 | 7.71 | 6.08 | 0.01 |
| **480** | 12.2 | 4.38 | 6.30 | 5.09 | 0.01 |
| **600** | 10 | 3.21 | 4.61 | 4.08 | 0.01 |
| **720** | 7.8 | 2.33 | 3.35 | 3.24 | 0.01 |
| **840** | 6.3 | 2.16 | 3.11 | 2.77 | 0.01 |
| **960** | 4.5 | 1.67 | 2.40 | 2.29 | 0.01 |
| **1080** | 2.6 | 1.56 | 2.24 | 1.87 | 0.01 |
| **1200** | 0.2 | 0.92 | 1.32 | 1.44 | 0.01 |
| **1320** | -1.9 | 0.89 | 1.28 | 1.14 | 0.01 |
| **1440** | -2.9 | 0.65 | 0.93 | 1.01 | 0.01 |
| **Avg** | | | | | 0.01 |

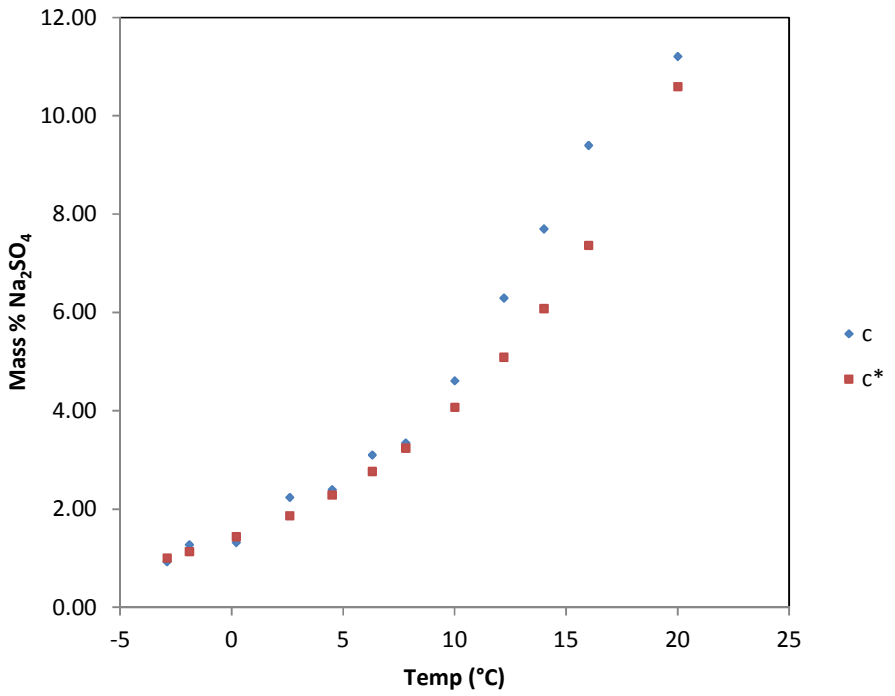


**Figure 50: Sodium sulphate concentration and saturation concentration for 2.2 g/l $Na_2SeO_4$ and cooling rate of 1°C/hr**

**Table 22: Results from cooling of 2.2 g/l sodium selenate brine at 2°C/hr**

| Selenium in brine | 2.2 g/l | NaCl $Na_2SO_4$ | 90 g/l 108 g/l | Cooling rate | 2°C/hr |
|---|---|---|---|---|---|
| **Time** | Temp | | $Na_2SO_4$ mass% of brine | | dm/dt |
| **Minutes** | °C | $SO_4$ % | c | c* | mass%/min |
| **0** | 20 | 7.7 | 11.07 | 10.60 | |
| **120** | 16.1 | 6.95 | 9.99 | 7.44 | |
| **180** | 13.7 | 5.39 | 7.75 | 5.91 | 0.02 |
| **240** | 11.9 | 4.41 | 6.34 | 4.94 | 0.02 |
| **300** | 10.1 | 3.05 | 4.38 | 4.12 | 0.02 |
| **360** | 8.4 | 2.92 | 4.20 | 3.45 | 0.02 |
| **420** | 6.3 | 2.3 | 3.31 | 2.77 | 0.02 |
| **480** | 4.5 | 1.69 | 2.43 | 2.29 | 0.02 |
| **540** | 2.7 | 1.41 | 2.03 | 1.89 | 0.02 |
| **600** | 0.8 | 0.96 | 1.38 | 1.54 | 0.02 |
| **660** | -1 | 0.82 | 1.18 | 1.26 | 0.02 |
| **720** | -3 | 0.64 | 0.92 | 1.00 | 0.02 |
| **Avg** | | | | | 0.04 |

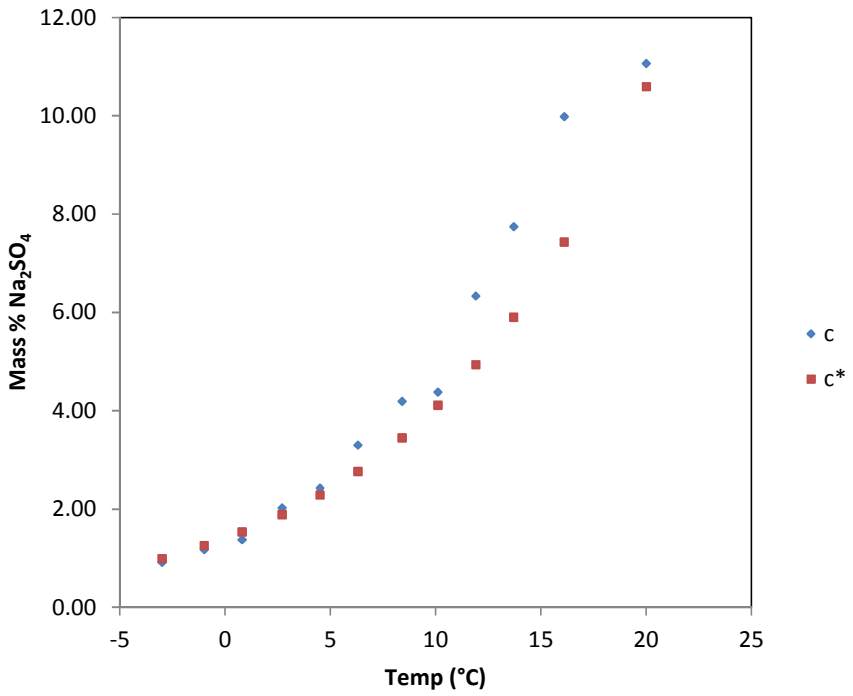


**Figure 51: Sodium sulphate concentration and saturation concentration for 2.2 g/l $Na_2SeO_4$ and cooling rate of 2°C/hr**

**Table 23: Results from cooling of 2.2 g/l sodium selenate brine at 4°C/hr**

| Selenium in brine | 2.2 g/l | NaCl $Na_2SO_4$ | 90 g/l 108 g/l | Cooling rate | 4°C/hr |
|---|---|---|---|---|---|
| **Time** | Temp | | $Na_2SO_4$ mass% of brine | | dm/dt |
| **Minutes** | °C | $SO_4$ % | c | c* | mass%/min |
| **0** | 20 | 8.26 | 11.87 | 10.60 | |
| **60** | 15.8 | 8.03 | 11.54 | 7.23 | |
| **90** | 14.5 | 5.35 | 7.69 | 6.39 | 0.05 |
| **120** | 12.5 | 4.37 | 6.28 | 5.25 | 0.04 |
| **150** | 10 | 3.50 | 5.03 | 4.08 | 0.04 |
| **180** | 8.1 | 2.64 | 3.80 | 3.35 | 0.04 |
| **210** | 6.4 | 2.02 | 2.90 | 2.80 | 0.04 |
| **240** | 4.4 | 1.87 | 2.69 | 2.27 | 0.04 |
| **270** | 2.4 | 1.47 | 2.11 | 1.83 | 0.04 |
| **300** | 0.8 | 0.92 | 1.32 | 1.54 | 0.05 |
| **330** | -2.1 | 0.84 | 1.21 | 1.11 | 0.04 |
| **360** | -3.5 | 0.68 | 0.98 | 0.94 | 0.04 |
| **Avg** | | | | | 0.04 |

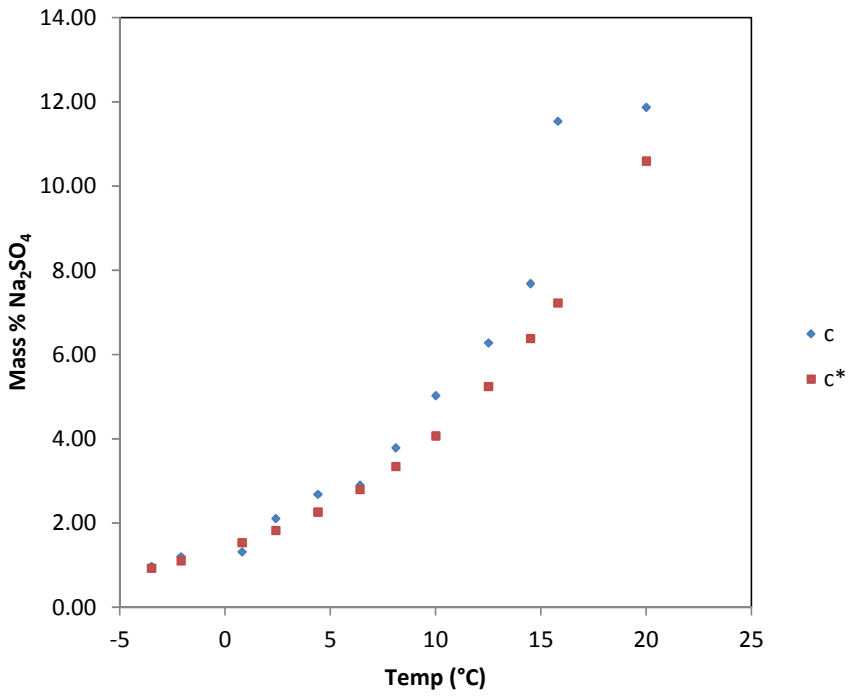


**Figure 52: Sodium sulphate concentration and saturation concentration for 2.2 g/l $Na_2SeO_4$ and cooling rate of 4°C/hr**

**Table 24: Uptake of selenium by sodium sulphate at differing selenium brine concentrations and mass deposition rates**

| | Sei n brine g/l | mass%/min | Se in salt mg/kg |
|---|---|---|---|
| S1 | 1 | 0.01 | 2654.8 |
| S2 | 1.6 | 0.01 | 4740.8 |
| S3 | 2.2 | 0.011 | 7359.4 |
| S4 | 1 | 0.021 | 2053.8 |
| S5 | 1.6 | 0.022 | 3838.0 |
| S6 | 2.2 | 0.021 | 5336.8 |
| S7 | 1 | 0.042 | 2830.6 |
| S8 | 1.6 | 0.043 | 4152.9 |
| S9 | 2.2 | 0.042 | 6314.5 |

The table to the left represents the results from the experiment described in section 6.4.2 on page 57.

The first column represents the sample number. The first column represents the concentration of selenium in the brine. The second column represents the rate of deposition of sodium sulphate, as calculated from Table 15 to Table 23 This data is represented in the report in Figure 31.

## 11.5 Data for investigation into coal power plant brine

**Table 25: Data from salt analysis of coal power plant brine experiment**

| mg/l | TS1 | TS2 | TS3 | TS4 | TS5 | TS6 |
|---|---|---|---|---|---|---|
| B | 0.000 | 0.000 | 0.000 | 0.000 | 0.000 | 0.000 |
| Si | 133.800 | 55.530 | 65.900 | 221.040 | 37.130 | 84.560 |
| Ba | 0.320 | 0.210 | 0.530 | 0.290 | 0.180 | 0.140 |
| Cu | 2.520 | 0.590 | 0.630 | 0.260 | 0.400 | 0.220 |
| P | 1494.000 | 688.500 | 1422.300 | 1423.300 | 696.000 | 1362.900 |
| V | 0.000 | 0.000 | 0.000 | 0.000 | 0.000 | 0.000 |
| Ca | 1816.300 | 254.480 | 2685.500 | 1388.200 | 1889.900 | 2273.500 |
| $Cl_2$ | 0.000 | 5.600 | 0.000 | 0.000 | 6.400 | 0.000 |
| Cd | 0.000 | 0.000 | 0.000 | 0.000 | 0.000 | 0.000 |
| Fe | 7.900 | 7.760 | 19.270 | 13.980 | 5.950 | 6.210 |
| Pb | 0.001 | 0.000 | 0.000 | 0.030 | 0.000 | 0.000 |
| Zn | 0.330 | 0.570 | 0.550 | 0.210 | 0.260 | 0.020 |
| K | 53724.000 | 26640.000 | 53896.000 | 53624.000 | 26827.000 | 53611.000 |
| S | 203707.000 | 160633.000 | 201573.000 | 213690.000 | 149861.000 | 220463.000 |
| Co | 0.000 | 0.000 | 0.000 | 0.000 | 0.000 | 0.000 |
| Mn | 0.020 | 0.000 | 0.090 | 0.050 | 0.180 | 0.001 |
| Se | 1.009 | 7.240 | 1.190 | 4.980 | 2.240 | 1.730 |
| Mg | 569.690 | 44.000 | 454.740 | 91.850 | 248.810 | 63.080 |
| Al | 5.740 | 4.100 | 4.080 | 5.800 | 4.970 | 5.340 |
| Cr | 0.300 | 0.200 | 0.280 | 0.300 | 0.210 | 0.160 |
| Mo | 0.020 | 0.000 | 0.040 | 0.000 | 0.001 | 0.000 |
| Sr | 2.540 | 0.270 | 7.110 | 1.310 | 6.560 | 3.260 |
| Na | 340805.000 | 202961.000 | 339361.000 | 358302.000 | 193843.000 | 371061.000 |
| As | 1.020 | 2.880 | 0.780 | 0.300 | 0.610 | 0.470 |
| Ni | 0.090 | 0.160 | 0.120 | 0.840 | 0.240 | 0.000 |
| Ti | 0.090 | 0.040 | 0.050 | 0.040 | 0.040 | 0.050 |
| Cl | 5.3 | 79.47 | 22.07 | 17.66 | 22.07 | 9.71 |

TS1 ➔ First salt taken. This salt was taken before any calcium sulphate precipitate formed.

TS2 ➔ Salt taken soon after calcium sulphate formed. Unwashed

TS3 ➔ Salt taken, calcium sulphate present. Unwashed

TS 4 ➔ Washed fraction of TS3.

TS 5 ➔ Salt taken, calcium sulphate present. Unwashed

TS 6 ➔ Washed fraction of TS5

**Table 26: Data from liquid analysis of coal power plant brine experiment**

| mg/L | Raw | Concentrate | #1 | #2 | #3 | #4 |
|---|---|---|---|---|---|---|
| **B** | 2.69 | 9.44 | 18.36 | 13.35 | 19.11 | 17.01 |
| **Si** | 8.66 | 4.42 | 7.84 | 5.96 | 8.50 | 7.66 |
| **Ba** | 0.06 | 0.11 | 0.22 | 0.17 | 0.24 | 0.22 |
| **Cu** | 0.30 | 0.60 | 1.28 | 0.89 | 1.31 | 1.13 |
| **$PO_4$** | 2.41 | 4.89 | 9.02 | 6.87 | 9.51 | 8.48 |
| **V** | 0.02 | 0.03 | 0.03 | 0.03 | 0.05 | 0.05 |
| **Ca** | 120.08 | 417.86 | 719.79 | 513.83 | 659.06 | 533.38 |
| **Cl2** | 0.36 | 0.40 | 6.50 | 0.21 | 0.21 | 0.19 |
| **Cd** | 0.00 | 0.00 | 0.00 | 0.00 | 0.00 | 0.00 |
| **Fe** | 0.29 | 0.11 | 4.86 | 1.22 | 1.42 | 0.87 |
| **Pb** | 0.01 | 0.00 | 0.00 | 0.02 | 0.03 | 0.02 |
| **Zn** | 0.20 | 0.05 | 0.15 | 0.14 | 0.19 | 0.17 |
| **K** | 92.32 | 370.53 | 729.87 | 502.91 | 723.96 | 683.37 |
| **$SO_4$** | 8514.66 | 30361.67 | 27980.01 | 26490.00 | 22248.99 | 21471.99 |
| **Co** | 0.02 | 0.02 | 0.02 | 0.02 | 0.03 | 0.04 |
| **Mn** | 0.01 | 0.07 | 0.23 | 0.19 | 0.31 | 0.28 |
| **Se** | 0.37 | 1.60 | 1.81 | 1.34 | 3.67 | 0.88 |
| **Mg** | 189.62 | 488.82 | 887.13 | 678.31 | 910.26 | 840.36 |
| **Al** | 0.13 | 0.10 | 0.56 | 0.30 | 0.23 | 0.17 |
| **Cr** | 0.01 | 0.03 | 0.04 | 0.03 | 0.04 | 0.04 |
| **Mo** | 0.01 | 0.06 | 0.15 | 0.11 | 0.17 | 0.18 |
| **Sr** | 3.40 | 11.56 | 16.10 | 14.65 | 17.48 | 16.56 |
| **Na** | 2955.24 | 9086.23 | 10392.30 | 8762.85 | 9165.19 | 8737.79 |
| **As** | 0.00 | 0.00 | 0.00 | 0.01 | 0.02 | 0.00 |
| **Ni** | 0.14 | 0.48 | 0.89 | 0.66 | 0.84 | 0.80 |
| **Ti** | 0.00 | 0.00 | 0.00 | 0.00 | 0.00 | 0.00 |
| **Cl** | 2752.44 | 8204.43 | 12952.83 | 10833.07 | 13670.64 | 12789.19 |

The table to the left represents the results from the experiment described in section 7.1 on page 61.

Raw ➔ This is the unprocessed coal power plant brine before any concentrating or salt removal had been performed. This is also represented by Table 7 on page 23.

Concentrate ➔ This is the brine after ice had been removed and crystallization of sodium sulphate was about to occur.

#1 ➔ Corresponds to salt sample TS1

#2 ➔ Corresponds to salt sample TS2

#3 ➔ Corresponds to salt samples TS3 and TS4

#4 ➔ Corresponds to salt samples TS5 and TS6